MERTK-mediated Signaling in the Retinal Pigment Epithelium: Insights into the Mechanism of RPE Phagocytosis

by

Shameka J. Shelby

A dissertation submitted in partial fulfillment
of the requirements for the degree of
Doctor of Philosophy
(Biological Chemistry)
in The University of Michigan
2012

Doctoral Committee:

Professor Debra A. Thompson, Chair
Professor Christin Carter-Su
Professor Bret A. Hughes
Professor Benjamin L. Margolis
Assistant Professor Hisashi Umemori

To my two favorite men, Juan and Zani for your patience, love, and support.

Acknowledgements

I would like to acknowledge all of the people who helped me to accomplish my goals. My mentor, Dr. Debra Thompson, has been instrumental in my success as a scientist. Her motherly guidance has helped to mold me into the person and scientist I am today. I'm overly grateful for her tireless efforts and patience during the course of my graduate career. I wouldn't have even considered graduate school without the guidance of my undergraduate advisors, Drs. Marion Carroll and Guangdi Wang, to whom I am also grateful. Also, my favorite high school teacher Mrs. Jenkins incited my passion for biology and encouraged me to follow my aspirations.

I am also grateful for the invaluable input and criticisms of my committee members, Drs. Bret Hughes, Christin Carter-Su, Hisashi Umemori, and Benjamin Margolis. I would especially like to thank Dr. Hughes, Dr. Carter-Su, and Dr. Margolis for reagents that were instrumental in the completion of my experiments. Ben literally saved my life with the plethora of antibodies he provided. Reagents and clones provided by Drs. Tony Pawson, Karen Colwill, Sirano Dhe-Paganon, and Xudong Huang were instrumental in the initial studies of MERTK and SH2-domain protein interactions. Additionally, the University of Michigan Protein Facilities Core, Kendricks Labs, and Dr. Mary Ann Gawinowics of Columbia University were also very helpful in conducting experiments that

were outside the scope of our lab. Dr. Steve Lentz will always have my appreciation for helping me out with all things related to confocal microscopy.

I would like to thank Dr. Christina McHenry for generating the MERTK constructs that I used almost daily. Naheed Hemati and Dr. Jared Chrispell were very helpful in teaching me many techniques during my early years in the lab. Current lab members including Austra Leipa, Monica Ray, Cameron Strong, and Anna Ganios were exceedingly helpful with everything ranging from taking care of animals to mini-preps. Frank Mei's expertise with PowerPoint and Photoshop were helpful in constructing signaling diagrams. I'd also like to thank Lin Jia for the awesome sections that she would always provide on a moment's notice. I'm forever indebted to Kecia Feathers for everything she's done for me. She's the only person I know that will come to lab at 3 AM just to help me. Thankfully I'll still be able to ask her my weekly stupid question for a few more years.

I'd also like to thank my family and friends. All of them have been very patient and understanding of this journey that no one in my family had any exposure to. Especially my mother and father, who have supported me and pushed me to become whatever I wanted to, regardless of where I'm from. Lastly, I'm so appreciative of my husband and my son. They both have had a profound impact on my life, and I only hope that I can return the favor.

Table of Contents

List of Figures

List of Tables

List of Abbreviations

AMD	Age-Related Macular Dystrophy
Arp2/3	Actin-Related Proteins
CD36	Cluster of Differentiation 36
CHM	Choroidermia
CP	Capping Protein
FAK	Focal Adhesion Kinase
GAP	GTPase Activating Proteins
GDI	GDP-Dissociation Inhibitors
GEF	Guanine Nucleotide Exchange Factors
GGTrII	Geranyl-Geranyl Transferase Type II
Grb2	Growth Factor Receptor Bound Protein 2
GTPase	Guanosine Nucleotide Triphosphatase
hTERT	Human Telomere Reverse Transcriptase
IS	Inner Segment
ITAM	Immunoreceptor Tyrosine-based Activation Motif
JMY	Junction Mediating Regulatory Protein
LIMK	LIM Kinase
MERTK	Mer Tyrosine Kinase Receptor
MFG-E8	Milk Fat Globule-EGF 8
MYRIP	Myosin VIIa and Rab Interacting Protein
NPF	Nucleation-Promotion Factors
OS	Outer Segment
Pak1	P21 Activating Kinase 1
PI3K	Phosphatidylinositol-3-Kinase
PKC	Protein Kinase C
Rab	Ras-related Proteins in the Brain
RCS	Royal College of Surgeons
REP	Rab Escort Proteins
RPE	Retinal Pigment Epithelium
RPE65	Retinal Pigment Epithelium 65 kDa Protein
Scar	Suppressor of cAMP Receptor
SH2	Src Homology 2
TAM	Tyro3/Axl/Mer
VASP	Vasodilator-Stimulated Phosphoprotein
WASH	WASP and SCAR Homolog
WASP	Wiskott-Aldrich Syndrome Protein
WAVE	WASP family Verprolin-homologous Protein

WH2	WASP Homology domain-2
WHAMM	WASP homolog associated actin membranes and microtubules
ZO	Zona Occludins

Abstract

A key function of the retinal pigment epithelium (RPE) is the phagocytic uptake of outer segment (OS) membranes shed from the distal tips of the photoreceptor cells in diurnal rhythm. The shedding and removal of effete OS membranes is essential for the normal function and renewal of the light-absorbing rod and cone photoreceptor cells. Mutations affecting the mechanism of RPE phagocytosis can result in inherited retinal degeneration. In the dystrophic Royal College of Surgeons (RCS) rat, a loss of function mutation in the gene encoding the receptor tyrosine kinase MERTK disrupts phagocytic uptake, but not binding, of shed OS membranes. As a consequence, a debris field forms in the subretinal space, blocking the supply of oxygen and nutrients to the photoreceptors resulting in retinal degeneration and vision loss. Activation of MERTK results in receptor autophosphorylation and interaction with a diverse array of signaling proteins. Using studies of recombinant protein interactions, this thesis shows that MERTK interacts with multiple SH2-domain proteins in the RPE, including effectors of Rho family GTPases that regulate cytoskeletal reorganization needed for phagocytic uptake. Signaling downstream of MERTK also results in tyrosine phosphorylation of cellular protein substrates. During peak phagocytosis by the RPE, MERTK activation was shown to stimulate the tyrosine

phosphorylation of RabGDIα, an effector of the Rab family of small GTPases that contribute to membrane localization. In addition, RabGDIα was shown to interact with Rab5 that is involved in early phagosome formation. These results suggest a direct role of MERTK in the regulation of membrane trafficking and cargo sorting in the RPE. The present findings extend our understanding of the role of MERTK in RPE phagocytosis. Identification of signaling partners and downstream effects of MERTK activation suggests multiple links to cytoskeletal rearrangement as well as a novel role in regulating phagosome trafficking in the RPE. Insights into the RPE phagocytic mechanism will further our understanding of the cell biology underlying the visual process and provide a foundation for studies aimed at therapeutic intervention in diseases of the retina.

Chapter I

Introduction

The retina

The vertebrate eye is one of the most complex structures of the body. Much of this is due to the highly specialized layer of light-sensitive tissue known as the retina. The vertebrate retina is the innermost layer of the eye and is composed of over 50 specialized cell types grouped together to form multiple layers [1]. Each layer of the retina has a specific function which contributes to its ability to serve as a sensory organ that turns light into neuronal signals that our brain processes to form vision. The retina is composed of 10 different sub-layers which are as follows (from innermost retina to outermost retina): the inner limiting membrane (ILM), ganglion cell layer (GCL), inner plexiform layer (IPL), inner nuclear layer (INL), outer plexiform layer (OPL), outer nuclear layer (ONL), external limiting membrane (ELM), photoreceptor inner segments (IS), photoreceptor outer segments (OS), and the retinal pigment epithelium (RPE) [2]. The choroid lies next to the RPE and serves to deliver oxygen and nutrients to the external layers of the retina including the RPE and the photoreceptors (Figure I-1).

The choroid is composed of five layers including Bruch's membrane, the choriocapillaris, two vascular layers: Haller's layer and Sattler's layer, and the

superchoroidea [3]. Of these layers, Bruch's membrane covers most of the basolateral membrane of the RPE and serves to effectively separate the RPE from the choroidal vasculature. The suprachoroid is the outermost layer of the choroid adjacent to the sclera. The RPE is a pigmented monolayer of hexagonal shaped cells which form part of the blood/retina barrier. These polarized cells are interconnected by tight junctions, which delineate two surfaces designated as the basolateral and apical membranes. The basolateral side shares space with Bruch's membrane, while the apical surface interacts directly with the OS of the photoreceptor cells. The apical surface contains microvilli which extend to surround the OS, establishing a structural interaction between the RPE and photoreceptor cells [4].

The sensory layers of the retina, also known as the neural retina, can be further divided into groups of three layers of nerve cell bodies and two layers of synapses. The nuclei of the rod and cone photoreceptors are located in the outer nuclear layer, adjacent to the outer plexiform layer where the photoreceptors synapse with the neural cells of the inner nuclear layer allowing for the neural signals generated from the rods and cones to be further processed. The inner nuclear layer contains the cell bodies of bipolar, horizontal, amacrine and Mueller cells. The bipolar cells are the most abundant and connect the photoreceptor and ganglion cell layers. There are more than ten subtypes of cone bipolar cells and only one subtype of rod bipolar cells [1]. This diversity of bipolar cells allows for the flexibility necessary to conduct signals stemming from many rod and cone photoreceptors. The cone bipolar cells directly connect cone photoreceptors to

ganglion cells and bridge synaptic connections with amacrine cells that synapse with rod bipolar cells. This allows cross talk between the rod and cone photoreceptors to enable rod signaling during dim light situations, and cone signaling during bright light. Each rod bipolar cell can synapse with one to four ganglion cells, in addition to synapsing with amacrine cells to allow further cross talk between the rod and cone photoreceptors. The horizontal cells receive inputs from the photoreceptors and conduct information laterally. Comparatively, there are relatively few synapses formed by bipolar cells with retinal ganglion cells, with the majority of the input from the bipolar cells transmitted by amacrine cells forming connections with bipolar and retinal ganglion cells [1].

Mueller cells fill the retinal space with cytoplasmic processes that reach the external limiting membrane. The inner plexiform layer is the second synaptic layer, and the site of synapses between ganglion, bipolar and amacrine cells. The third layer of neural cells is the ganglion cell layer, where the cell bodies of the ganglion cells lie. Ganglion cells are the only output neurons in the retina and possess the unique ability to process and transmit information from the retina to the visual processing centers in the brain. The axons from the ganglion cells bundle into tracts that continue to form the nerve fiber layer. The bundled tracts run radially along the inner surface of the retina and eventually meet at the optic nerve. The optic nerves leave the orbit, cross the optic chiasm, and innervate the optic tectum to generate the visual response [5].

The retinal pigment epithelium

The RPE is a monolayer of polarized neuroepithelial cells that are post-mitotic and highly metabolically active as evidenced by the large number of mitochondria on the basolateral region of the cytoplasm [6]. They also harbor numerous melanosomes which give the RPE its pigmented appearance [7]. Akin to other epithelial cells, the RPE has apical and basolateral surfaces. The cells adhere to one another through complexes that form several types of junctions between them, namely gap, adherens, and tight junctions. Gap junctions are distributed along the lateral membrane and form intercellular pores that allow exchange of small molecules between cells. Adherens junctions are adhesive junctions, which are linked to intermediate filaments and the actin cytoskeleton. Tight junctions are normally located toward the apical surface of epithelial cells and form a paracellular gate that regulates permeability. Tight junctions are linked to the actin cytoskeleton and the adherens junctions by the Zona occluden (ZO) proteins. [8].

The RPE functions in transporting vitamins and nutrients to the neural retina (particularly the photoreceptors), retinoid processing, and phagocytosis of effete OS membranes. The basolateral surface of the RPE is directly adjacent to Bruch's membrane and together with the tight junctions form a blood-retinal barrier between the neural retina and the fenestration of the choriocapillaris [9]. The RPE serves to transport glucose, retinol, and nutrients from the choroidal blood-supply to the photoreceptors, and in opposite transports water, ions, and metabolic waste from the neural retina out to the choroid through the differential

expression of ion channels and pumps on the apical and basolateral surfaces [10, 11]. The RPE also participates in vitamin A metabolism necessary for the visual response of photoreceptor cells that use 11-cis retinal based pigments to absorb light. The RPE regenerates 11-cis-retinal for use by the photoreceptors, in which the photoisomerization of 11-cis-retinal to all-trans-retinal occurs [12]. Finally, a major critical function of the RPE is the phagocytosis of spent photoreceptor OS, which lie in direct contact with the apical surface of the RPE [4] (Figure I-2).

The photoreceptors

The photoreceptor cells are unique ciliated cells that have become specialized in structure and function for sensing light and signaling. These neurons are composed of four parts: the synaptic terminal, nucleus, a central body or inner segment, and a distal end or OS that contains membranous sacks or discs which house the visual pigment opsin and the phototransductive machinery [13]. Photoreceptor OS contain a high concentration of opsins and unsaturated phospholipids that are denatured and oxidized by light exposure, causing a need for renewal. OS proteins are synthesized and new membranes are added to the base of the OS daily [14, 15]. For rod photoreceptors, this complex process has been shown to involve the visual pigment rhodopsin. Mice lacking rhodopsin failed to grow and maintain OS, implicating rhodopsin in the synthesis of OS membranes [16]. Additionally, mutations in the C-terminal tail of rhodopsin displayed defective trafficking to the OS, effectively stalling at the IS [17]. Subsequent studies using a two-hybrid approach identified the Smad

anchor for receptor activation (SARA) as a binding partner of rhodopsin's C-terminal tail which uses multiple domains to interact with and fuse nascent rhodopsin molecules with the existing OS [18].

Spent membranes are shed from the OS tips and removed from the subretinal space by RPE phagocytosis [19]. RPE cells extend microvilli from the apical cell membrane that surrounds the OS. Following OS shedding, particles are phagocytized by the RPE cell, where they are carried through the process of phagosome maturation to become lysosomes and their contents are degraded [20]. This process of clearance of effete OS membranes is essential for the viability and function of the photoreceptors. Failure of phagocytosis results in accumulation of OS membranes in the sub-retinal space, leading to photoreceptor degeneration and blindness, as observed in the Royal College of Surgeons (RCS) rat [21]. Defective phagocytosis of shed OS may also contribute to the pathology of age-related macular degeneration (AMD) in humans [22, 23] (Figure I-3).

The processes of photoreceptor renewal, OS shedding, and RPE phagocytosis are highly regulated. Photoreceptor OS are damaged due to light exposure, and newly synthesized OS proteins are effectively trafficked up to the tips for replacement [14]. In addition, OS shedding and renewal exhibit peaks and lows in response to light exposure, with a burst of OS shedding beginning at light onset and tapering off during the dark [24-26]. Further studies revealed that OS shedding is influenced by a circadian-like light-dark cycle, including a clear burst of shedding and clearance occurring about one hour after light onset for rod

photoreceptors and one hour after dark onset for cones in mice [27]. Remarkably, this synchronized shedding of OS can be maintained over a period of three days in the absence of light, suggesting that OS shedding is not regulated by light alone but is also responsive to a light-entrained circadian rhythm [28].

Phagocytosis

Phagocytosis is a specialized form of endocytosis capable of ingesting solid particles over 0.5 μM, bringing them from outside the cell to inside the cell. The particles are normally recognized by receptors on the cell surface which initiate a signal transduction cascade that facilitates ingestion of the large particle through actin-myosin contractility, phagosome formation, and eventually lysosome formation [29]. As evidenced by previous studies, RPE phagocytosis appears to share a conserved mechanism with other professional phagocytes [30]. However, the mechanism of RPE phagocytosis is not yet understood to the extent of other phagocytic mechanisms, including Fcγ-receptor mediated ingestion of opsonized foreign particles [31], and Tyro/Axl/Mer (TAM) family signaling in the clearance of apoptotic cells by macrophages [32, 33].

Fcγ-receptor mediated phagocytosis of opsonized particles

One of the most well-defined mechanisms of phagocytosis occurs in the immune system and involves the recognition of IgG opsonins bound to foreign particles by the constant regions of Fcγ-receptors in macrophages [34]. Fcγ-receptors are members of a superfamily of tyrosine kinase-associated receptors which lack intrinsic tyrosine kinase activity. Upon binding to its ligand IgG, the

Fcγ-receptor is tyrosine phosphorylated on residues located within an immunoreceptor tyrosine-based activation motif (ITAM) domain by the activity of Src family kinases. This results in the creation of docking sites for Src homology 2 (SH2) domain-containing proteins, including the non-receptor tyrosine kinase Syk, which recruits additional proteins including Vav and Rac to form a signaling complex [31, 35, 36]. The proteins Syk, Vav, and Rac are of central importance in Fcγ-receptor signaling. Syk is critical for ITAM-dependent phagocytosis, and its silencing results in loss of the ability to internalize opsonized particles [37]. Rac is a member of the Rho-family G proteins, also known as Rho guanosine nucleotide triphosphatases (Rho GTPases). Members of this superfamily act as molecular switches, cycling between inactive GDP-bound and active GTP-bound conformations, downstream of a number of cell surface receptors to regulate a diverse array of cellular events including cytoskeletal reorganization, activation of protein kinases, and regulation of cell growth [38]. As a testament to the importance of Rac1 to Fcγ-receptor signaling, Rac1 has been shown to be required for FcγR-mediated phagocytosis [39]. In addition, the Vav family proteins function as guanine nucleotide exchange factors (GEF) for Rac1 [40].

TAM receptor-mediated phagocytosis of apoptotic cells

The TAM family of receptor tyrosine kinases function in critical cellular processes including tissue homeostasis, inflammation, autoimmune responses, innate immunity, and phagocytic clearance of apoptotic cells [32]. All three receptors function in macrophages to promote phagocytosis, however only MERTK was shown to be essential for phagocytosis of apoptotic cells [33].

Members of the TAM family consist of three domains: an extracellular ligand binding domain including a N-terminal immunoglobin-like domain and fibronectin type III repeats, a transmembrane region, and a cytoplasmic domain containing a catalytic domain with a conserved KWAIAES sequence [41-43]. The TAM receptors and their ligands protein S and Gas6, are known to function as dimers [44-47]. The structurally similar ligands contain multiple γ-carboxyglutamic acid residues that complex with Ca^{2+} and negatively charged phosphatidylserine residues on the outer leaflet of apoptotic cells. This interaction potentially serves as a bridge between the apoptotic cell and the receptor to initiate phagocytosis [48-50]. Ligand binding to the TAM family receptors activates their intrinsic kinase activity and result in autophosphorylation of tyrosine residues in the cytoplasmic domain of the receptors [51]. The phosphorylated receptors then recruit SH2 domain proteins and phosphotyrosine binding (PTB) domains which signal in other diverse processes within the cell [52, 53] (Figure I-4).

Dimerization and activation of the TAM receptors recruits a host of proteins which have not yet been definitively linked to cytoskeletal rearrangement. However, it is known that MERTK is the predominant receptor involved in the clearance of apoptotic cells [54], and that it works in concert with αvβ5 integrin to initiate phagocytosis [55]. In addition, MERTK interactions with growth factor receptor bound protein 2 (Grb2), Src, Vav, focal adhesion kinase (FAK), and phosphatidylinositol-3-kinase (PI3K) have been demonstrated and are thought to be important in MERTK-mediated phagocytosis of apoptotic cells [56-62]. Perhaps the most direct link of MERTK to the cytoskeleton is through

interaction with Vav1 that subsequently activates Rho family GTPases required for actin remodeling.

OS phagocytosis by the RPE

Phagocytic uptake of OS by the RPE is a highly specialized process that involves OS shedding, recognition, binding, ingestion, and the breakdown and recycling of photoreceptor components [4]. The mechanism underlying this receptor-mediated process has not yet been fully defined, but key protein components have been identified including MERTK, αvβ5 integrin, cluster of differentiation 36 (CD36), FAK, and Rac1 [30, 63]. Recognition of spent OS by the RPE appears to occur similarly to TAM receptor signaling in clearance of apoptotic cells. Studies of bovine rod OS showed that the plasma membranes contain high levels of phosphatidylserine [64]. Later studies also suggested that when compared to phosphatidylethanolamine and phosphatidylcholine, phosphatidylserine is the preferred phospholipid expressed in the OS and bound by the RPE [65]. MERTK is the predominate TAM family receptor expressed in the RPE, while Tyro3 is also expressed but its loss does not affect RPE phagocytosis in the *Tyro3-/-* mouse [66]. In cultured cells, both protein S and Gas6 stimulate phagocytosis of OS by RPE cells [67]. However, studies in knockout mice revealed that Gas6 is not essential for RPE phagocytosis. In addition, protein S has been shown to stimulate MERTK phosphorylation in RPE cells in the absence of Tyro3 [66].

Much work has been done to identify the mechanism of OS binding to the RPE. The activation of αvβ5 integrin, a cell surface adhesion molecule that is

expressed on the apical surface of RPE cells, is required for binding OS, with αvβ5 integrin loss-of-function resulting in delayed-onset retinal degeneration in mice [68, 69]. Binding of effete membranes by αvβ5 integrin involves recognition of RGD motifs on ligands that bind the OS, including the secreted glycoprotein milk fat globule–EGF 8 (MFG-E8) which is presumed to exist on the OS surface or in the subretinal space [68, 70]. αvβ5 integrin also contributes to maintaining a strong interaction between the RPE and photoreceptors [71], as well as functioning in the synchronization of circadian OS phagocytosis by the RPE. Following activation of αvβ5 integrin, FAK is phosphorylated on activating tyrosine residues and upon ingestion of OS, dissociates from αvβ5 [72]. In the absence of β5, diurnal activation of FAK is lost, resulting in the dampening of the burst of ingestion that follows OS shedding [73]. Tetraspannin CD81 has been shown to work in concert with αvβ5 integrin to initiate OS binding [74]. Integrin signaling may also affect the process of cytoskeletal rearrangement in the RPE. Recent studies have shown that Rac1, a Rho family GTPase that functions in regulating actin polymerization acts downstream of αvβ5 integrin signaling in the RPE phagocytosis [63].

Critical insight into the mechanism of OS uptake has been gained through studies of the Royal College of Surgeons (RCS) dystrophic rat, a classic model of retinal dystrophy [75]. The RCS rat has a disruption in the process of the uptake of spent OS by the RPE, resulting in the formation of a debris field between the RPE and retina that blocks the supply of oxygen and nutrients to the photoreceptor cells [22, 76, 77]. Identification of *Mertk* as the disease gene in the

RCS rat demonstrated that the retinal dystrophy is caused by a 2 kb deletion in the *Mertk* gene, producing a truncated and inactive protein [78]. *Mer-/-* mice also exhibited a similar retinal phenotype [79-81]. *MERTK* was subsequently identified as a human retinal dystrophy gene, based on the finding of loss-of-function mutations in patients with autosomal recessive retinitis pigmentosa [82-84]. *MERTK* is a very polymorphic gene which produces many functional forms of the protein in humans [82, 84-86]. The finding of *MERTK* as a disease gene in humans, rats, and mice led to subsequent studies by Vollrath and colleagues showing that the phenotype could be corrected by viral gene transfer. Subretinal injections of a virally delivered MERTK rescued vision in the rats by preserving photoreceptor OS structure and correcting the RPE phagocytosis defect, further supporting that MERTK loss-of-function is responsible for the RCS phenotype [87]. Studies in cultured RPE cells also showed that MERTK is required for the uptake of OS added to cultures [88].

Despite the importance of MERTK in RPE phagocytic uptake, little is known about its signaling partners and their functions in the RPE. To date, the only protein shown to interact with MERTK in the RPE is myosin II [89]. This interaction is necessary for myosin II to be recruited to the phagosome during OS ingestion [89]. Additional proteins that have been shown to be involved with phagocytic uptake, but not directly linked to MERTK include PI3K, PKC, scavenger receptor CD36, annexin A2, and Rac1 [63, 90-95].

Cytoskeletal rearrangement in phagocytosis

Phagocytic uptake of OS by the RPE requires rearrangement of the actin cytoskeleton, a feature in common with the mechanism associated with other phagocytosis receptors including Fcγ and CR3 [29, 34, 96-98]. At the center of each of these receptor-mediated phagocytic mechanisms are small monomeric G-proteins, primarily Rho family and actin related proteins (Arp) family GTPases [99]. The Rho family GTPases, specifically Rac1, Cdc42, and Rho A are responsible for conducting signals leading to cytoskeletal rearrangement [29]. The action of specific Rho family GTPases in conducting signals for cytoskeletal rearrangement differs in various systems, in that Rac1 and Cdc42 act downstream of Fcγ-receptors, whereas Rho is required downstream of CR3 complement receptor signaling [100, 101]. The Wiskott-Aldrich syndrome Protein (WASP) and Suppressor of cAMP receptor/WASP family Verprolin-homologous (Scar/WAVE) proteins are key effectors downstream of Rac and Cdc42 [102]. In Fcγ receptor signaling, Rac1 stimulates actin polymerization by activating WAVE [103], PI(4)P 5-kinase, and Pak1[104, 105]. Cdc42 also contributes to actin polymerization by binding and activating WASP [106]. Members of the Arp family also function downstream of Rho family effectors and directly regulate the actin cytoskeleton during phagocytosis [107] (Figure I-5).

Actin remodeling in phagocytosis

Actin is one of the most highly conserved proteins between species. It is a 42 kDa globular protein that forms monomers (G-actin) which assemble to form polarized filamentous actin (F-actin), an essential component of the cytoskeleton.

Actin filaments grow and shrink by addition or loss of monomeric actin from either the barbed or pointed ends. Newly formed actin monomers are predominantly added to the barbed ends, while removal of actin monomers occurs at the pointed ends [108]. The mechanism of actin assembly occurs in three stages which include the formation of new actin filaments (nucleation), increase in filament length (capping and uncapping), and reduction of length and number of filaments (severing and depolymerization) [29].

Actin nucleation

For actin polymerization to occur, the formation of newly synthesized actin monomers must be initialized by actin-nucleating proteins. Formins, tandem-monomer-binding nucleators, and the Arp2/3 protein complex make up three major families of actin-binding proteins that regulate nucleation [108]. Of the three, the Arp2/3 complex is the major actin nucleator in cells and has the most well-defined mechanism of action. The Arp2/3 complex is composed of 7 subunits, including Arp2, Arp3, and 5 additional ARPC1–5 subunits, and functions with the aid of nucleation-promoting factors (NPF) [109, 110]. NPFs including WASP, N-WASP, WAVE, SCAR, WASP homolog associated with actin, membranes and microtubules (WHAMM), WASP and Scar homolog (WASH), and junction mediating regulatory protein (JMY), interact with actin through their WASP Homology 2 (WH2) domains and with Arp2/3 complex through their central acidic domains [111]. Upon activation of the Rho family GTPases, NPFs are activated and dimerize forming a bridge between the Arp2/3 complex and actin [112]. Arp2 and Arp3 become activated and interact with the pointed end of

the daughter filament while the remaining subunits interact with the mother filament [113]. The Arp2/3 complex completes the nucleation step by creating newly synthesized filaments which extend from the sides of existing filaments at a 70° angle to form branched f-actin [108].

Actin capping and uncapping

The nucleation of actin is highly regulated. Capping protein (CP) has the ability to bind the barbed end of actin filaments and “cap” their addition or loss of any actin monomers [114]. This function is necessary to maintain a consistant level of monomeric g-actin within the cell to promote Arp2/3 complex-mediated filament nucleation and branching [115, 116]. In addition, CP plays an instrumental part in the control of cell shape and movement by regulating the direction and length of the actin cytoskeleton [117]. While capping is important, “un-capping” the barbed end of actin is needed for effective polymerization. CP inhibitors include indirect regulators that bind to actin directly and inhibit CP from binding to the barbed-end of actin, and direct regulators that bind to the capping protein itself. Indirect inhibitors include formins and the scaffolding protein vasodilator-stimulated phosphoprotein (VASP), all of which induce actin polymerization at barbed ends through incorporation of actin monomers bound to the actin-binding protein profilin [118, 119]. The two major direct interacting regulatory proteins are V-1 and CARMIL which use distinct mechanisms to inhibit CP [120].

Actin severing and depolymerization

Actin filaments are continuously reorganized through the highly regulated processes of polymerization and depolymerization occurring during and after ingestion of foreign particles. Actin depolymerization is controlled by the 16 kDa actin regulatory protein, actin depolymerization factor (ADF)/cofilin. ADF/cofilin functions through severing actin filaments to increase the number of branching points at which polymerization and depolymerization occur [121]. Under normal circumstances, ADF/cofilin binds to actin filaments at a 1:1 ratio [122], however the ratio of ADF/cofilin to actin dictates the action of the enzyme. During times of low ADF/cofilin relative to actin, ADF/cofilin severs rapidly and transiently and then stabilizes F-actin, whereas high cofilin/actin ratios cause polymerization [123]. ADF/cofilin activation is directly regulated by LIM kinase (LIMK) via phosphorylation. Serine phosphorylation on the N-terminus of ADF/cofilin by LIMK yields an inactive cofilin protein, while dephosphorylation produces activity [124]. Further regulation of ADF/cofilin includes the phosphorylation of LIMK by p21-activated kinase 1 (PAK1), which is also an effector of Rho family GTPases [105, 125].

Gelsolin is another severing protein involved in actin depolymerization. As with ADF/cofilin, it can serve as a severing protein, but differs in that gelsolin is a much larger protein that can also serve as a capping protein and is regulated by intracellular calcium and $PI(4,5)P_2$ concentration [126-129]. In the presence of high intracellular calcium concentration, gelsolin changes confirmation to expose actin binding sites [130]. This confirmation is reversed under conditions of low

calcium and PI(4,5)P_2 [131, 132]. Gelsolin and ADF/cofilin share structural similarities in their actin binding sites. In addition, gelsolin has been implicated in cytoskeletal changes associated with pseudopod formation during the early stages of Fcγ receptor-mediated phagocytosis, but not in CR3-mediated phagocytosis [133].

Myosin activity in phagocytosis

Although actin polymerization is critical for cytoskeletal rearrangement, formation and trafficking of the phagosome cannot occur without closure and movement of the newly formed actin filaments. Myosins are a superfamily of ATP-dependent motor proteins which provide actin-based motility [134, 135]. In Fcγ-receptor signaling, multiple myosins including IC, II, Va, IXb, and X have been identified at different stages of particle uptake and trafficking [136-139]. In mouse macrophages, myosin IC was found at the top of the phagocytic cup, suggesting a role in phagosome closure. The activity of myosin IC is controlled by phospholipid expression at the point of phagocytic uptake. In the presence of PI3K inhibitors, myosin IC failed to close the phagosome in murine macrophages [56, 137, 140]. Myosin X also functions in phagosome cup closure and is downstream of PI3K signaling. Myosin X contains three pleckstrin homology domains, one of which is used for recruitment to the forming phagosome to aid in cup closure [138]. Non-muscle myosin II and IXb have been implicated in the formation of the phagocytic cup, with myosin II shown to participate in a squeezing motion of the cytoskeleton to surround the particle [139-142]. Myosin

Va localizes to the fully internalized phagosome and is thought to mediate short range movements of the phagosome [143] (Figure I-5).

Actin-binding proteins in the RPE

Studies focused on the identification of proteins involved in cytoskeletal rearrangement in the RPE have identified three actin-binding proteins reported to function in the phagocytic mechanism: annexin II, myosin II, and myosin VIIa [30]. Annexin II is a calcium and phospholipid dependent protein that has been shown to associate with phagosomes in macrophages [144]. In studies of a differentiated RPE cell line that retains phagocytic activity, annexin II was shown to be up-regulated after differentiation, consistent with involvement in phagocytosis [145]. Recent studies of annexin II further solidified its involvement in RPE phagocytosis, showing that it is recruited to the early phagocytic cup, and is required for normal uptake of spent OS. These studies also demonstrated that annexin II phosphorylation is subject to circadian regulation of OS shedding and phagocytosis in the RPE [94].

As mentioned above, myosin II has been shown to directly interact with MERTK and is required for phagocytic uptake in the RPE [89]. This suggests that myosin II function in the RPE may mimic its function in Fcγ-receptor-mediated phagocytosis in formation of the phagocytic cup. Myosin VIIa is also expressed in the RPE and its function has been studied in more detail than that of myosin II. Mutations in *MYOSIN VIIa* cause Usher syndrome type 1B (USH1B), which accounts for the disease in up to 50% of patients with Usher syndrome that is characterized by deafness and early-onset retinal degeneration [146, 147].

Mutant myosin VIIa mice, also known as Shaker 1 mice [148], display an absence of melanosomes from the apical processes of the RPE [149], and a slower rate of disk membrane renewal [150]. Subsequent studies demonstrated that myosin VIIa is involved in the trafficking of phagosomes in the RPE following phagocytic uptake [151]. Recent studies have further solidified the role of myosin VIIa a as a transporter in the RPE, demonstrating that the translocation of RPE65, a retinoid isomerase with a direct role in the visual cycle, is regulated by myosin VIIa [152].

Phagosome maturation and trafficking

Following the closure of the phagocytic cup, the newly formed phagosome is trafficked within the cell to further mature and eventually degrade its contents. Regulation of membrane trafficking is performed by a large subfamily of the Ras superfamily of GTPases, called Ras-related proteins in the brain (Rab) GTPases [153-155]. Like other small Ras family GTPases, Rabs are molecular switches that cycle between active and inactive forms to regulate membrane movement throughout the cell [156, 157]. Rabs are involved in exocytosis and endocytosis, as well as the movement of larger particles in phagocytosis [158]. There are over 70 different Rab GTPases, and the function of at least 36 of these has been identified [159]. Each Rab has a specific role in membrane trafficking, with activities that can vary based on the signal provided by the initializing engulfment receptor. Of these, Rab5 has a well-defined role in early endosome formation, while Rab7 functions in endosome maturation and trafficking to the late endosome [160, 161].

Recruitment of Rab proteins to various membrane compartments is regulated through a large group of effector proteins [161]. Post-translational modification of Rab proteins by geranylgeranyl transferase type II (GGTrII) allow for reversible interaction and localization to the membrane [162, 163]. Rab activation and regulation of subcellular localization is regulated by multiple proteins including guanine nucleotide exchange factors (GEF), GTPase activating proteins (GAP), Rab escort proteins (REP), and GDP dissociation inhibitors (GDI). Due to the high concentrations of free magnesium within the cell, Rab GTPases normally do not cycle spontaneously to the GTP-bound form [164]. Therefore GEFs are required to catalyze the exchange of GDP to GTP in Rab GTPases [165]. GAPs perform the opposite action by speeding up the hydrolysis of bound GTP to GDP [166-168]. Rab proteins perform their requisite functions when associated with the membrane, and effector proteins REP and GDIs serve to facilitate their activities. REPs are responsible for binding newly synthesized Rab proteins and facilitating their recruitment to GGTrII to allow for the prenylation of the Rab to occur [162, 169-171]. GDIs inhibit the dissociation of GDP from Rab GTPases, transport them from the membrane to the cytosol, and deliver them to subsequent membrane locations requiring their activity [172-174]. In addition, the affinity of GDIs for Rabs is thought to be regulated by phosphorylation. Previous studies demonstrated that p38 MAPK is an enhancer of Rab5-RabGDI complex formation during endocytosis [175]. Also, pharmacologically induced tyrosine phosphorylation of RabGDI2 (β) resulted in its increased affinity for certain GDIs [176]. These results suggest that the

phosphorylation of RabGDI by various kinases may have a regulatory or gain-of-function effect on the activity of the Rab-RabGDI complex (Figure I-6).

Rab GTPases and effectors in the RPE

To date, only five Rab GTPases have been shown to function in the RPE including Rabs 8, 11, 27A, 32, and 38. Studies in cultured human telomere reverse transcriptase (TERT)-immortalized RPE cells demonstrated involvement of Rab8 and Rab11 in cilliary membrane formation [177, 178]. The function of Rab27A has been the most intensely studied and shown to form a complex with myosin Va, myosin VIIa, and myosin VIIa and Rab-Interacting Protein (MYRIP) to mediate melanosome transport [179-183]. The function of Rab38 was elucidated in studies of Rab38-deficient or “chocolate” mice, finding that Rab38 is required for the stability of melanosomes in the RPE, and that Rab32 may partially compensate for Rab38 loss-of-function [7, 184].

The only effector of Rab GTPases known to function in the RPE is REP1/ Choroideremia (CHM) [185]. Mutations in *REP1* in humans result in a complete lack of the protein and subsequent degeneration of the choroid, RPE, and the photoreceptors [169, 171, 186]. Individuals with CHM mutations exhibit an accumulation of undegraded OS in RPE phagosomes, suggesting that CHM could be involved in phagocytic uptake. Recent studies in human fetal RPE cells in which REP-1 was silenced have provided evidence for the involvement of REP1 in the mechanism of OS degradation within the phagolysosome [187]. There have been no reports of GDI function in the RPE, but given the similarities

of their structure and function with REPs, it is very likely that GDIs act in a similar capacity in the RPE.

Synopsis of dissertation

MERTK signaling plays a crucial role in the mechanism of RPE phagocytosis required for the survival of the photoreceptor cells of the retina. The goal of the studies presented in this dissertation was to identify signaling proteins that regulate RPE phagocytosis downstream of MERTK activation resulting in tyrosine phosphorylation of the receptor and cellular proteins. The work presented describes investigations of MERTK interactions with SH2-domain proteins, and MERTK-dependent phosphorylation of proteins involved in RPE phagocytosis.

Chapter II describes studies to identify SH2-domain proteins that interact with MERTK via recognition of phosphotyrosine residues. Pulldowns performed using recombinant proteins showed interaction of the SH2-domain proteins Grb2, PI3K, Vav3, and Src with MERTK in vivo and in vitro. Silencing of Grb2 in cultured RPE cells demonstrated a requirement for Grb2 in phagocytic activity. PI3K was implicated in phagosome formation. MERTK signaling was necessary for activation of Src, providing a possible link to integrin signaling and Rho family GTPases. These findings suggest that MERTK signaling contributes to regulation of cytoskeletal rearrangement through Rho family GTPases in the RPE.

Chapter III describes studies designed to identify proteins in the RPE/choroid whose tyrosine-phosphorylation correlates with phagocytic activity.

RabGDIα was found to be differentially phosphorylated during phagocytic uptake, indicating a potential regulatory role of membrane trafficking through its interaction with Rab GTPases. Tyrosine-phosphorylation of RabGDIα was MERTK dependent and affected its binding affinity for Rab GTPases. This represents the novel finding that MERTK signaling is likely to play a direct role in regulating phagosome formation and maturation in the RPE.

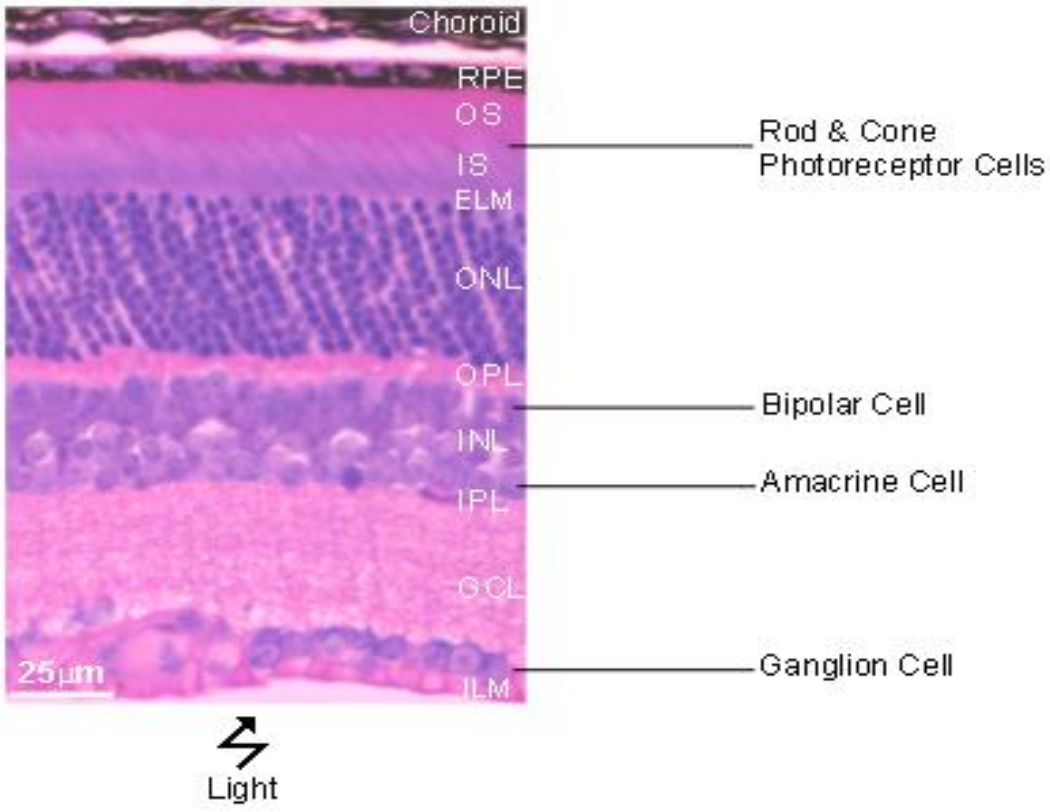

Figure I-1. Structure of the layers of the retina. Plastic embedded section from a wild-type mouse stained with Lee's stain (Methylene Blue and Basic Fuchsin) shows the histology of a normal mouse retina. The layers, viewed here from top to bottom are: the retinal pigment epithelium (RPE), outer segments (OS), inner segments (IS), external limiting membrane (ELM), outer nuclear layer (ONL), outer plexiform layer (OPL), inner nuclear layer (INL), inner plexiform layer (IPL), ganglion cell layer (GCL), and inner limiting membrane (ILM).

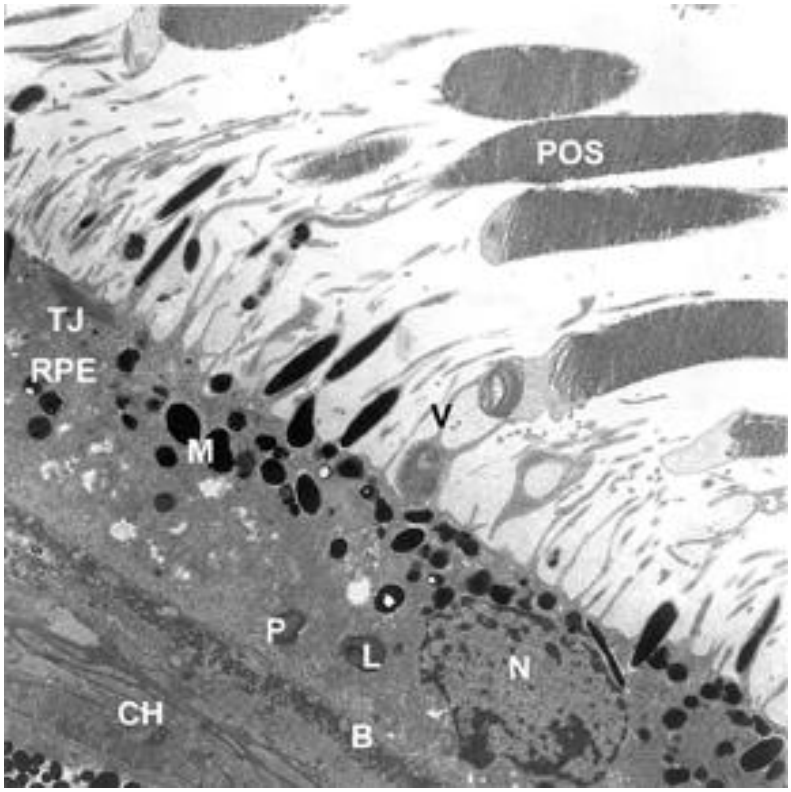

Figure I-2. Structure of the retinal pigment epithelium. An ultrathin section of mouse retina imaged by transmission electron microscopy shows the normal morphology of the retinal pigment epithelia (RPE) adjacent to the photoreceptor outer segment (POS) and the choroid (CH). Labeled are the cell nucleus (N), Bruch's membrane (B), tight junction (TJ), phagosome (P), melanosomes (M), lysosomes (L), and apical microvilli (V). This figure is used with permission from [188].

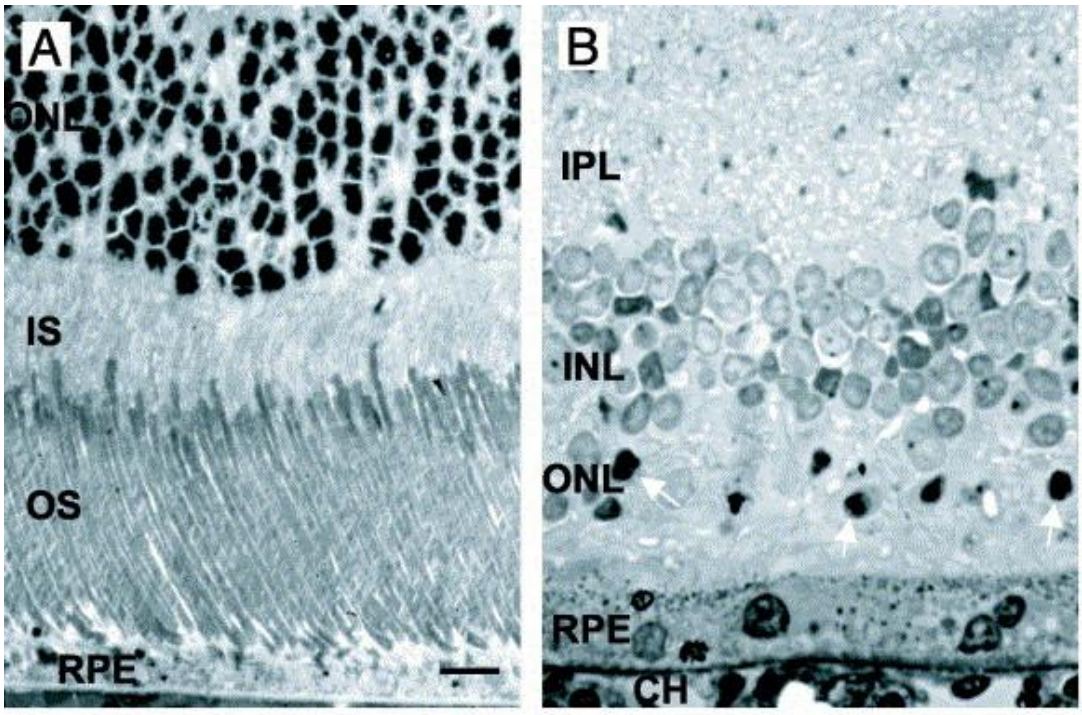

Figure I-3. Formation of a debris field and destruction of the retina in the RCS rat. An semi-thin section of rat retina stained with toluidine blue and imaged by light microscopy shows the normal morphology of the retina (A) in contrast to the retina of a 4 week old dystrophic rat (B). Note the thinning of the neural retina and very few remaining photoreceptors in the dystrophic rat (indicated by the arrows). Labeled are the retina pigment epithelium (RPE), outer segments (OS), inner segments (IS), choroid (CH), outer nuclear layer (ONL), inner nuclear layer (INL), and inner plexiform layer (IPL). This figure is used with permission from [189].

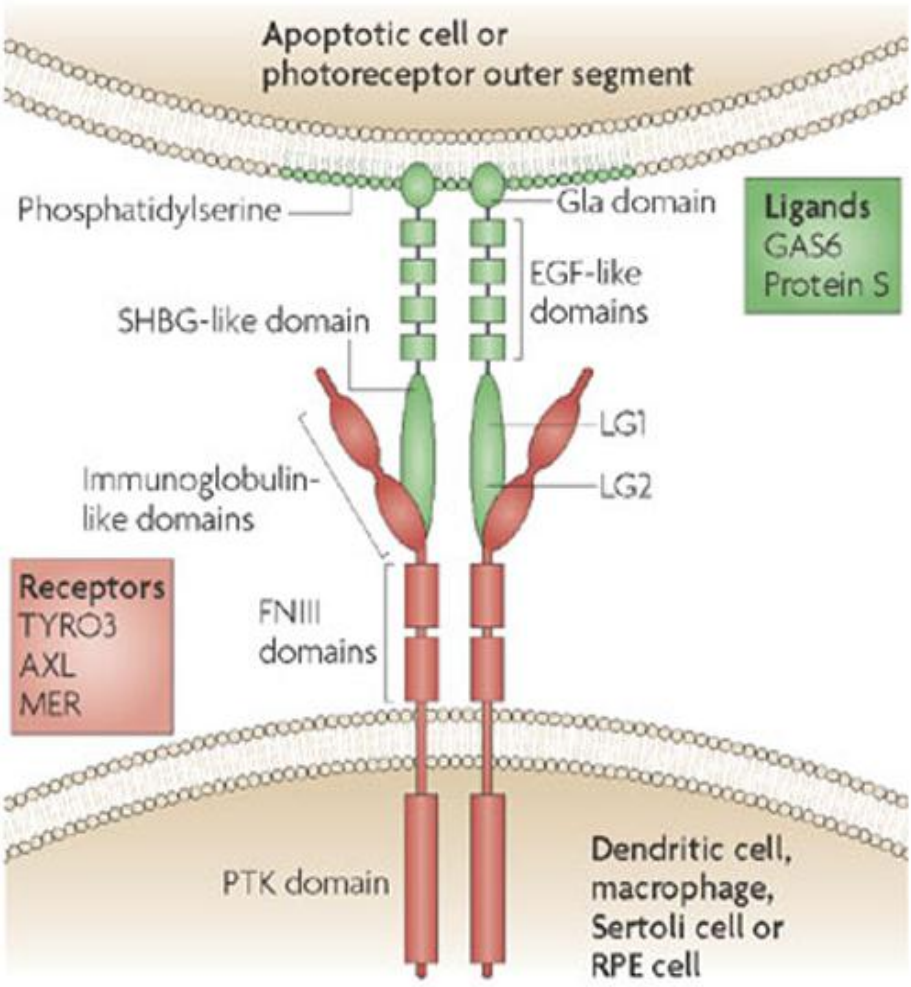

Figure I-4. Tyro/Axl/Mer receptor structure and ligand binding. Schematic of TAM receptor structure depicting the three domains present in this receptor family, including immunoglobulin-like, fibronectin type III (FNIII), and phosphotyrosine kinase (PTK) domains. Also shown are TAM receptor immunoglobulin-like domain interactions with the ligands protein S and Gas6 through sex hormone binding globulin (SHBG) like domains. The ligands are composed of three domains including two C-terminal laminin G (LG), epidermal growth factor-like, and Gla domains which bind to phosphatidylserine and serve to bridge the spent cell or membrane to the receptors. Both TAM receptors and ligands form dimers to execute activation. This figure is used with permission from [51].

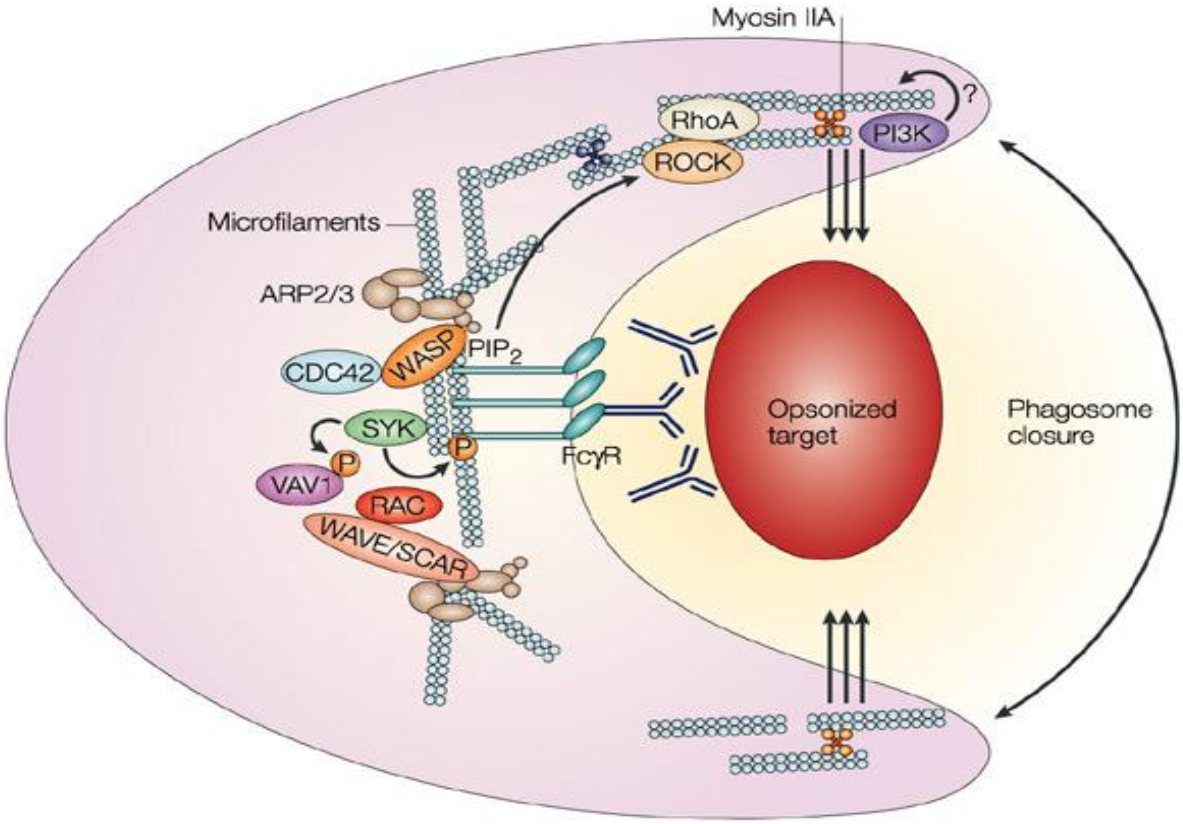

Figure I-5. Fcγ-receptor-mediated cytoskeletal rearrangement. Schematic showing Fcγ-receptor-mediated phagocytosis of opsonized particles. Particle recognition by FcγR results in activation of Syk intracellular tyrosine kinase and its tyrosine phosphorylation of Vav1, a guanine nucleotide exchange factor for Rac and Cdc42 GTPase. Rac and Cdc42 downstream effectors, including Wiskott-Aldrich syndrome protein (WASP) and WASP family verprolin-homologous protein (WAVE/SCAR), stimulate actin-related protein 2/3 (Arp2/3) to initiate actin polymerization. Further regulation of cytoskeletal rearrangement involves PI3K generation of PIP_2 that regulates WAVE and WASP. The Rho family GTPase Rho A and Rho-associated coiled-coil containing protein kinase (ROCK) regulate the activity of myosin IIA in phagosome closure. This figure is used with permission from [190].

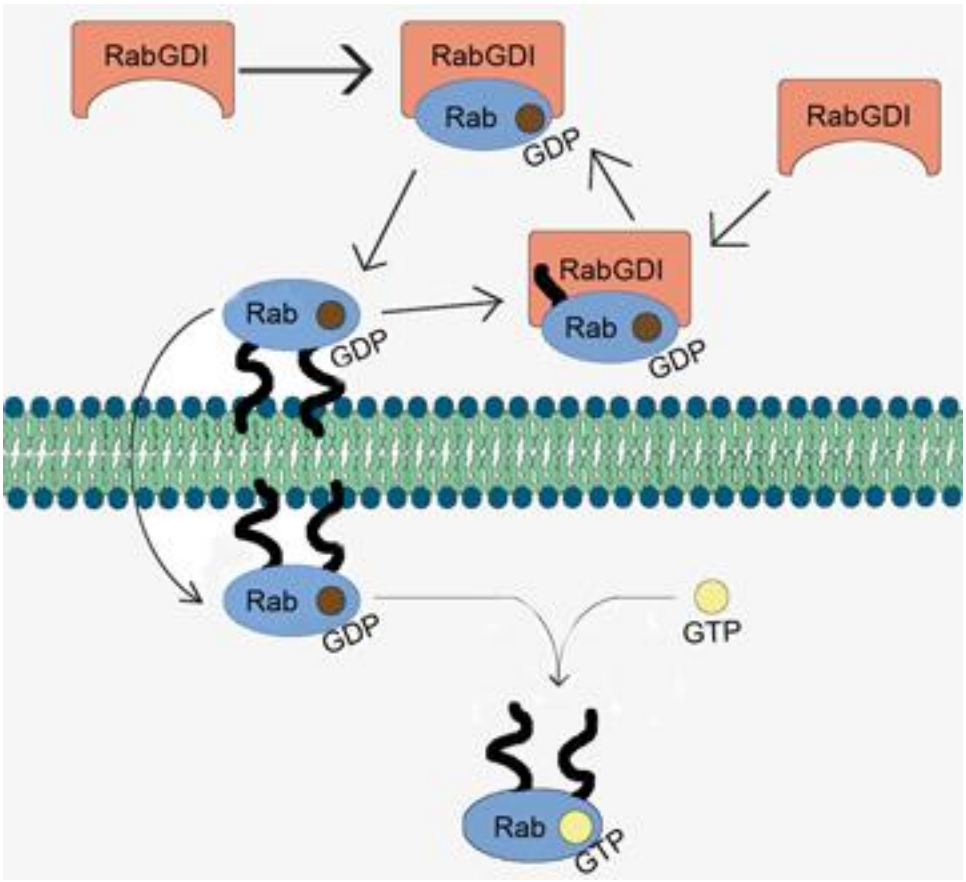

Figure I-6. Rab GTPase cycling mechanism. Schematic showing cycling of Rab GTPases between the membrane and cytosol facilitated by RabGDI. RabGDI recognizes and binds prenylated and GDP-bound Rab GTPases, thereby helping to stimulate GTP hydrolysis and their return to the originating membrane. Adapted from [191].

Chapter II

MERTK Interactions with SH2-Domain Proteins in the Retinal Pigment Epithelium

Abstract

The receptor tyrosine kinase MERTK plays an essential role in the phagocytic uptake of shed photoreceptor membranes by the retinal pigment epithelium (RPE). A fundamental aspect of signal transduction by receptor tyrosine kinases involves autophosphorylation of tyrosine residues that recruit Src-homology 2 (SH2)-domain proteins to the receptor intracellular domain. The goal of the current study was to evaluate the interactions of human MERTK with SH2-domain proteins present in the RPE. The MERTK intracellular domain was expressed as a 6xHis-fusion protein (6xHis-rMERTK$_{571-999}$), purified and phosphorylated. Ni^{2+}-NTA pull downs were performed using 6xHis-rMERTK$_{571-999}$ in incubations with recombinant phosphotyrosine-recognition sequences expressed as GST-fusion proteins. In addition, pull downs of native SH2-domain proteins were performed using 6xHis-rMERTK$_{571-999}$ with protein homogenates from rat RPE/choroid. In western analysis of the recovered proteins, MERTK interactions were detected with both recombinant and native GRB2, PIK3R1 (P85α), VAV3, and SRC. In cultured RPE-J cells incubated with rod outer

segments (OS), siRNA knockdown of Grb2 had no effect on OS binding, but significantly reduced OS uptake. P85α localized to early phagosomes along with Rab5 and Eea1. Phosphorylation and activation of Src was detected downstream of phagocytosis and Mertk activation. These findings suggest that MERTK signaling in the RPE involves a cohort of SH2-domain proteins with the potential to regulate cytoskeletal rearrangement and membrane movement. Identification of the SH2-domain signaling partners of MERTK is an important step toward further defining the mechanism of RPE phagocytosis that is central to the function and survival of the retina.

Introduction

Vertebrate photoreceptor cells function under conditions of high metabolic demand and light exposure that result in chronic damage to lipid and protein components of their specialized outer segment (OS) membranes [4]. As a result, photoreceptor cells undergo a process of continual renewal involving the addition of new membranes at the base of the OS just above the connecting cilium, and shedding spent membranes from the OS tips [14]. The retinal pigment epithelium (RPE) removes the shed debris from the subretinal space by phagocytic uptake [19], a process that is critical for photoreceptor cell survival, as these cells depend on close association with the RPE for oxygen and nutrients, and for ionic homeostasis of the subretinal space [22]. A key insight into the molecular mechanism of phagocytic uptake by the RPE resulted from the discovery that

inherited retinal degeneration in Royal College of Surgeons (RCS) dystrophic rats results from a deletion in the gene encoding Mertk [78]. As a consequence of this loss-of-function mutation, shed OS membranes can be bound but not taken up by the RPE [88]. Subsequent studies identified disease-associated mutations in the gene encoding human MERTK in individuals affected by a relatively rare form of juvenile-onset retinitis pigmentosa [82, 84, 192-194].

MERTK is a receptor tyrosine kinase belonging to the TAM receptor family (Tyro-3, Axl, Mer), whose ligands include the vitamin K-dependent proteins growth arrest-specific protein 6 (gas6) and protein S [44], as well as the retinal dystrophy-gene products Tulp1 and Tubby [195]. MERTK is expressed in monocytes and tissues of epithelial and reproductive origin [196] where it contributes to a number of cellular processes including cell proliferation and survival, down-modulation of pro-inflammatory signals, and clearance of apoptotic cells [79]. Studies of the mechanism of apoptotic clearance in transfected HEK-293T cells suggest that MERTK signaling involves cross-talk with αvβ5 integrin, resulting in activation of focal adhesion kinase (FAK) via Src family non-receptor tyrosine kinases(SFKs) [55]. Studies of MERTK interactions in the RPE also have suggested a role for myosin II in the phagocytic mechanism [89].

A central step in the MERTK signaling mechanism is the activation of receptor tyrosine kinase activity resulting in trans-autophosphorylation. Three tyrosine residues, Y-749, Y-753, and Y-754, present within the activation loop of

the (human) MERTK-kinase domain have been identified as sites of autophosphorylation [197]. Receptor tyrosine phosphorylation serves to generate docking sites for signaling molecules, including Src-homology 2 (SH2) domain proteins that function as enzymes and adapter proteins [52]. Previous studies of MERTK-associated proteins in myeloid cells identified interactions with multiple SH2-domain proteins [59, 61, 62]. The fundamental role of SH2-domain proteins in MERTK-downstream signaling suggests that they play an essential role in the mechanism of RPE phagocytosis. In the present study, analysis of expression, protein interactions, and functional assays have been used to identify SH2-domain proteins in the RPE with the potential to signal downstream of MERTK and upstream of cellular remodeling. The findings suggest that MERTK interacts with multiple signaling partners in the RPE, including SH2-domain proteins that regulate cytoskeletal rearrangement and membrane movement in other professional phagocytes.

Results

Development of study tools and focus

To identify potential MERTK-signaling partners in the RPE, expression analysis was coupled with a screening strategy that focused on candidate SH2-domain proteins selected from an extensive cDNA library encoding the corresponding phosphotyrosine-recognition sequences as GST-fusion proteins [52]. The recombinant human SH2-domains (rSH2-domains) were expressed in

E. coli and purified by GSH-affinity and size-exclusion chromatography. Constructs encoding the human MERTK cytoplasmic domain, $rMERTK_{571-864}$ [198] and $rMERTK_{571-999}$, were expressed in *E. coli* as 6xHis fusion proteins and purified using Ni^{2+}-NTA affinity and size-exclusion chromatography. To confirm autophosphorylation of tyrosine residues in the kinase domain, $rMERTK_{571-864}$ was subjected to analysis of tryptic peptides using MALDI/MS/MS. Ion fragmentation patterns for three peptides designated P1, P2, and P3 identified tyrosine phosphorylation of three sites in the catalytic domain, Y749, Y753, and Y754, in agreement with previously published data [197] (Figure II-1). To evaluate protein-protein interactions, Ni^{2+}-NTA pull downs were performed using $rMERTK_{571-999}$ (corresponding to the full-length MERTK intracellular domain) with purified rSH2-domain fusion proteins, as well as with rat RPE/choroid homogenates. Candidates for analysis included SH2-domain proteins previously implicated in MERTK downstream signaling, and expression in the RPE was evaluated at the transcript and protein level in cultured RPE-J cells, and in RCS congenic and dystrophic rats. The combined results led to a focus on protein families previously implicated in mechanisms of phagocytic uptake, including growth factor receptor-bound proteins (GRB), phosphatidylinositol 3-kinase regulatory subunit alpha (PIK3R1), vav proto-oncogenes (VAV), and SRC-family kinases (SFKs), as described in detail below.

GRB2

A key role of GRB proteins is their ability to function as adapters for GEF proteins involved in RAS activation of downstream kinases that regulate multiple

signaling processes and biological activities, including NF-κB control of inflammation and regulation of motor proteins involved in cellular movement [60, 199]. Previous studies in hematopoietic cells identified MERTK interactions with GRB2 [59], pointing to the importance of defining the role of GRB proteins in RPE phagocytosis. In the current study, semi-quantitative RT-PCR was used to evaluate expression in mouse RPE/choroid, retina, brain, and liver. Transcripts encoding Grb2 were seen at relatively high levels in RPE/choroid when compared to levels present in retina, brain, and liver (Figure II-2A). In contrast, transcripts encoding the Grb7 isoform were low in RPE/choroid and high in liver, whereas transcripts encoding the Grb10 isoform were high in RPE/choroid and retina, and low in liver. Assays of potential MERTK interactions using Ni^{2+}-NTA pull downs of 6xHis-rMERTK$_{571-999}$ incubated with rSH2-domain fusion proteins showed strong recovery of the recombinant GRB2 protein (Figure II-2B), which far exceeded that of recombinant GRB7 and GRB10, suggesting specificity in the interactions of MERTK with GRB isoforms. Analysis of endogenous protein expression on western blots showed strong Grb2 immunoreactivity in RPE/choroid from RCS congenic and dystrophic rats [75, 200], with less in the rat RPE-J cell line [72] (Figure II-2C). Pull downs of endogenous proteins from mouse RPE/choroid homogenates using 6xHis-rMERTK$_{571-999}$ resulted in specific recovery of Grb2 seen on western blots (Figure II-2D), and was not obtained using 6xHis-rMERTK$_{571-864}$ missing the C-terminal sequence (data not shown). Immunohistochemical analysis of retina/RPE/choroid cryosections from BALB/c mice confirmed the presence substantial *Grb2* expression in both the RPE and

neural retina, with marked immunoreactivity present in the interneuron and ganglion cell layers (Figure II-2E), consistent with the fundamental role of Grb2 in a wide range of signaling processes. Taken together, these findings demonstrate the ability of the current approach to capture MERTK interactions with endogenous proteins, and are consistent with previous studies showing GRB2 binding to MERTK-Y867 [59].

Grb2 effects on RPE phagocytosis

To evaluate the effect of Grb2 loss-of-function on RPE phagocytosis, siRNAs were used to deplete *Grb2* transcripts in sub-confluent rat RPE-J cells, followed by quantitative assays of OS binding and uptake. Transient transfection of RPE-J cells with a pool of four Grb2 targeting siRNAs resulted in efficient knockdown at both the transcript and protein level (Figure II-3A, B). In contrast, *Grb2* expression was retained in cells transfected with a control non-targeting siRNA. Equivalent levels of Mertk and β-actin were present in both treated and control cells. Furthermore, phalloidin staining of the actin cytoskeleton, and immunostaining with antibodies against the ZO-1 protein present in tight junctions showed little disruption of cellular integrity (Figure II-4A). In assays of phagocytic uptake using bovine OS labeled with AlexaFluor 555, RPE-J cells treated with *Grb2* targeting siRNAs exhibited significantly less activity (~60% at the 6 h time point) than cells treated with control non-targeting siRNA ($p < 0.0005$) (Figure II-3C, D). In both cases, OS binding was unaffected ($p > 0.05$). Taken together, these findings support the view that the interaction of endogenous Grb2

with MERTK contributes, directly or indirectly, to the phagocytic activity of the RPE.

PIK3R1

Stimulation of phosphoinositide-3-kinase (PI3K) activity by activated receptor tyrosine kinases plays a central role in downstream signaling mechanisms, including those involved in regulating inflammatory responses [201, 202]. Analysis of the expression of the PI3K regulatory subunit (*Pik3r1, P85α*) in mouse tissues showed that transcript levels were relatively high in RPE/choroid compared to levels in retina and brain (Figure II-5A). Ni^{2+}-NTA pull downs with 6xHis-rMERTK$_{571-999}$ showed specific recovery of a PIK3R1-fusion protein corresponding to the SH2-domain present in the amino-terminal half of the regulatory subunit (PIK3R1-N), which was not seen with a fusion protein corresponding to the SH2-domain present in the carboxy-terminal half (PIK3R1-C)(Figure II-5B). Western analysis showed equivalent levels of Pik3r1 protein in RPE/choroid from congenic and dystrophic rats, and higher levels in RPE-J cells (Figure II-5C). Pull downs of 6xHis-rMERTK$_{571-999}$ incubated with RPE/choroid homogenates showed specific recovery of the endogenous Pik3r1 protein from both congenic and dystrophic samples (Figure II-5D). Immunohistochemistry on mouse retina/RPE/choroid cryosections showed strong Pik3r1 immunoreactivity in the RPE and photoreceptor inner segments, and less intense labeling present in the inner retina (Figure II-5E). Taken together, these results are the first to

demonstrate a direct interaction of MERTK with PI3K *in-vitro* and with native RPE protein.

PI3K in the early phagosome

Previous studies have shown that PI3K participates in early events necessary for phagosome formation and maturation [203]. To investigate the role of Pik3r1 relative to phagosome formation in the RPE, cultured RPE-J cells were incubated with or without bovine rod OS, and indirect immunofluorescence microscopy was performed using antibodies against Pik3r1, as well as two markers for phagosome formation: early endosomal antigen 1 (Eea1) and Rab5 GTPase [202]. Localization of Eea1 and Rab5 with ingested OS was shown by co-labeling with rhodopsin (Figure II-6) In control cells without added OS, the labeling of Pik3r1 appeared diffuse, Eea1 was seen in small discrete vesicles distributed throughout the cytoplasm (Figure II-7A), and Rab5 appeared in a widespread punctate pattern (Figure II-7B). In RPE-J cells incubated with rod OS, Pik3r1 was seen to co-localize with Eea1 in vesicular structures surrounding the ingested material (Figure II-7A). These structures were similar in appearance to those showing colocalization of Eea1 with Rab5 (Figure II-7B), consistent with the role of Rab5 as a PI3K effector and established participant in early endosome/phagosome formation [204]. The finding that Pik3r1 can engage in direct interaction with rMERTK in the RPE, and also colocalizes with an early phagosome marker, suggests that PI3K activity plays a role in the initial steps of phagosome formation in the RPE.

VAV proteins

The VAV family of proteins, VAV1, VAV2, and VAV3 serve as guanine nucleotide exchange factors (GEFs) for Rac1 GTPase that contributes to cytoskeletal rearrangement through effects on actin polymerization [40]. Previous studies reported that VAV1 undergoes interaction with MERTK independent of receptor phosphorylation status [62]. In the current study, analysis of expression in mouse RPE/choroid showed transcripts encoding all three Vav isoforms (Figure II-8A). Pull-down assays with 6xHis-rMERTK$_{571-999}$ showed interaction with rSH2-domain fusion proteins corresponding to VAV1 and VAV3, but not VAV2 (Figure II-8B). Western analysis showed both Vav1 and Vav3 were present in protein homogenates of RPE/choroid from congenic and dystrophic rats, but not RPE-J cells (Figure II-8C). Pull downs from RPE/choroid homogenates showed interaction of 6xHis-rMERTK$_{571-999}$ with endogenous Vav3, but not with Vav1 (Figure II-8D). Immunohistochemical analysis of retina/RPE/choroid cryosections showed punctate localization of Vav3 in the RPE, and diffuse labeling in the inner retina (Figure II-8E). Viewed together, these findings suggest that the association of VAV3 comprises the predominant MERTK interaction occurring with VAV family members in the RPE.

SRC

SFKs are intracellular tyrosine kinases that act downstream of receptor activation to powerfully impact signaling. SFKs have been shown to play a role in apoptotic cell clearance by dendritic cells [61] and to contribute to

immunoreceptor signaling activated upon particle uptake [205]. In the current study, analysis of expression in mouse RPE/choroid identified transcripts encoding nearly the entire Src family, including Src, *Fyn*, *Fgr*, *Yes*, *Hck*, *Lyn*, and *Lck* (Figure II-9A). Transcripts encoding *Hck*, *Fyn*, and *Yes* appeared to be relatively more abundant in RPE/choroid versus retina. Pull-down assays with 6xHis-rMERTK$_{571-999}$ showed specific interaction with the rSH2-domain fusion proteins corresponding to SRC and HCK (Figure II-9B). Western analysis showed that Src was present in the RPE/choroid from congenic and dystrophic rats, and RPE-J cells, while Hck protein levels were significantly lower in each case (Figure II-9C). However, rMERTK$_{571-999}$ pull downs with RPE/choroid homogenates from congenic and dystrophic rats showed interaction with endogenous Src, but interaction with Hck was not detected (Figure II-9D). Immunohistochemical analysis of Src showed strong labeling throughout the RPE, as well as the inner retinal layer (Figure II-9E). In the RPE, significant labeling extended toward the apical microvilli. These results suggest that Src is a candidate for direct interaction with MERTK and the regulation of downstream effects on RPE function.

SRC activation downstream of MERTK

Previous studies of apoptotic cell clearance have proposed that SFKs facilitate crosstalk between MERTK and αvβ5 integrin in downstream signaling to RAC1 involved in cytoskeletal reorganization [55, 63, 72], however, the mechanistic details and the specific SRC-family member involved have not been elucidated. In the current study, the activation status of SRC was evaluated using

an antibody that recognizes the active form of the protein that is phosphorylated on tyrosine residue 416 (pY416). This analysis showed formation of pY416 SRC in HEK-293T cells transfected with active full-length MERTK, but not with kinase-dead MERTK (Figure II-10A). In addition, formation of pY416 Src was seen in the RPE/choroid of congenic RCS rats sacrificed during peak phagocytic uptake, but not those sacrificed before light onset, and was not found in dystrophic rats sacrificed at either time (Figure II-10B). pY416 Src was also seen in RPE-J cells incubated with rod OS, appearing highest at 30 and 45 min post feeding (Figure II-10C). At corresponding times, a decrease in Mertk immunostaining was also seen. As the blots were probed with antibody specific for the receptor C-terminal sequence [78], this decrease likely reflects loss of the C-terminal fragment (60 kDa) as a result of proteolysis initiated by activation of MERTK that is notable for releasing the soluble N-terminal ectodomain [206, 207]. Viewed together, these findings suggest that SRC activation in the RPE can result from direct interaction with activated MERTK, but leave open the possibility that additional SFKs may function downstream of MERTK signaling.

Discussion

Phagocytic uptake by the RPE requires multiple activities that regulate cellular plasticity, including cytoskeleton reorganization and membrane remodeling, and also contribute to down-modulating pro-inflammatory responses. Although not required for binding of effete membranes, MERTK signaling is

essential for initiating phagocytic uptake. The current studies show that MERTK interactions in the RPE/choroid and other phagocytic cell types involve an overlapping set of core SH2-domain proteins that are not down regulated in response to MERTK loss-of-function in the RCS rat. These findings lead to a new appreciation of the phagocytic mechanism adapted to the highly-specialized function of the RPE.

Changes in actin polymerization needed for cytoskeletal reorganization are regulated by members of the Rho family of GTPases, including the small G-proteins Rac1, Cdc42, and RhoA [29]. Activation of Rho family GTPases requires interaction with guanine nucleotide exchange factors (GEFs) necessary for GDP/GTP exchange [40]. These include the VAV family of SH2-domain proteins that act as GEFs for Rac1 involved in regulating F-actin recruitment. Previous studies in macrophages showed that VAV1 interacts with MERTK independent of its phosphorylation status [62]. In the current studies, both VAV1 and VAV3 were shown to interact with MERTK as recombinant proteins, but only native Vav3 was found to interact in assays of endogenous rat RPE proteins. Vav3 was also the major isoform seen in the RPE using immunohistochemical analysis. In contrast, expression of VAV family proteins was not detected in cultured RPE-J cells that retain the capacity to perform MERTK-mediated phagocytic uptake. In addition, previous studies of Vav2/3 knockout mice have shown that Vav loss of function results in a glaucoma phenotype, but not retinal degenerative disease [208]. Taken together, these findings are consistent with the view that direct activation of VAV proteins by MERTK is not essential for the uptake phase of phagocytosis,

but likely fulfills another signaling role downstream of MERTK activation in the RPE.

Recent studies have shown that RAC1 activation occurs downstream of αvβ5 integrin, but does not require MERTK, suggesting that integrin signaling through the CRKII/p130CAS/DOCK180/ELMO complex is the primary mechanism involved in activating RAC1 in the RPE [63]. A model of MERTK mediated phagocytosis based on these studies invokes the involvement of SFKs in crosstalk between MERTK and αvβ5 integrin in regulating downstream signaling to RAC1 [55, 63, 72, 209]. Crosstalk between integrins, Rho-family GTPases, and SFKs is well documented in signaling involved in cellular adhesion [210]. The current studies establish that MERTK interacts with recombinant SRC, as well as with endogenous Src in the rat RPE. In addition, activation of MERTK promotes Src activation as evidenced by phosphorylation of Y416. Transcripts encoding the known mammalian SFKs, with the exception of *Blk*, were detected in mouse RPE/choroid. This suggests there are multiple opportunities for SFKs to directly participate in MERTK signaling in the RPE, including crosstalk with integrins involved in cytoskeletal reorganization. This mechanism also has the potential to make significant contributions to cellular motility, in that SFKs are important in regulating other Rho family GTPases, including RhoA which functions to induce actomyosin contractility [211].

Myosin motor proteins responsible for actin motility are an important driving force in phagosome formation [36]. In the RPE, myosin II has been shown to interact with MERTK and contribute to phagosome formation [89], whereas

myosin VIIa has been implicated in phagosome trafficking [151]. Previous studies of MERTK-associated proteins in hematopoietic cells identified the adapter protein GRB2 [59] and established that this interaction is a prerequisite for phagocytic clearance of apoptotic cells [60]. In addition, GRB2 signaling to myosin and dynamin via the RAS pathway has been shown to induce membrane ruffling and cell migration [212]. The current studies show that MERTK interacts with endogenous Grb2 present in the RPE. Consistent with previous findings that Y867 is required for the interaction of recombinant MERTK and GRB2 [59], native Grb2 was found to interact with the full-length rMERTK$_{571\text{-}999}$ intracellular domain, but not with rMERTK$_{571\text{-}864}$. In addition, knockdown of Grb2 was found to inhibit the phagocytic uptake of ROS by RPE-J cells in culture, although it was not established whether this was due to a direct effect on the phagocytic mechanism or other aspects of cell function and viability. Taken together, these findings point to a conserved role for GRB2 in apoptotic cell clearance, endocytosis, and RPE phagocytosis.

In phagocytic uptake by macrophages, formation of the phagocytic cup as well as phagosome maturation require the involvement of both class I and III PI3Ks [203]. In Fc-receptor signaling, one role of PI3K is to generate the phosphoinositides that recruit RAB5 GTPase and early-endosomal markers (including EEA1) to the phagosome [201, 202, 204]. Previous studies using the PI3K inhibitors wortmannin and LY294002 have shown that loss of PI3K activity inhibits RPE phagocytosis [90]. In hematopoetic cells, the PIK3R1 regulatory subunit of class I PI3K has been shown to interact indirectly via GRB2 with a

FMS-MERTK chimera [59]. In the current studies, recombinant MERTK was shown to interact with endogenous Pik3r1, but the possibility that endogenous Grb2 contributed to this interaction cannot be excluded. However, studies using purified recombinant proteins also showed that PIK3R1 interacts with the $rMERTK_{571-999}$ intracellular domain. The site of this interaction, as well as those of VAV3 and SRC, are not predicted using various algorithms [213] and remain to be experimentally determined. Taken together, these findings suggest that PI3K can undergo both direct and indirect interactions with MERTK. The finding that Pik3r1 colocalizes with both Eea1 and Rab5 GTPase in phagosomes formed during uptake of OS by RPE-J cells suggests that this mechanism is conserved among professional phagocytes.

In immune cells, an important role of MERTK is to dampen pro-inflammatory responses resulting from apoptotic cell binding [214]. This is accomplished in part by GRB2 and PI3K signaling downstream of autophosphorylation of MERTK-Y867 that results in down regulation of NF-κB [59, 60]. Studies in dendritic cells also have shown that SRC signaling downstream of MERTK plays an important role in immunomodulation [61]. The finding that GRB2, PI3K, and SRC likely contribute to MERTK signaling in the RPE raises the important possibility that this mechanism plays a critical role in controlling inflammatory responses elicited by OS uptake, as well as those associated with aging and disease.

Establishing the identities of MERTK-interacting SH2-domain proteins in the RPE provides new insight into downstream signaling potentially linked to

various aspects of the phagocytic mechanism. The role of MERTK loss-of-function in inherited retinal degeneration suggests that key signaling partners may be candidates for involvement in this group of diseases. Thus, increased knowledge of the phagocytic mechanism has the potential to advance our understanding of the causes of RPE dysfunction occurring in aging and disease, as well as to further efforts to develop targeted therapeutic strategies to improve RPE function.

Materials and methods

Animals

Experimental procedures involving animals were performed in accordance with the guidelines and under the approval of the University Committee on Use and Care of Animals at the University of Michigan, and were in compliance with the statement for ethical care and use of animals of the Association for Research in Vision and Ophthalmology (ARVO). C57BL/6J and BALB/C mice were bred from animals obtained from the Jackson Laboratories. Pigmented dystrophic (RCS-*p*+) and non-dystrophic (RCS-*rdy*+*p*+) rats were bred from the strains described in [75, 200]. Mice and rats were housed in a 12-h/12-h light–dark cycle (~300 lux room light) and were euthanized by CO_2 inhalation approximately 2 h after light onset, at a time when levels of RPE phagocytic uptake are near maximal [28].

Materials

Primary antibodies: GRB2, Santa Cruz Biotechnology; PIK3R1, VAV1, VAV3, and HCK, Millipore; c-SRC, pY416 SRC, and EEA1, Cell Signaling Technology; GAPDH, Ambion; β-actin and RAB5, Abcam. AlexaFluor 555, AlexaFluor 488-conjugated anti-rabbit IgG, AlexaFluor 555-conjugated anti-mouse IgG, and Sybr safe were from Invitrogen. Complete protease inhibitors, PhosSTOP phosphatase inhibitors, Fugene transfection reagent, and AmpliTaq Gold polymerase were from Roche Diagnostics. Ni^{2+}-NTA resin, RNeasy kit, Superscript II, and oligo-dT were from Qiagen. RPE-J and HEK-293T cells were from ATCC. Other chemicals and reagents were from Sigma. The pcDNA 3.1+ expression vectors encoding full-length MERTK and kinase-dead R844C-MERTK have been previously described [84].

RT-PCR analysis of SH2-domain protein expression

Total RNA was isolated from freshly-dissected RPE/choroid, retina, liver, and brain from C57BL/6 mice using the RNAeasy kit, and first-strand cDNAs were generated using Superscript II and oligo-dT. Sequences encoding SH2-domain proteins of interest were amplified with gene-specific primers flanking at least one intron in the genomic sequence (Table S1), using AmpliTaq Gold polymerase and the following cycling conditions: 1 cycle at 95°C for 10 min, followed by 28 cycles at 95°C for 2 min, 60°C for 45 sec, 72°C for 2 min. Primers for hypoxanthine-guanine phosphoribosyltransferase (Hprt) served as a control. PCR products were analyzed by electrophoresis on agarose gels stained with

Sybr safe. Comparisons of the relative levels of different gene products were made using the same RT reaction in amplifications containing a single pair of primers.

Western analysis of SH2-domain protein expression

Dissected samples of RPE/choroid from dystrophic and congenic RCS rats were harvested at times corresponding to peak phagocytic uptake [28], and confluent cultures of the rat RPE-J cell line that retains Mertk expression [72] were harvested after 3 days in culture. Tissues and cells were homogenized in 20 mM MOPS, 2 mM EGTA, 5mM EDTA, 1% Triton X-100, 1mM DTT, protease and phosphatase inhibitors; cellular debris was removed by low speed centrifugation; and protein concentrations of the supernates were determined using a modification of the Lowry method [215]. Protein samples (7.5 µg) were dissociated in 1xSDS sample buffer, electrophoresed on 10% polyacrylamide gels, and transferred to nitrocellulose. Blots were blocked and incubated with primary antibodies specific for SH2-domain proteins of interest, then with alkaline phosphatase-conjugated secondary antibodies, and developed using 5-bromo-4-chloro-3'-indolyphosphate p-toluidine and nitro-blue tetrazolium chloride.

Immunohistochemical analysis

Eyes from BALB/c mice perfused with 4% paraformaldehyde were washed with PBS, transitioned to sucrose/OCT, and flash frozen. Retinal cross sections (10 µm) were washed with PBS and permeabilized with PBS-T (0.125% Triton X-100); blocked with 1% bovine serum albumin, 10% normal goat serum, and

0.125% Triton X-100; and incubated with primary antibodies for 2 h, then with fluorophore-conjugated secondary antibodies for 1 h. Species and dilutions of primary antibodies were as follows: Rabbit anti-Grb2 (1:300), anti-Pik3r1 (1:300), anti-Vav3 (1:300), anti-Src (1:300), anti-Rab5 (1:300); Mouse anti-Eea1 (1:300); AlexaFluor 488 anti-rabbit IgG (1:500); AlexaFluor 555 anti-mouse IgG. Images were obtained by confocal fluorescence microscopy (Leica SP5). For immunohistochemistry with RPE-J cells, the cultures were challenged with isolated bovine rod OS [216], washed 3 times with PBS, and fixed with 4% paraformaldehyde for 30 min at room temperature. The cells were then processed using the same methods as for retinal cross sections.

rSH2-domain protein expression and purification

GST-tagged constructs in pGEX2T vectors encoding the phosphotyrosine-recognition sequences of SH2-domain proteins were previously generated from a library representing nearly the complete set of known SH2-domain proteins [217]. The constructs were transformed into BL21 DE3 Gold bacteria and large scale cultures were grown in Terrific Broth with glycerol plus ampicillin at 37°C to an OD_{600} of 0.8. Isopropyl β-D-1-thiogalactopyranoside (final concentration 0.1 mM) was added and the cells were incubated at 15°C overnight. The cells were pelleted and resuspended in phosphate buffered saline and lysed by French press. Glutathione-agarose beads were incubated with cleared lysates for 1 h at 4^{o}C, washed with 10 volumes of PBS- 1% TritonX100, and eluted with buffer containing 8 mM glutathione, 50 mM Tris-HCl, pH 9.5. Fractions were collected

and analyzed on SDS gels, and those containing rSH2-domains were pooled, concentrated to 1 mL, and loaded on a Sephacryl S-200 HR column (21 x 1 in). Fractions were collected at a rate of 0.5 mL/min, analyzed on SDS gels, and those containing purified rSH2-domains were pooled and concentrated.

rMERTK expression and purification

Two His-tagged expression constructs encoding the human MERTK cytoplasmic domain, amino acid residues 571 to 864 (6xHis-rMERTK$_{571-864}$) [23] and 571 to 999 (6xHis-rMERTK$_{571-999}$), in the pET28a-LIC vector were amplified in bacterial cells as described above for rSH2-domains, with kanamycin replacing ampicillin in the cultures. Cells were pelleted and resuspended in lysis buffer containing 50 mM Tris-HCl, 500 mM NaCl, 5% glycerol, 1 mM β-mercaptoethanol, 2 mM imidazole, and 200 µM phenylmethylsulfonyl fluoride (PMSF) at pH 8, and lysed by French press. Ni^{2+}-NTA resin was incubated with cleared supernatants with shaking for 1 h at 4^{o}C, washed with 10 volumes of 10 mM imidazole in lysis buffer, and eluted with 200 mM imidazole in lysis buffer. The eluate was concentrated to 1 mL, chromatographed on Sephacryl S-200 HR as described above, evaluated on SDS gels, pooled, and concentrated. Recombinant MERTK was autophosphorylated by incubating with 10 mM ATP, 10 mM $MgCl_2$ in gel filtration buffer at room temperature for 3 h and was stored at -80°C.

Phosphotyrosine analysis by MALDI/Mass Spectrometry

Purified, phosphorylated 6xHis-rMERTK$_{571-864}$ was digested by addition of porcine trypsin in 50 mM ammonium bicarbonate, 0.05% SDS, and incubated overnight at 37°C. The digested peptides were subjected to TiO_2 selection to enrich for phosphorylated peptides and evaporated to dryness in a SpeedVac. The sample was dissolved in 5 µL 60% Acetonitrile and 0.1% Trifluoroacetic acid. 1 µL of sample was spotted on MALDI target plates and peptides were separated by liquid chromatography. Phosphopeptide analysis of the separated peptides was performed using a 4700 MALDI TOF/TOF mass spectrometer (Applied Biosystems) with peptide mass analysis using UniProt by the University of Michigan Protein Core Facility.

rMERTK pull downs of rSH2-domains and native SH2-domain proteins

Purified GST-tagged-rSH2-domain proteins (10 µg) were incubated with 6xHis-rMERTK$_{571-999}$ (10 µg) in 50 mM NaH_2PO_4, 300 mM NaCl, 10 mM imidazole, and 0.1 µM PMSF for 1h at 4^{o}C. 50 µL of Ni^{2+}-NTA resin slurry was added and the incubation was continued for an additional 0.5 h. The beads were collected by brief centrifugation, washed three times in binding buffer including 50 mM imidazole, and eluted with binding buffer containing 500 mM imidazole. Negative controls omitted the 6xHis-tagged-rMERTK$_{571-999}$. For native tissue, protein homogenates from RPE/choroid were obtained as described for western analysis. Ni^{2+}-NTA pull downs of the protein homogenates with 6xHis-tagged-rMERTK$_{571-999}$ (10 µg) were performed as described above.

Cell culture and transfections

HEK-293T cells were maintained in DMEM supplemented with 10% FBS, 1 mM sodium pyruvate, and 1 mM penicillin/streptomycin at 37°C in 5% CO_2. HEK-293T cells were transiently transfected with full-length MERTK and kinase-dead R844C-MERTK using FuGENE as recommended (Roche). Rat RPE-J cells were maintained in Dulbecco's modified Eagle's medium (DMEM) supplemented with 4% fetal bovine serum (FBS), and 1 mM non-essential amino acids at 33°C in 5% CO_2. Rat Grb2 siRNAs were obtained as a Smartpool (Thermo Scientific) containing mixtures of four different duplexes to minimize silencing of unintended targets. ON-TARGET plus non-targeting siRNA (at the same concentration as the total pool of targeting siRNAs) served as a negative control. RPE-J cells (32,000 cells per well) were passaged into eight-well chamber slides, and 24 h later each well was transfected with 0.5 µg of the siRNAs plus 3.75 µL of DharmaFect 3 transfection reagent as recommended (Dharmacon). The cells were incubated with the siRNAs for 48 h, the medium was changed, and 24 h later the cells were transfected a second time and incubated for an additional 24 h. Cell viability was assessed by trypan blue staining, and was equivalent in cultures treated with targeting and non-targeting siRNAs. Phagocytosis assays were performed 5 days after siRNA transfection.

Phagocytosis assays

Rod OS were isolated from bovine eyes [216] and covalently labeled with AlexaFluor 555 [68]. RPE-J cells were cultured for 6 days in eight-well chamber slides, and then incubated with 10 OS per cell for 4 h at 33°C. Unbound OS were

removed by washing the cells 3 times with PBS containing 0.2 mM $CaCl_2$ and 1 mM $MgCl_2$, and the cells were fixed in 4% paraformaldehyde. To distinguish total and bound OS, duplicate samples were incubated before fixation with 0.2% trypan blue to quench fluorescence [218] as shown in supplementary Fig. 2B. Slides were mounted using Prolong Gold containing DAPI, and were visualized by fluorescence microscopy (Eclipse E800; Nikon). Images were taken from 10-12 random fields (0.100 mm^2 per field) for each group. OS with a diameter of at least 2 μm were quantified manually per viewing field. Counts of ingested AlexaFluor 555-labeled OS were obtained from trypan blue treated samples, while total OS counts (bound plus ingested) were obtained from duplicate untreated samples. For each condition, assays were repeated three times and results represented as a mean ± standard error.

Outside Contributions: Kecia Feathers generated RNA for RT-PCR samples. Lin Jia prepared sections for immunohistochemical staining. Xudong Huang generated constructs for $rMERTK_{571-999}$ and purified protein for $rMERTK_{571-898}$. Christina McHenry generated constructs for MERTK wild-type and the MERTK R844C mutant. Tony Pawson and Karen Colwill provided expression constructs for rSH2-domain proteins. Phosphotyrosine analysis of $rMERTK_{571-898}$ was conducted by the University of Michigan Protein Core Facility.

Gene	Forward primers 5’ to 3’	Reverse primers 3’ to 5’
Grb2	GCCATCGCCAAATATGACTT	GAGCATTTCTTCTGCCTTGG
Grb7	CAGCGCAGCCATTCATCGCA	TGGCTCTCCCGGACCAGGAAC
Grb10	ATGCCTGGCGTAAGCGGAGC	AGGTCTGCCCATCATCCTCGCA
PI3K(p85)	GTGGCTGGGGAATGAAAATA	CCGGTGGCAGTCTTGTTAAT
Vav1	CTACGGGATCTGCTGATGGT	CTGCCGTAGGGTTTCATTGT
Vav2	GCGAGAAGGTGATGTGGTGAAG	TAGGGCAGGTGATGGTGGAA
Vav3	TTTCTGAGACGGATGGAAGG	ATGGAAGAGCCGAGTTGTCA
Src	TACACAGCCCGGCAAGGTGC	TCATGCAGGGACTCGGGGCA
Fgr	CGTGTGGTCCTTTGGGATTCTG	AGGCTGGTACTGTGGTTCTGTGGA
Fyn	ACACAGCAAGACAAGGTGCGAAGT	TCGTGCAGGGAGATCGGGCA
Yes	GCTGCTCAGATCGCTGATGGCA	GCCTCAGGAGCTGTCCACTTGA
Hck	CACCAAAGGGAGCTACTCGT	TCTTTCTCCCATGGCTTCTG
Lyn	TAGAAGAGCATGGGGAATGG	GAAAGCTCCTGCACTGTTCC
Lck	GGCAGCCCAGATTGCAGAGGG	GGGATTCGACCGTGGGTGACG
HPRT	CAAACTTTGCTTTCCCTGGT	CAAGGGCATATCCAACAACA

Table II-1. PCR primer sequences used to amplify transcripts encoding SH2-domain proteins.

A

	Position	Sequence	Mass (Da)
P1	748 – 755	IpYSGDYpYR	1323.7
P2	748 – 759	IYSGDpYYRQGR	1457.6
P3	748 – 759	IYSGDpYpYRQGR	1537.6

B

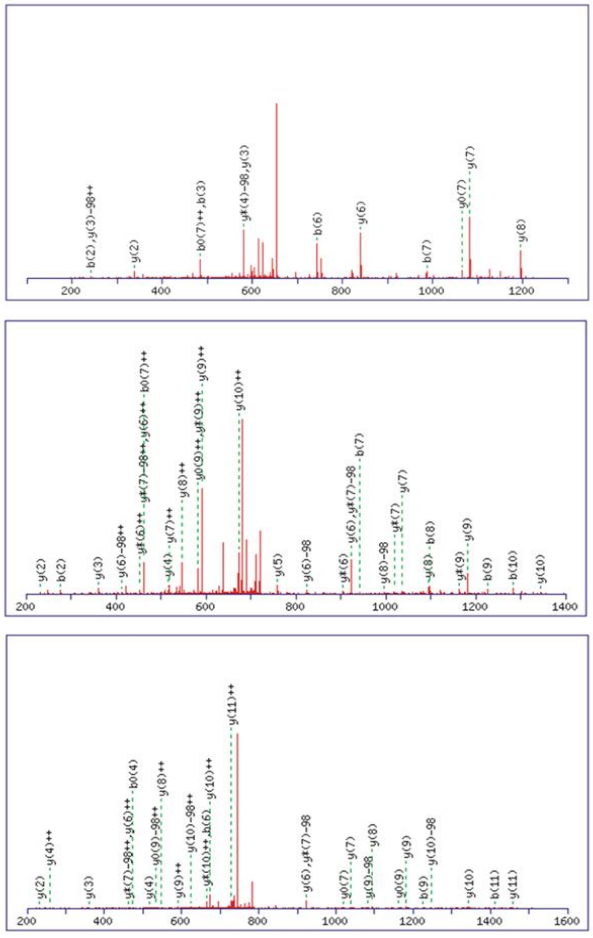

Figure II-1. Ion fragmentation patterns for MALDI-MS/MS phosphopeptide analysis. Purified 6xHis-rMERTK$_{571 – 864}$ was autophosphorylated by addition of ATP and digested by addition of porcine trypsin. Phosphopeptides were selected by TiO_2 enrichment and separated by LC and subjected to MALDI-MS/MS analysis. (A) Summary of peptides sequenced by MALDI/MS/MS analysis. (B) Ion fragmentation data for fragments P1, P2, and P3 are shown. Peaks labeled with the letter “b” followed by numbers correspond to fragments with masses that have matches in the UniProt database. Autophosphorylation was detected at three sites in the catalytic domain of human MERTK (Y749, Y753, and Y754) in agreement with Ling et al. [197].

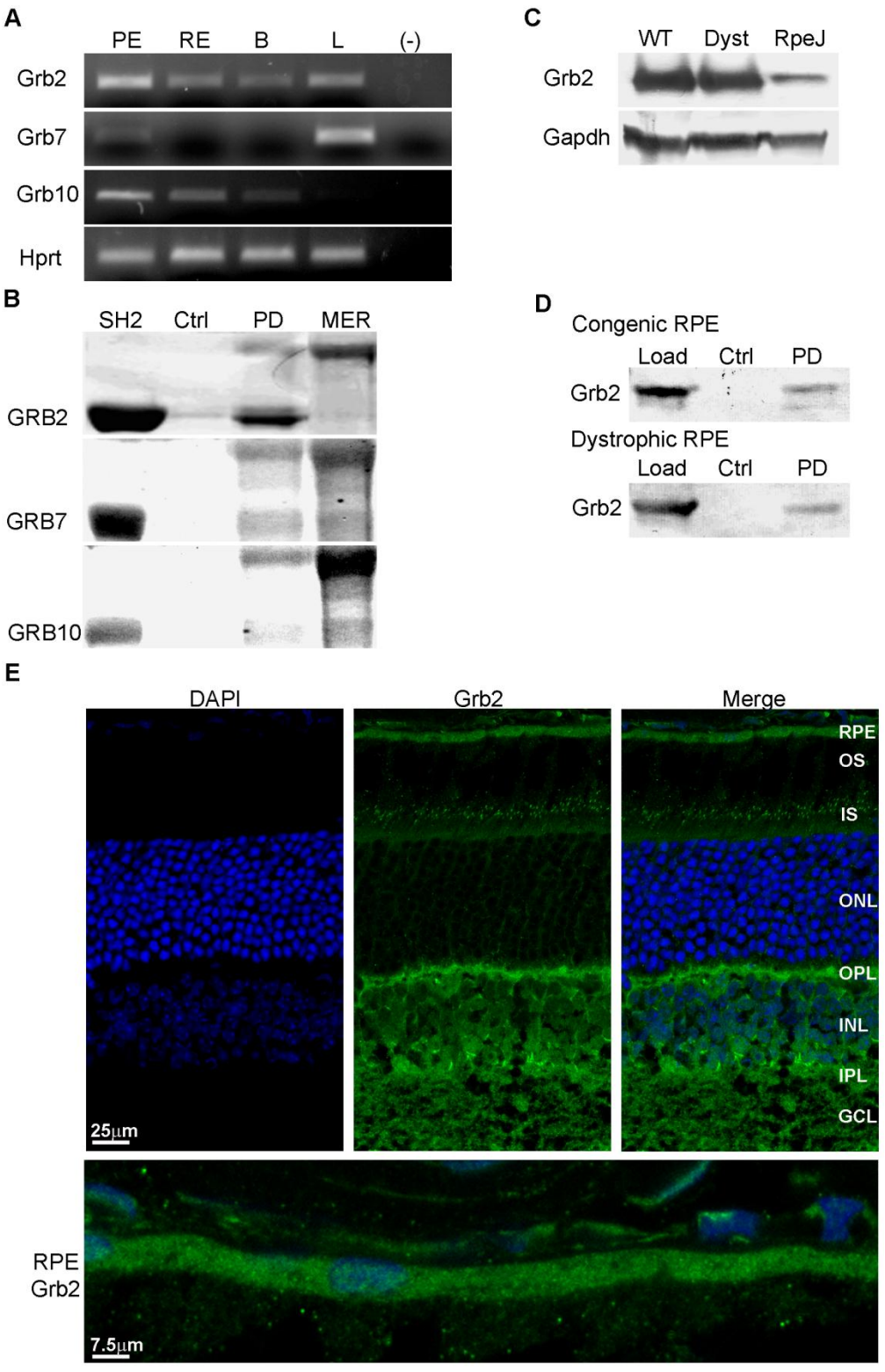
A
PE
RE
B
L
(-)
Grb2
Grb7
Grb10
Hprt
C
WT
Dyst
RpeJ
Grb2
Gapdh
B
SH2
Ctrl
PD
MER
GRB2
GRB7
GRB10
D
Congenic RPE
Load
Ctrl
PD
Grb2
Dystrophic RPE
Load
Ctrl
PD
Grb2
E
DAPI
Grb2
Merge
RPE
OS
IS
ONL
OPL
INL
IPL
GCL
25μm
RPE
Grb2
7.5μm

Figure II-2. Grb2 is expressed and interacts with MERTK in the RPE. (A) *Grb* and *Hprt* transcripts amplified by RT-PCR from mouse RPE/choroid, retina, brain, and liver total RNA. Hprt primers served as control. PE, RPE/choroid; RE, retina; B, brain; L, liver; (-), no cDNA. (B) 6xHis-rMERTK$_{571-999}$ and GRB GST-SH2-domains were purified from *E. coli* and their interactions evaluated using Ni^{2+}-NTA pull downs. Coomassie blue-stained proteins of SDS gels are shown. SH2, GRB GST-SH2 domain loading control; Ctrl, negative control omitting rMERTK; PD, pull down of GRB SH2-domain and rMERTK$_{571-999}$; MER, rMERTK$_{571-999}$ loading control. (C) Grb protein immunoreactivity on western blots of RPE/choroid protein homogenates from 4 wk old RCS congenic and dystrophic rats at 2 h post light-onset, and of RPE-J cell homogenates, probed with antibodies specific for Grb2. WT, congenic RCS-rat RPE/choroid; Dyst, dystrophic RCS-rat RPE/choroid; RpeJ, RPE-J cells. (D) Ni^{2+}-NTA pull downs of endogenous proteins from RPE/choroid homogenates from RCS congenic and dystrophic rats incubated with or without 6xHis-rMERTK$_{571-999}$. Western blots of the recovered proteins were probed with antibodies against Grb2. Load, input RPE/choroid homogenate; Ctrl, Ni^{2+}-NTA resin with homogenate alone; PD, pull down including rMERTK$_{571-999}$ and homogenate. (E) Grb2 localization on retina/RPE/choroid cryosections from 4 wk old BALB/c mice imaged using indirect immunofluorescence with confocal microscopy. A selected area of RPE was enlarged to show specific localization to the cell layer. RPE, retinal pigment epithelium; OS, outer segments; IS, inner segments; ONL, outer nuclear layer; OPL, outer plexiform layer; INL, inner nuclear layer; IPL, inner plexiform layer; GCL, ganglion cell layer.

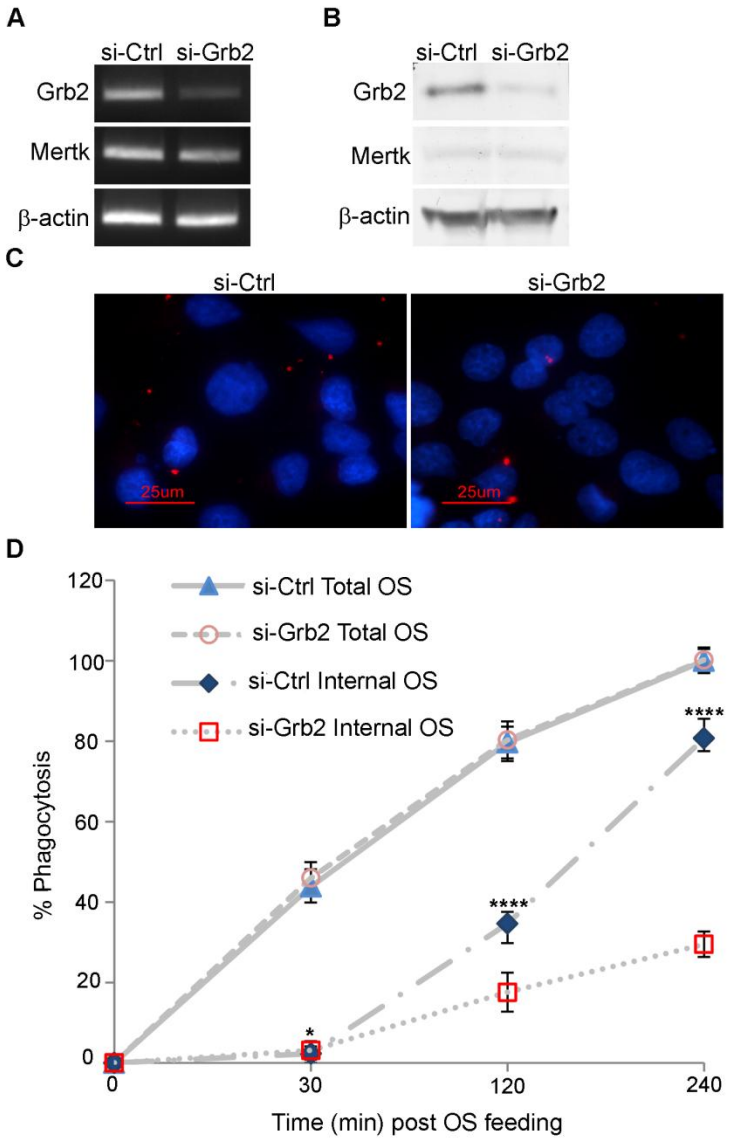

Figure II-3. Grb2 silencing decreases phagocytic uptake in RPE cells. RPE-J cells were transfected with a pool of Grb2 targeting siRNAs or a non-targeting siRNA control, and expression was evaluated 5 days later. (A) Transcript levels for *Grb2*, *Mertk*, and *β-actin* evaluated using RT-PCR. (B) Protein levels of Grb2, Mertk, and β-actin evaluated by western blot analysis of RPE-J cell homogenates. (C-D) Phagocytic activity assays. (C) Transfected cells were incubated with AlexaFluor 555-labeled bovine rod OS for 4 h and quenched by addition of trypan blue. Images shown are representations of total labeled OS ingested by cells. Labeled OS are shown in red and nuclei are shown in blue. (D) OS ingestion and binding were quantified for three independent assays and plotted as a percentage of control total OS after 4 h which was set as 100%. Error bars represent mean ± SEM, n=3. p values were calculated using Student's *t* test, and are as shown: p**<0.05, p****<0.00005.

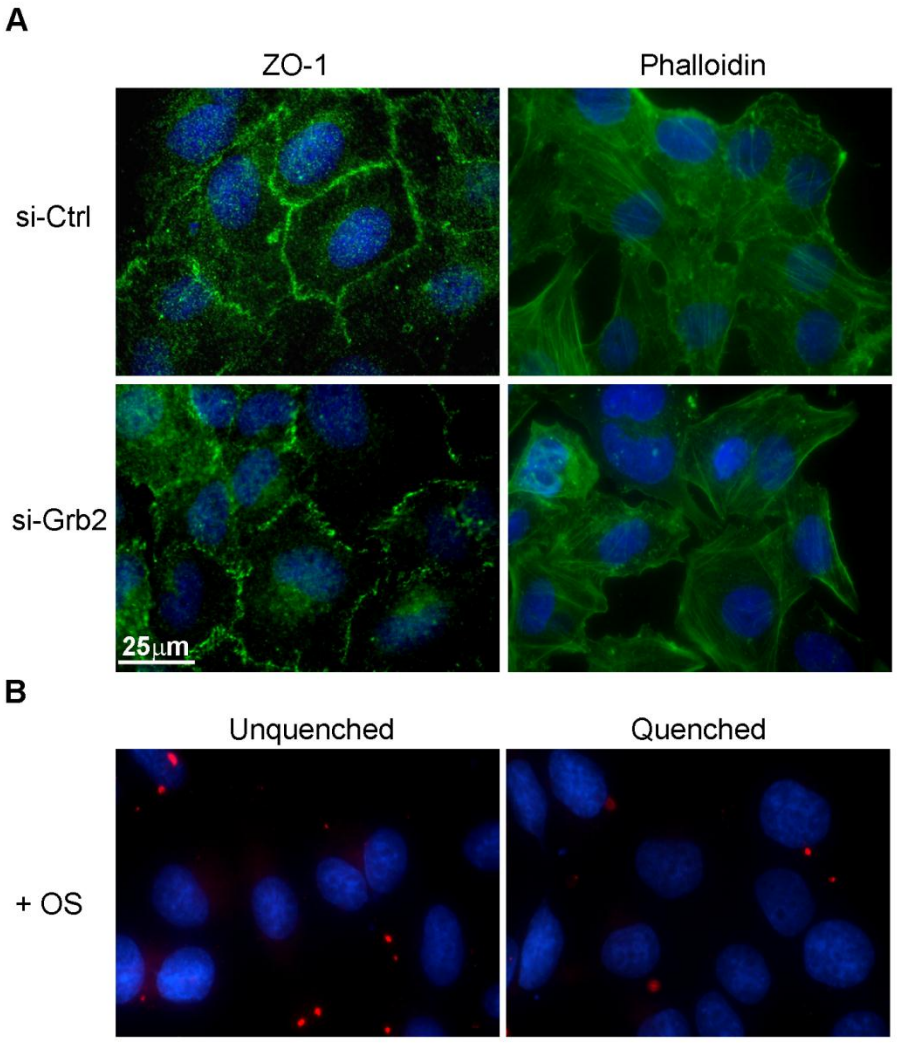

Figure II-4. Morphology of transfected cells in RPE phagocytosis assays and quenching of AlexaFluor 555-OS fluorescence. RPE-J cells were transfected with a pool of Grb2 targeting siRNAs or a non-targeting siRNA control. (A) Morphology of transfected cells were assessed by evaluating ZO-1 immunostaining and actin staining by phalloidin using fluorescence confocal microscopy. (B) Quenching of external and bound AlexaFluor 555-OS fluorescence in transfected RPE-J cells was performed by incubation with trypan blue. Images shown are cells transfected with si-Ctrl and fixed at 2 hours after feeding OS.

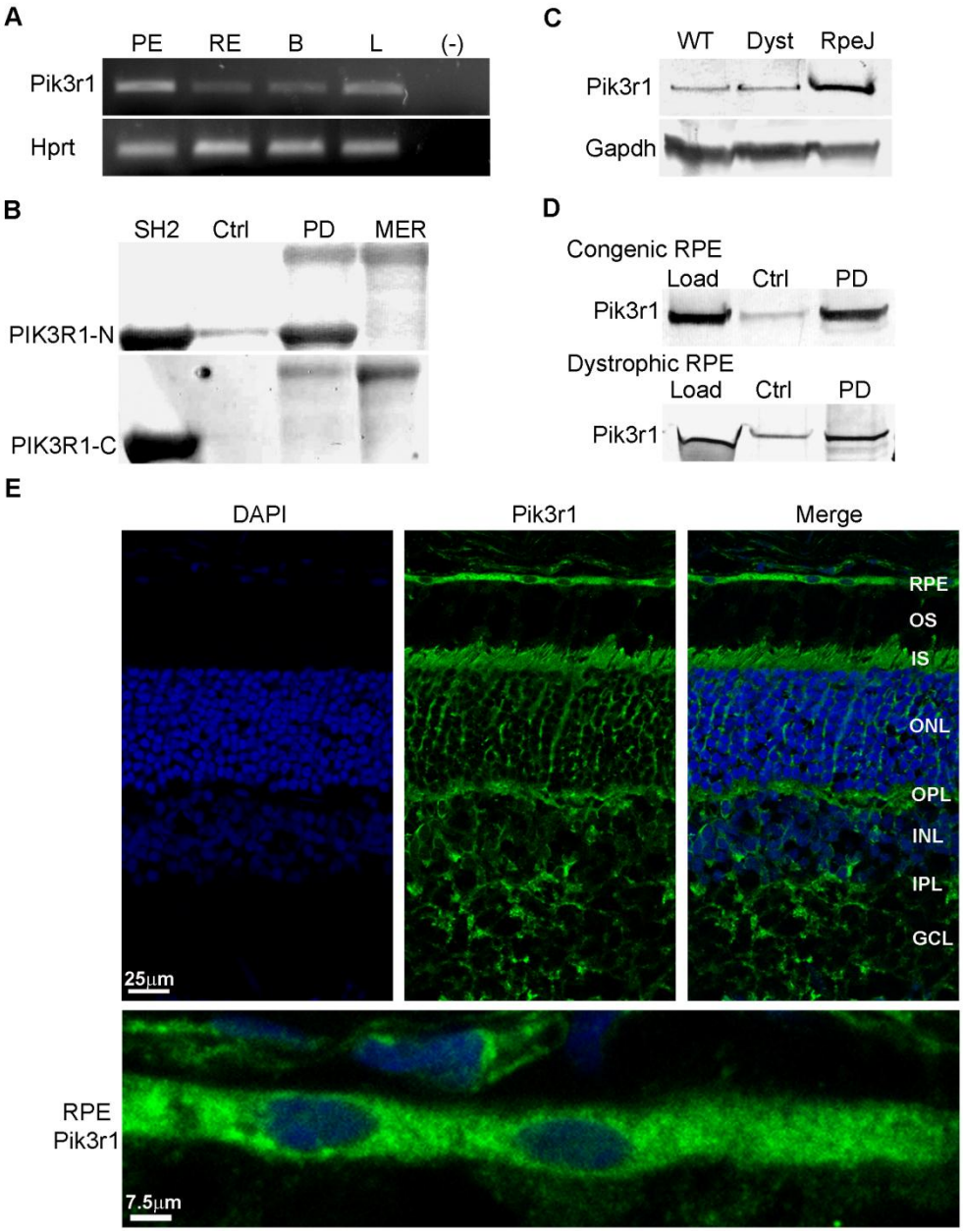

Figure II-5. Pik3r1 is expressed and interacts with MERTK in the RPE. (A) Pik3r1and Hprt transcripts amplified from mouse tissues by RT-PCR. (B) Ni2+-NTA pull downs of recombinant PIK3R1 GST-SH2 domains incubated with or without 6xHis-rMERTK571-999 and evaluated on SDS-gels. (C) Pik3r1 immunoreactivity on western blots of rat RPE/choroid and RPE-J cell homogenates. (D) Ni2+-NTA pull downs with RPE/choroid protein homogenates from RCS congenic and dystrophic rats incubated with or without 6xHis-rMERTK571-999, and evaluated by western analysis with antibodies against Pik3r1. (E) Pik3r1 localization on cryosections of mouse retina/RPE/choroid. Details as in Fig. II-2.

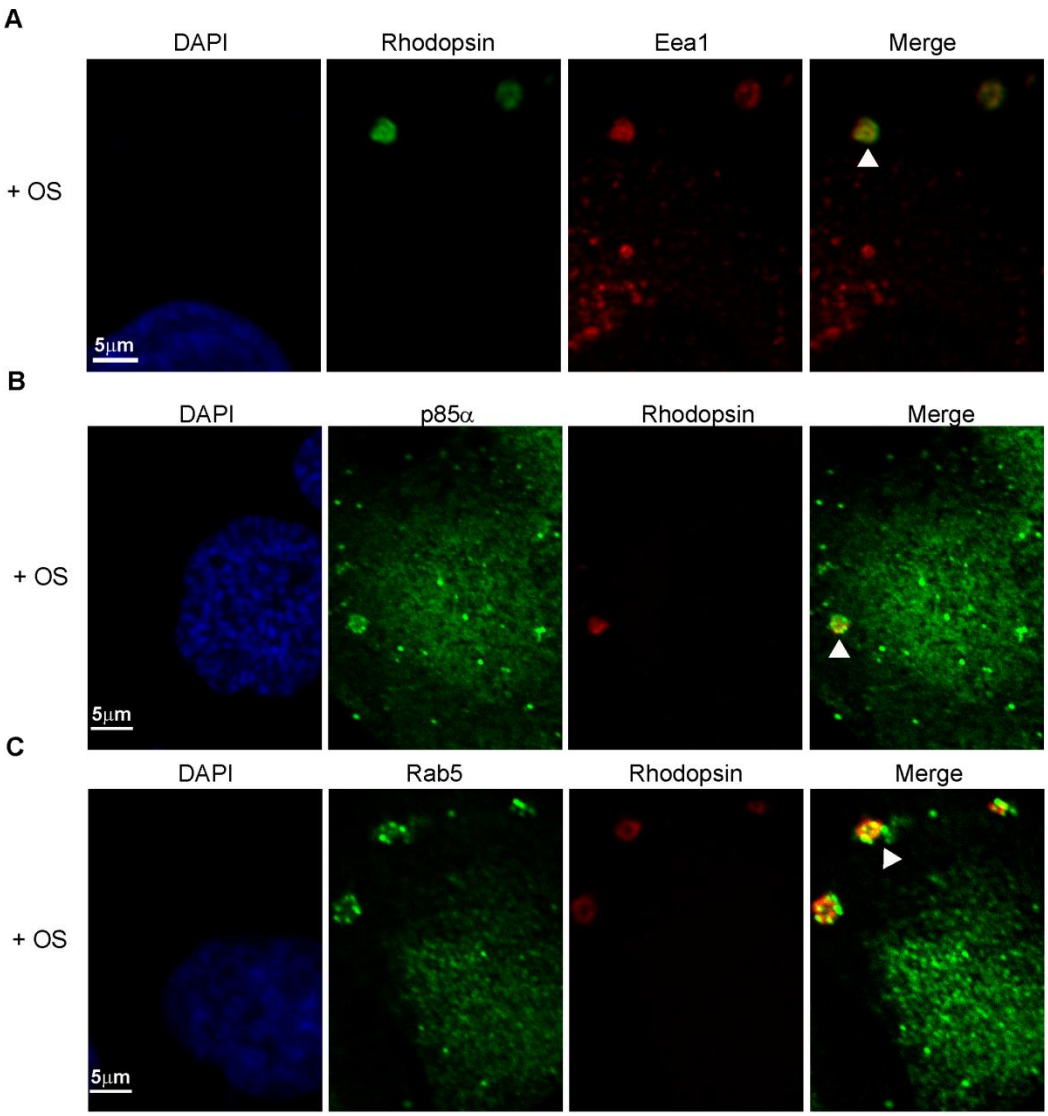

Figure II-6. Rhodopsin colocalization with Pik3r1, Eea1, and Rab5 in OS fed RPE-J cells. RPE-J cells were incubated with isolated bovine OS for 4 h. Cells were fixed and stained with anti-rhodopsin and anti-Eea1 (A), anti-Pik3r1 and anti-Eea1(B), or anti-Rab5 and anti-Eea1 (C), with AlexaFluor 488 and 555 as secondary and viewed using fluorescence confocal microscopy. Areas showing co-localization appear as yellow in the merged images and are marked by white arrowheads.

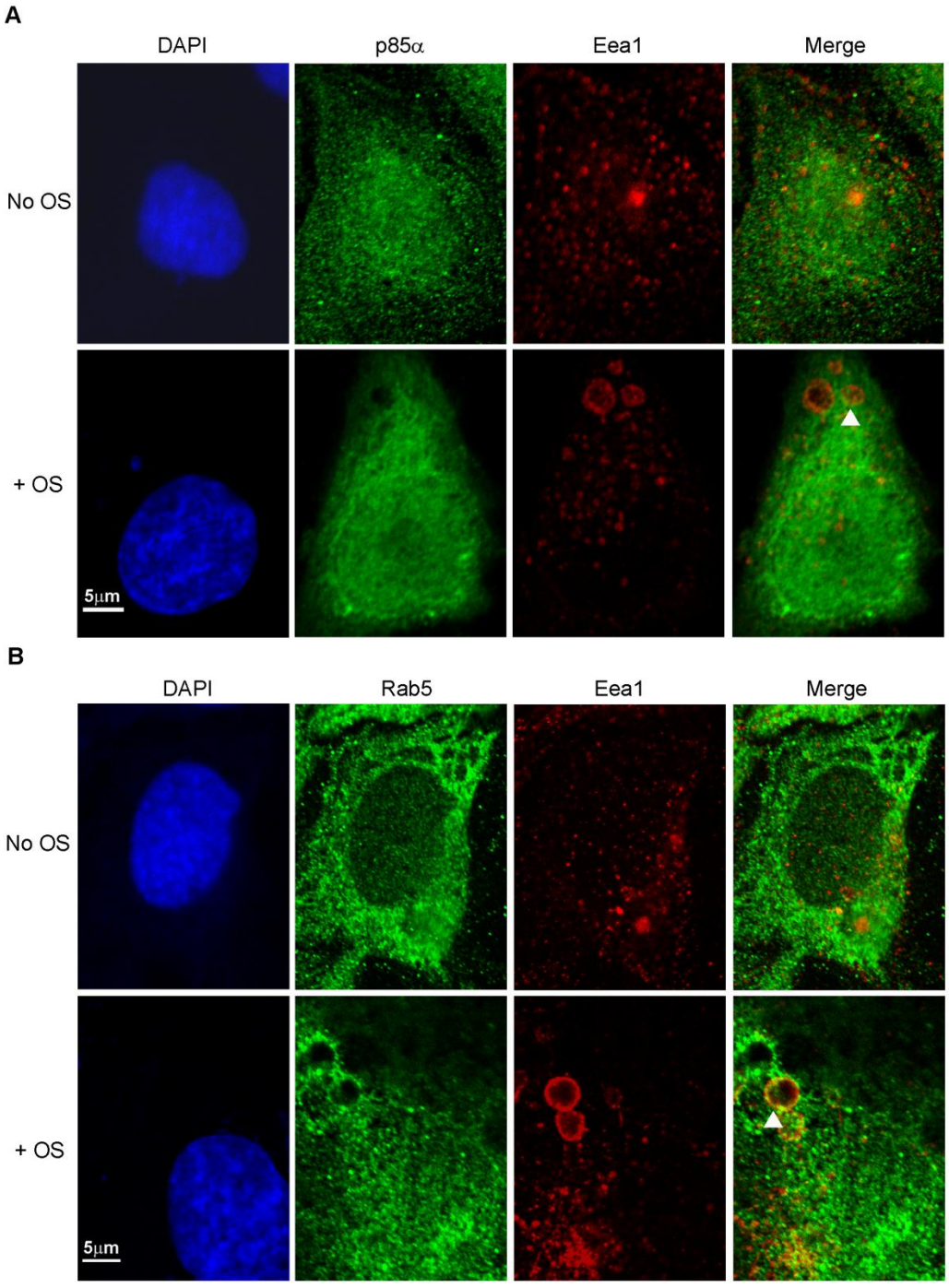

Figure II-7. Pik3r1 colocalizes to early phagosomes with Eea1 and Rab5 during OS uptake. RPE-J cells were incubated with, or without, isolated bovine OS for 4 h. Cells were fixed and stained with anti-Pik3r1 and anti-Eea1 with AlexaFluor 488 secondary (A), or anti-Rab5 and anti-Eea1 with AlexaFluor 555 secondary (B), and viewed using fluorescence confocal microscopy. Areas showing co-localization appear as yellow in the merged images and are marked by white arrowheads.

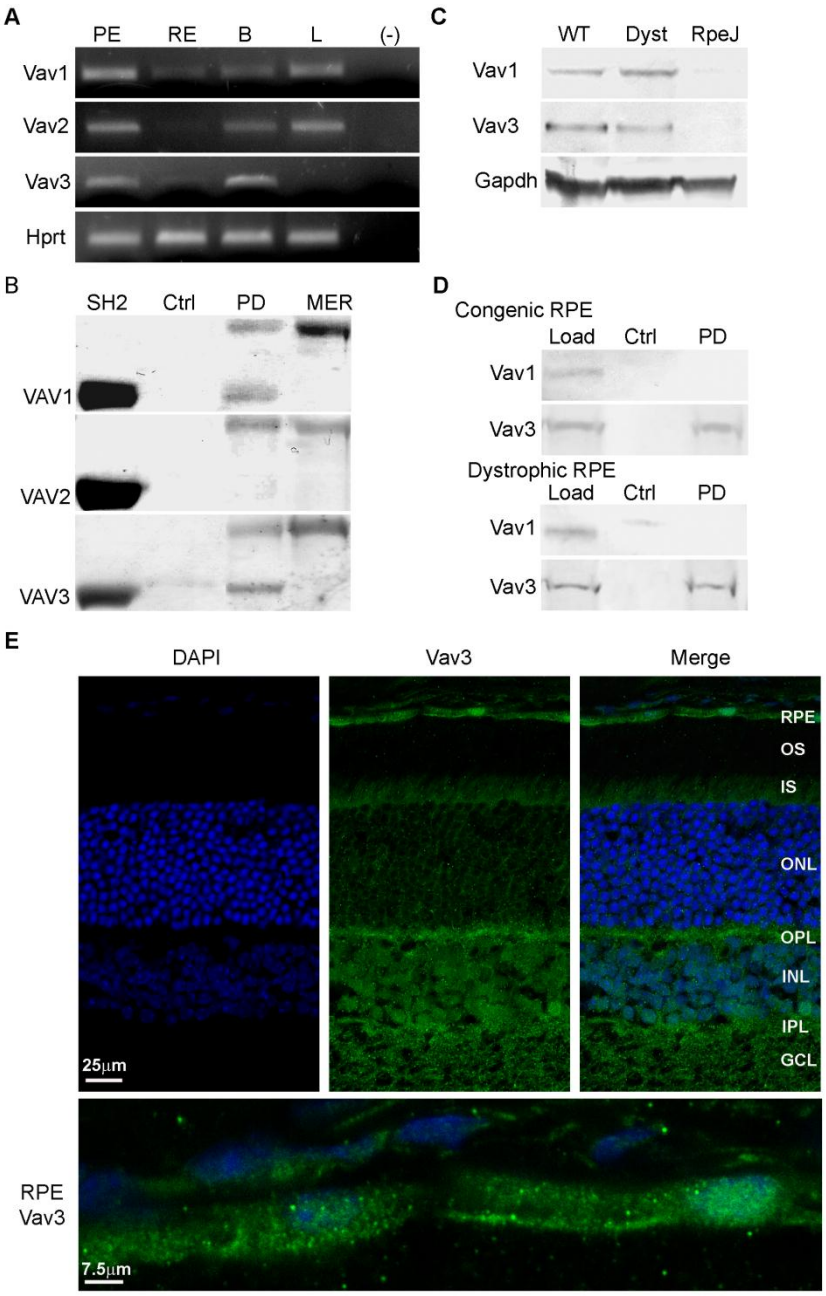

Figure II-8. Vav3 is expressed and interacts with MERTK in the RPE. (A) Vav and Hprt transcripts amplified from mouse RPE/choroid by RT-PCR. (B) Ni2+-NTA pull downs of recombinant VAV GST-SH2 domains incubated with or without 6xHis-rMERTK571-999 and evaluated on SDS-gels. (C) Vav protein immunoreactivity on western blots of rat RPE/choroid and RPE-J cell homogenates. (D) Ni2+-NTA pull downs with RPE/choroid protein homogenates from RCS congenic and dystrophic rats incubated with or without 6xHis-rMERTK571-999, and evaluated by western analysis with antibodies against Vav1 and Vav3. (E) Vav3 localization on cryosections of mouse retina/RPE/choroid.Details as in Fig. II-2.

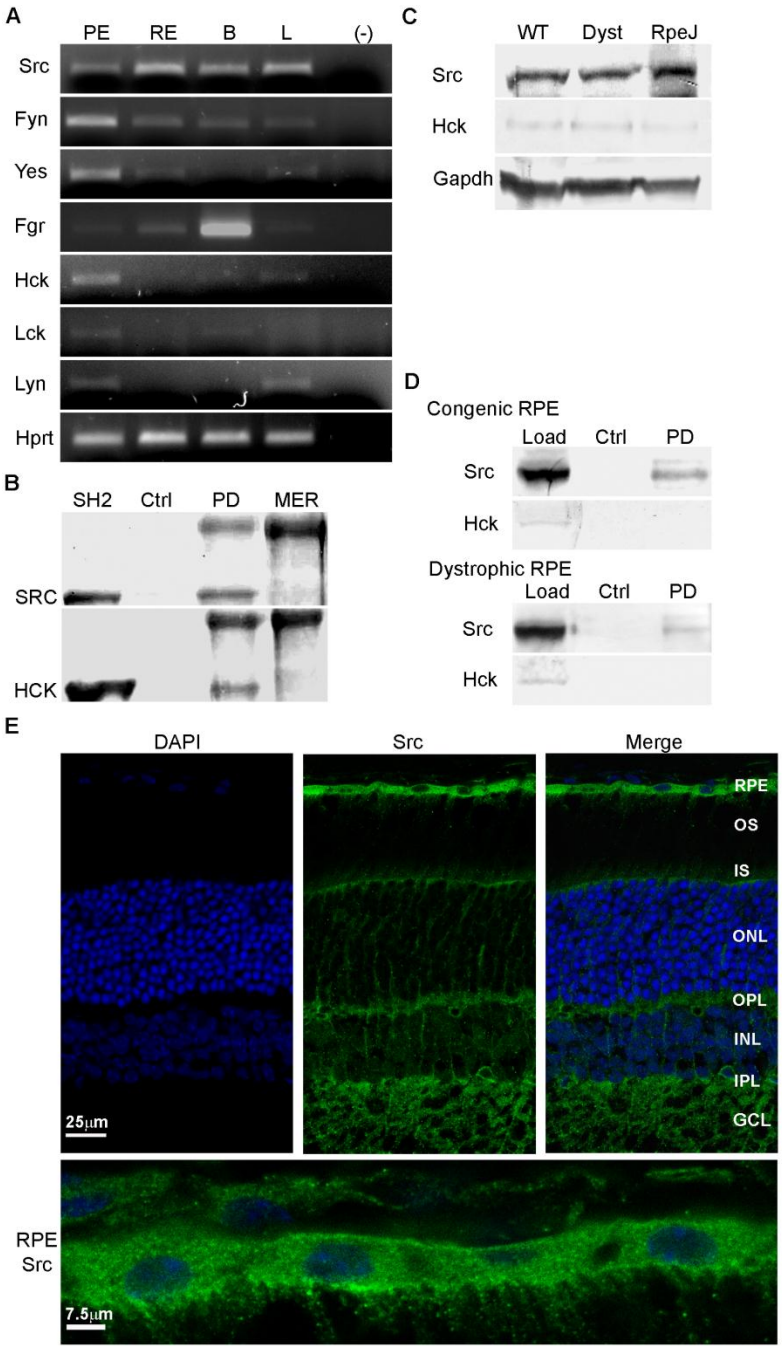

Figure II-9. Src is expressed and interacts with MERTK in the RPE. (A) Src family kinase and *Hprt* transcripts amplified from mouse RPE/choroid by RT-PCR. (B) Ni^{2+}-NTA pull downs of recombinant SRC and HCK GST-SH2 domains incubated with or without 6xHis-rMERTK$_{571-999}$ and evaluated on SDS-gels. (C) Src and Hck immunoreactivity on western blots of rat RPE/choroid and RPE-J cell homogenates. (D) Ni^{2+}-NTA pull downs with RPE/choroid protein homogenates from RCS congenic and dystrophic rats incubated with or without 6xHis-rMERTK$_{571-999}$, and evaluated by western analysis with antibodies against Src and Hck. (E) Src localization on cryosections of mouse retina/RPE/choroid. Details as in Fig. II-2.

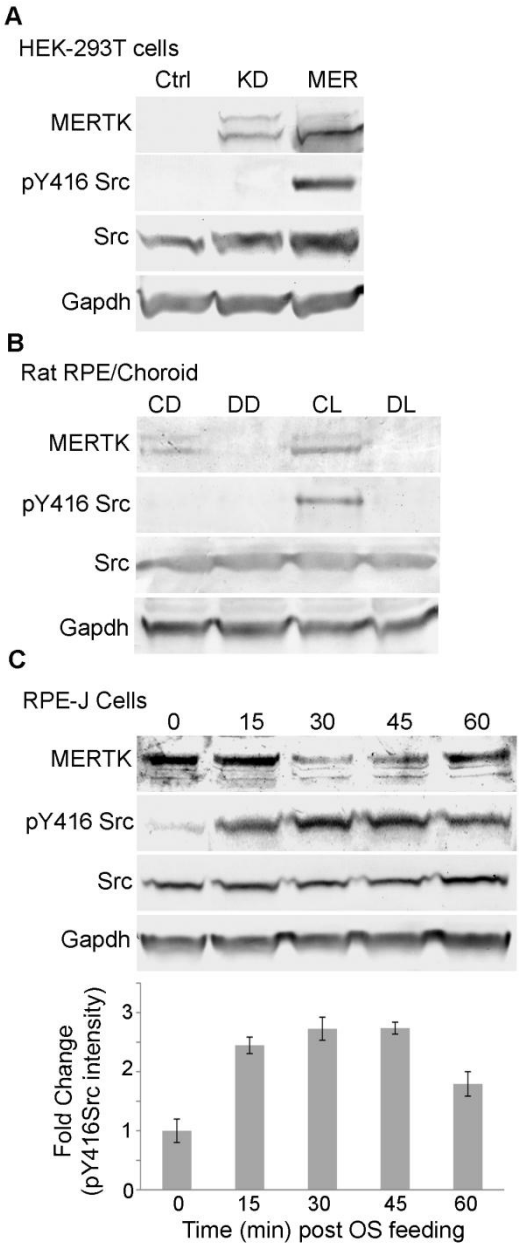

Figure II-10. Src is phosphorylated on Y416 in response to MERTK activation in the RPE. Immunoreactivity of antibodies recognizing pY416 Src, Src, Mertk (c-terminal antibody), and Gapdh on western blots of cell and tissue homogenates. (A) HEK-293T cells transfected with full length MERTK (Mer) or kinase-dead R844C-MERTK (MerKD). (B) RPE/choroid homogenates from 4 wk old RCS congenic and dystrophic rats harvested at 1 h prior to light onset, and 1.5 h post light onset (peak of phagocytic uptake). CD, congenic rat RPE/choroid in the dark; DD, dystrophic in the dark; CL, congenic at peak activity; DL, dystrophic taken at peak activity. (C) RPE-J cells were incubated with OS and lysed at times indicated, followed by western blot analysis. Results for pY416 Src are plotted as the mean fold change in band intensity. Error bars represent mean ± SEM, n=3.

Chapter III

Tyrosine Phosphorylation of RabGDI Downstream of MERTK Activation in the RPE

Abstract

Rod and cone photoreceptor cells undergo a process of continual renewal involving daily shedding of outer segment (OS) membranes that are cleared from the subretinal space by phagocytic uptake into retinal pigment epithelium (RPE). In the Royal College of Surgeons (RCS) dystrophic rat, a loss-of-function mutation in Mer tyrosine kinase (MERTK) blocks this phagocytic mechanism. In the present study, two-dimensional western analysis coupled with MALDI-mass spectrometry (MS) and peptide mass fingerprinting were used to evaluate protein tyrosine phosphorylation in the RPE/choroid of congenic and dystrophic RCS rats. Largely overlapping patterns of tyrosine phosphorylation were detected in all samples collected before or during peak phagocytic activity. A marked exception was tyrosine phosphorylation of Rab GDP dissociation inhibitor 1 (RabGDIα) that was detected only in congenic animals during peak phagocytic uptake. Localization of RabGDIα in the RPE showed a distribution overlapping that of MERTK and cSrc. In transfected HEK293T cells, phosphorylation of RabGDIα occurred downstream of MERTK signaling and required cSrc activation. In retinal

cross sections and cultured RPE-J cells challenged with isolated OS, RabGDIα colocalized with MERTK and cSrc. In addition, the presence of active MERTK caused a decrease in the interaction of RabGDIα and Rab5. Collectively, the present studies suggest that MERTK-stimulated tyrosine phosphorylation of RabGDIα likely regulates Rab5 participation in early phagosome formation occurring during OS uptake by the RPE. These findings provide the first evidence of a direct role of MERTK in regulating membrane trafficking that is integral to the mechanism of phagosome formation and maturation.

Introduction

A key function of the retinal pigment epithelium (RPE) is the phagocytic uptake of outer segment (OS) membranes shed from the distal tips of the photoreceptor cells [219]. In the Royal College of Surgeons (RCS) dystrophic rat, disruption of this process results in the formation of a debris field between the RPE and retina that blocks the supply of oxygen and nutrients to the photoreceptor cells and results in profound retinal degeneration [22]. The disease in the RCS rat is caused by a loss-of-function mutation in the gene encoding MERTK [78]. Disease-associated mutations in *MERTK* have also been identified in individuals with autosomal recessive retinitis pigmentosa [82-84].

MERTK is a member of the Tyro3/Axl/Mer family of receptor tyrosine kinases that play critical roles in tissue homeostasis, inflammation, autoimmune responses, and innate immunity [32]. Activating ligands are the structurally-related proteins growth-arrest-specific protein 6 (Gas6) and anti-coagulant

protein S [44, 45]. Novel ligands identified in recent studies include Tubby and Tulp1 [195]. Ligand binding activates MERTK intrinsic tyrosine kinase activity, resulting in autophosphorylation of tyrosine residues in the receptor intracellular domains and subsequent recruitment of SH2 domain-containing proteins, as well as tyrosine phosphorylation of downstream proteins [59].

Recent studies have indicated the involvement of SH2 domain proteins Grb2, PI3K, and Src that may signal to small G-proteins which regulate cytoskeletal rearrangement in MERTK-mediated phagocytosis (Chapter II). Other studies identified myosin II [89] and annexin II [94] as actin-binding proteins necessary for RPE phagocytic uptake, providing a direct link to cytoskeletal rearrangement. Proteins involved in phagosome trafficking and degradation in the RPE have also been recently identified. Myosin VIIa has been shown to function in trafficking of phagosomes post-engulfment [151]. Rab escort protein 1 (REP1)/Choroideremia gene (CHM), an effector of Rab small G-proteins involved in membrane trafficking, has also been implicated in the degradation of phagolysosomes but does not contribute to phagocytic uptake [169, 185, 187].

As an approach to understanding the mechanism of MERTK signaling that initiates OS uptake in the RPE, the profiles of tyrosine phosphorylated proteins present in the RPE/choroid of congenic and dystrophic RCS rats were compared before and after light onset, corresponding to times of low and high shedding and phagocytic uptake, respectively [27]. The results suggest that MERTK activation is responsible for the tyrosine phosphorylation of Rab GDP dissociation inhibitor

alpha (RabGDIα). RabGDIα is an effector of Rab GTPases involved in regulating their movement from membrane to membrane, thus linking MERTK signaling to the function of Rab GTPases active in endosome formation and maturation, as well as phagocytosis [155, 174, 220]. These findings point to a novel role of MERTK in regulating the factors that control membrane movement and remodeling in the mechanism of phagocytic uptake by the RPE.

Materials and Methods

Animals

All experiments were conducted in accordance with the ARVO statement for the Use of Animals in Ophthalmic and Vision Research and approved by the University of Michigan Committee on the Use and Care of Animals. C57BL/6J and Balb/C mice were bred from animals obtained from the Jackson Laboratories. Pigmented dystrophic (RCS-*p*+) and non-dystrophic (RCS-*rdy*+*p*+) rats were bred from previously described strains [75, 200]. Mice and rats were housed in a 12-/12-h light–dark cycle (~300 lux room light) and were euthanized by CO_2 inhalation.

Materials

Primary antibodies: Src, pY416-Src, and pY527-Src, Cell Signaling Technology; Xpress, Invitrogen; RabGDIα, Sy systems; GAPDH, Ambion; Rab5, Abcam; EEA1, BD Labs. Secondary antibodies: AlexaFluor 488-conjugated anti-Rabbit IgG, AlexaFluor 555-conjugated anti-mouse IgG, Invitrogen. Complete protease inhibitors, PhosSTOP phosphatase inhibitors, protein-G agarose,

Fugene, and AmpliTaq Gold polymerase were from Roche Diagnostics. *Pfu* Ultra polymerase was from Stratagene. Ni^{2+}-NTA resin, RNeasy kits, Superscript II, and oligo-dT were from Qiagen. RPE-J and HEK293T cells were from ATCC. Sybr safe was from Invitrogen. Other chemicals and reagents were from Sigma. The pcDNA 3.1+ expression vectors encoding full-length MERTK and kinase-dead R844C-MERTK have been previously described [8]. Src family kinase inhibitors PP1, PP2, and PP3 analog were gifts from Dr. Christin Carter-Su. Antibodies to MERTK and anti-phosphotyrosine were gifts from Drs. Douglas Vollrath and Benjamin Margolis, respectively.

Western analysis

RPE/choroid was dissected from groups of 3 dystrophic and 3 congenic RCS rats at 30 days of age, euthanized 1.5 h before or 2 h after light onset. The tissues were homogenized in 20mM MOPS, 2mM EGTA, 5 mM EGTA, 1% Triton X-100, 1mM DTT, plus protease and phosphatase inhibitors. All cultured cells were harvested in the same buffer. Cellular debris was removed by low speed centrifugation and protein concentrations of supernates were determined by modified Lowry assay [215]. For one-dimensional analysis: protein samples (7.5µg) were separated by SDS-polyacrylamide electrophoresis (PAGE), transferred onto nitrocellulose membranes that were blocked, incubated with primary antibody, washed, incubated with alkaline phosphatase-conjugated secondary antibodies, and developed using 5-bromo-4-chloro-3'-indolyphosphate p-toluidine and nitro-blue tetrazolium chloride. For two-dimensional analysis: protein samples (300µg) were separated in the first dimension by isoelectric

focusing, and in the second dimension by SDS-PAGE, and the proteins transferred onto polyvinylidene difluoride (PVDF). Blots were blocked, incubated with a monoclonal anti-phosphotyrosine antibody, then with horse radish peroxidase-conjugated secondary antibody, and developed with 3,3′-diamino benzidine.

MALDI-mass spectrometry (MS) and peptide mass fingerprinting

For in-gel digestion of proteins, gel spots were transferred to clean tubes and hydrated in water. The gel pieces were washed twice with 100 μl 0.05 M Tris, pH 8.5/ 30% acetonitrile for 20 min with shaking, then with 100% acetonitrile for 1-2 min. After drying for 30 min under vacuum, the samples were digested by adding 0.08 μg modified trypsin (sequencing grade, Roche Molecular Biochemicals) in 13-15 μl 25 mM Tris, pH 8.5, and incubating overnight at 32°C. Peptides were extracted with 2X 50 μl 50% acetonitrile/ 2% TFA, and the combined extracts were dried. Matrix solution was prepared by making a 10 mg/mL solution of 4-hydroxy-α-cyanocinnamic acid in 50% acetonitrile/ 0.1% TFA and adding two internal standards, angiotensin and ACTH 7-38 peptide. The dried digest was dissolved in 3 μl matrix/standard solution and 0.5 μl was spotted onto the sample plate, completely dried, and washed twice with water. MALDI mass spectrometric analysis was performed on the digest using an Applied Biosystems Voyager DE Pro mass spectrometer in the linear mode. For peptide mass search, peptide masses were entered into search programs to search the SwissProt database for a protein match. Programs used were Mascot at www.matrixscience.com and MS-Fit at http://prospector.ucsf.edu.

Immunohistochemical analysis

Balb/C mouse eyes were obtained from animals perfused with 4% paraformaldehyde, washed with PBS, transitioned to sucrose/OCT, flash frozen and retina/RPE/choroid cryosections generated (10 μm). Rat RPE-J cells were maintained in DMEM supplemented with 4% FBS and 1 mM non-essential amino acids at 33°C in 5% CO_2. For immunohistochemical analysis, cells were cultured for 6 days on eight-well chamber slides, then incubated with bovine rod outer segments [216] at a ratio of 10 OS per RPE cell for 4 h at 33°C. Unbound OS were removed by washing the cells 3 times with PBS containing 0.2 mM $CaCl_2$ and 1 mM $MgCl_2$, and the cells were fixed in 4% paraformaldehyde for 30 min at room temperature. Sections and cells were permeabilized with PBS-Triton X-100 (0.125%); blocked with 1% bovine serum albumin (BSA), 10% normal goat serum, and 0.125% Triton X-100; incubated with primary antibody for 2 h; washed and incubated with fluorochrome-conjugated secondary antibody for 1 h. Primary antibodies were used as follows: Rabbit anti-RabGDI (1:300), anti-Src (1:300), anti-Rab5 (1:300); Anti-MERTK (1:300). Mouse anti-EEA1 (1:300); RabGDI (1:200). Secondary antibodies dilutions were: AlexaFluor 488 anti-Rabbit IgG (1:500); AlexaFluor 555 anti-mouse IgG (1:500). Slides were cover mounted using Prolong Gold containing DAPI, and images were obtained using confocal fluorescence microscopy (Leica SP5).

Transfection and immunoprecipitation

Human embryonic kidney (HEK-293T) cells were maintained in Dulbecco's modified Eagle's medium (DMEM) supplemented with 10% fetal

bovine serum (FBS), 1 mM sodium pyruvate, and 1 mM penicillin/ streptomycin at 37°C in 5% CO_2. The cells were transiently transfected using FuGENE according to the manufacturer's recommendations with the following expression vector constructs alone or in pairs: pcDNA 3.1+ encoding full-length human MERTK or kinase-dead R844C-MERTK [84]; pcDNA3.1/HisC encoding full-length human RabGDIα generated using RT-PCR with gene specific primers (Table III-1) and total human RPE/choroid RNA. Total RNA was prepared from isolated human RPE/choroid using the RNAeasy kit, and first-strand cDNAs were generated using Superscript II and oligo-dT. At 48 h post-transfection, the cells were lysed by sonicating in 20 mM MOPS, 2 mM EGTA, 5 mM EGTA, 1% Triton X-100, 1 mM DTT, protease and phosphatase inhibitors; cellular debris was removed by low speed centrifugation; and protein concentrations in the supernatant were determined by modified Lowry [215]. Aliquots of 200 µg protein were incubated with primary antibody overnight at 4°C, then with protein G-agarose for 2 h at 25°C. The beads were washed three times in 150 mM NaCl and 25 mM Tris at pH 7.2; eluted with 0.1 M glycine-HCl pH 3.0; and samples pH adjusted by addition of 1 M Trizma base, pH 10.0. To reduce saturated activation of MERTK observed in transiently transfected HEK-293T cells in the presence of serum [84], unless noted, cells were serum starved for 18 h. Cells in selected experiments were treated with 4-amino-5-(4-methylphenyl)-7-(t-butyl)pyrazolo[3,4-d]pyrimidine (PP1), PP2, or the inactive analog 4-amino-7-phenylpyrazol[3,4-d]pyrimidine (PP3) for 60 min [221, 222]. To reactivate MERTK to initial levels, serum was added onto the cells for 10 min before cell lysis.

RT-PCR expression analysis

Total RNA was isolated from C57BL/6 mouse RPE/choroid, retina, and from rat RPE-J cells using the RNAeasy kit, and first-strand cDNAs were generated using Superscript II and oligo-dT. Sequences encoding Rab family proteins were amplified with gene-specific primers flanking at least one intron in the genomic sequence (Table III-2), using AmpliTaq Gold polymerase and the following cycling conditions: 1 cycle at 95°C for 10 min, followed by 28 cycles at 95°C for 2 min, 60°C for 45 sec, 72°C for 2 min. Primers for hypoxanthine-guanine phosphoribosyltransferase (Hprt) served as a control. PCR products were analyzed by electrophoresis on agarose gels stained with Sybr safe.

Microarray analysis

Mouse RPE/choroid total RNA was isolated as described above, assayed by Agilent BioAnalyzer 2100, and converted into biotinylated, fragmented, and cleaned cRNA using Affymetrix GeneChip One-Cycle Target Labeling and Control Reagents. The cRNAs were hybridized with Affymetrix Mouse Genome 430_2.0 arrays that were washed and stained with streptavidin-phycoerythrin and antibody, and optically read with a Hewlett-Packard GeneArray Scanner. CHP/.CEL files were generated using the Affymetrix Microarray Suite of programs. Four independent replicates were performed. The quality of the GeneChip hybridizations was excellent according to Affymetrix QC criteria, including average 3’/5’ ratios, background, standard deviation, background, raw Q (noise), scalar factor, and percent present. Data were considered only for probe sets for which a majority of replicates were called as present.

Normalization (quantile method) and calculation of signal intensities was performed using the RMA software package from the R project (http://www.r-project.org/).

Results

Differential tyrosine phosphorylation of RabGDIα in the RPE

The fundamental role of MERTK signaling in OS phagocytosis suggests that tyrosine phosphorylation is likely to regulate key molecular mechanisms in the RPE. To evaluate the steady-state pattern of protein tyrosine phosphorylation, and the potential changes occurring during phagocytic uptake, two-dimensional western analysis was performed on RPE/choroid preparations from cohorts of young adult pigmented dystrophic (RCS-*p*+) and non-dystrophic congenic (RCS-*rdy*+*p*+) rats. Animals were euthanized 1.5 h before, or 2 h after, light onset; the latter time corresponding to the peak of phagocytic activity [27]. On blots probed with a phosphotyrosine-specific monoclonal antibody, the pattern of phosphorylated proteins in each of the four conditions exhibited significant overlap (Figure III-1). No differences were seen between the phosphorylation patterns of dystrophic animals before and after light. Differences between dystrophic and congenic rats before light were also minimal and largely reflected differences in intensity, with dystrophic animals exhibiting apparently higher phosphorylation levels overall. A marked difference in the pattern of tyrosine phosphorylation that correlated with phagocytic activity was seen as a series of closely spaced signals of similar size present only in congenic rats that

were euthanized after light onset (encircled on upper left panel of Figure III-1). The corresponding protein was identified by MALDI-MS as Rab GDP dissociation inhibitor 1 (RabGDIα or GDI1) (Table III-3). GDIs are proteins that regulate members of the family of Rab GTPases involved in vesicular trafficking by slowing the rate of the GDP/GTP exchange [223]. RabGDIα is expressed mainly in neural tissues where it functions in vesicular trafficking within cells [224, 225]. The co-migration of RabGDIα with the phosphotyrosine signals on the two-dimensional westerns was confirmed by stripping the blots and reprobing with an antibody specific for RabGDIα (Figure III-2A). The pattern of multiple spots seen likely reflects heterogeneity in extent and nature of posttranslational modifications, as RabGDIα can be phosphorylated on multiple serine and tyrosine residues [175, 176, 226, 227]. Western analysis of RPE/choroid protein samples evaluated on one-dimensional SDS-gels confirmed the presence of RabGDIα immunoreactivity in both congenic and dystrophic rats (Figure III-2B).

RabGDIα localization in the RPE

Immunohistochemical analysis of RabGDIα in cryosections of retina/RPE/choroid from 4 wk old albino Balb/C mice euthanized during peak phagocytic activity showed strong labeling of the RPE, OS, and synaptic and ganglion cell layers of the neural retina. In high magnification images of the RPE, RabGDIα labeling could be seen extending toward both apical and basal regions of the RPE cells (Figure III-3A). Previous studies have shown that MERTK localizes to the apical microvilli of the RPE [66]. Double-labeling studies showed overlap in the distribution of RabGDIα and the pattern of MERTK

immunostaining, indicating that a site of RabGDIα is likely to be in the apical microvilli (Figure III-3B). The independence of RabGDIα expression relative to the functional status of MERTK, as well as its expression in various layers of the retina, is consistent with its role as an effector of small GTPases that play a variety of roles in membrane trafficking.

RabGDIα phosphorylation downstream of MERTK and Src activation

The affinity of the interaction of RabGDIα for Rab GTPases, as well as its membrane localization within cells, is regulated by multiple posttranslational modifications [175, 176, 226, 227]. To evaluate the effect of MERTK activity on the tyrosine phosphorylation of RabGDIα, HEK-293T cells were co-transfected with expression constructs for wild-type MERTK or a kinase-dead R844C-MERTK mutant. Western blots of anti-phosphotyrosine immunoprecipitations probed for RabGDIα (Xpress-tag) showed that phosphorylated RabGDIα was recovered from co-transfections with wild-type MERTK but not mutant MERTK (Figure III-4A). Previous studies of RhoGDI, a GDI for Rho family GTPases, have shown that phosphorylation of RhoGDI occurs through interaction with Src [228]. MERTK has also been shown to interact with and activate Src in the RPE resulting in phosphorylation on tyrosine residue 416 (pY416-Src) [229] (Chapter II). Immunohistochemical analysis of Src and RabGDIα in cryosections of retina/RPE/choroid from 4 wk old albino Balb/C mice during peak phagocytic activity showed overlap in the distribution of RabGDIα and Src on the apical surface of the RPE (Figure III-4B). In HEK-293T cells cotransfected with expression constructs encoding MERTK and RabGDIα, western analysis showed

that formation of active pY416-Src, but not inactive pY527-Src, depended on the presence of wild-type rMERTK (Figure III-4C). To evaluate the requirement for Src activity in the MERTK-mediated tyrosine phosphorylation of RabGDIα, immunoprecipitations were performed with HEK-293T cells transfected with MERTK and RabGDIα that were pretreated with Src family kinase inhibitors PP1 and PP2, or the inactive analog PP3. Western analysis of the active form of Src, pY416-Src, showed that PP1 and PP2 inhibitors, but not PP3, inhibited Src family kinases downstream of MERTK (data not shown). PP1 and PP2 were also found to inhibit the tyrosine phosphorylation of RabGDIα in the transfected cells (Figure III-4D).

RabGDI interaction with MERTK and Src

To further evaluate the potential involvement of Src in tyrosine phosphorylation of RabGDIα, immunopreciptations were performed using the co-transfected cells to assay for protein-protein interactions. Western analysis of MERTK on pulldowns using antibodies against Xpress (tagged RabGDIα) showed that RabGDIα interacted with wild-type but not mutant MERTK (Figure III-5A). Pull downs using antibodies against Src showed its direct interaction with wild-type rMERTK, but not with kinase-dead R844C-rMERTK (Figure III-5B). Pull downs using antibodies against Src showed that rRabGDIα (Xpress) could be recovered only in the presence of wild-type rMERTK (Figure III-5C). This was also the case for pull downs using antibodies specific for pY416-Src (Figure III-5D).Taken together, these findings are consistent with phosphorylation of RabGDIα occurring downstream of Src activation by MERTK.

RabGDIα localization during phagocytic uptake

To determine the sub-cellular localization of RabGDIα relative to that of MERTK and Src during phagocytic uptake, indirect immunofluorescence microscopy was performed on cultured RPE-J cells incubated with or without bovine rod OS. In control cells without added OS, RabGDIα immunolabeling appeared diffuse throughout the cytoplasm. In cells incubated with rod OS, co-localization of MERTK with RabGDIα was seen near the edges of the cell in association with apparent phagosomes (Figure III-6A). Similarly, Src immunolabeling was diffuse in the absence of OS, and appeared to colocalize with RabGDIα after addition of OS (Figure III-6B).

Expression of Rab GTPases in the RPE

To identify potential candidates for involvement in RPE phagocytosis, the expression of Rab family GTPases was evaluated in preparations of total RNA from native tissues. Affymetrix gene chip hybridization data for C57BL/6 mouse RPE/choroid showed relatively high average intensities for multiple Rabs including those: 1) reported to fulfill specific functions in the RPE; 2) known to function in the early stages of endocytosis/phagocytosis; 3) involved in polarized cell functions; 4) that facilitate ER to golgi transport (Table III-4). Analysis of comparative RT-PCR data for congenic and dystrophic RCS rat RPE/choroid, congenic RCS rat retina, and RPE-J cells in culture confirmed that: 1) Rab 27A and 38 are preferentially expressed in RPE/choroid, but are lost from RPE-J cells that retain phagocytic competence; 2) Rabs 5 and 14 that are involved in early endosome formation [202, 230], and Rab 7 which is involved in endosome

maturation [231] are expressed at high levels in RPE and retina, and are also retained in RPE-J cells (Figure III-7).

RabGDIα and Rab5 interact in the RPE

Rab5 was considered to be a strong candidate for involvement in the mechanism of phagosome formation in the RPE, having been previously shown to colocalize with early-endosome markers on phagosomes [232], including early endosome antigen 1 (EEA1) that recognizes phosphatidylinositol 3-phosphate present in such vesicles [202]. Immunohistochemical analysis showed that Rab5 localization in the RPE overlapped with that of RabGDIα with Rab5 appearing to be dispersed throughout the RPE, while RabGDIα staining appeared to trend toward the apical and basal regions of the monolayer of cells (Figure III-8A). In cultured RPE-J cells challenged with isolated rod OS, RabGDIα and Rab5 were seen to colocalize in structures that appeared to be phagosomes (Figure III-8B). To investigate the effects of RabGDIα tyrosine phosphorylation on its interaction with Rab5, immunoprecipitations of transfected HEK-293T cells were performed. Direct interaction of RabGDIα with Rab5 could be demonstrated in the presence of kinase dead R844C-rMERTK, but not wild-type rMERTK (Figure III-8C). These findings are consistent with a mechanism in which changes in the phosphorylation status of RabGDIα regulate Rab5 localization and activity in the early stages of RPE phagocytosis. The observed localization, tyrosine phosphorylation, and known role of GDIs are consistent with potential involvement of RabGDIα in regulating early phagosome formation in the RPE through effects on associated Rab GTPases.

Discussion

Rab GTPases play a fundamental role in intracellular membrane trafficking. The finding that RabGDIα is regulated by tyrosine-phosphorylation occurring downstream of MERTK provides the first direct link between receptor activation and the mechanism of membrane movement essential for RPE phagocytosis. These observations expand the current understanding of the MERTK signaling in the RPE and provide new insight into the phagocytic mechanism necessary for the function and survival of photoreceptor cells in the vertebrate retina. A model of MERTK signaling in the RPE is shown in Figure III-9.

Previous studies have explored the mechanisms involved in cytoskeletal remodeling necessary for RPE phagocytosis. Activation of αvβ5 integrin is an essential component of this process, as it initiates downstream activation of focal adhesion kinase (FAK) [72] and the Rho family GTPase Rac1 that regulates actin polymerization [63]. Both Rho family GTPases and actin-related proteins (Arp) family GTPases are known to act as effectors in multiple phagocytic mechanisms, including those initiated by complement and Fcγ receptors [100, 107, 233]. Myosin also plays an essential role in cytoskeletal remodeling needed for phagocytic uptake, participating in both the formation and closure of the phagocytic cup in professional phagocytes [136]. The finding that MERTK undergoes direct interaction with myosin II suggests that receptor signaling contributes to the regulation of motor protein activity in phagocytosis in the RPE [89].

Upon ingestion, newly formed phagosomes undergo a maturation process involving multiple membrane trafficking events [234]. A second GTPase superfamily, Ras-related proteins in the brain (Rab) GTPases, plays a key role in regulating the membrane flow necessary for phagosome maturation and phagolysosome formation [235]. Essential for both exocytosis and endocytosis, Rab GTPases are involved in cargo sorting, coordinating vesicle motility, and SNARE-mediated fusion in many cell types [153-155, 161]. The importance of Rab GTPases in RPE function is consistent withthe current finding that at least half the known Rab GTPases are expressed. Previous studies have shown that Rab GTPases play critical roles in melanosome motility and maturation in the RPE [182, 184]. Complex formation involving Rab27A, myosin Va, myosin VIIa, and Rab-Interacting Protein (MYRIP) mediates melanosome transport [179, 180, 182, 183]. Rab38 function is required for melanosome stability that is defective in the “chocolate mouse”, with Rab32 able to partially substitute for Rab38 in the RPE [7, 184]. Rab5 is known to play a pivotal role in early endosome formation in many cell types [160] and has been shown to associate with phagosomes and phagolysomes containing fractions in the RPE [236].

Rab GTPases are responsive to signals provided by the initializing receptor, with recruitment to specific membranes regulated by multiple effector proteins [161]. Post-translational modification by geranylgeranyl transferase type II (GGTrII) facilitates the reversible interaction of Rab GTPases with membranes [162, 163]. Activation and subcellular localization is further regulated by guanine nucleotide exchange factors (GEF); by GTPase activating proteins (GAPs); by

Rab escort proteins (REPs) that facilitate recruitment of newly synthesized Rab GTPases to GGTrII for prenylation; and by GDP dissociation inhibitors (GDI) that inhibit the transport Rab GTPases from membrane to the cytosol, and membrane to membrane [155, 164, 185].

Previous studies identified REP1/choroideremia (CHM) as an important effector of Rab GTPases in the RPE [185]. Mutations and deletions in the REP1 gene in patients result in a complete absence of the protein and degenerative disease affecting the choroid, RPE, and photoreceptor cells [169, 171, 186, 237]. In addition, CHM patients exhibit an accumulation of undegraded OS in RPE phagosomes, suggesting involvement of CHM in the mechanism of phagocytic uptake. Recent studies in human fetal RPE cells with silencing of the CHM gene have implicated REP1 in the mechanism of OS degradation occurring in the phagolysosome [187]. In contrast to the limited disease phenotype in CHM, mutations in the *GDI1* gene encoding RabGDIα cause severe systemic disease: X-linked mental retardation [238, 239]. There have been no previous reports of RabGDIα function in the RPE, but given the similarity of their structure and function, it seems likely that both effectors function in a similar capacity in regulating membrane trafficking in the RPE.

In the present studies, phosphotyrosine profiling identified RabGDIα phosphorylation occurring in native RPE/choroid in a manner consistent with MERTK-mediated signaling during phagocytic uptake. Previous studies have shown that the affinity of RabGDIα for various Rab GTPases is regulated, in part, by phosphorylation occurring primarily on serine/threonine residues [175, 240,

241], and phosphorylation by p38 MAPK has been shown to act as an enhancer of Rab5-RabGDI complex formation during endocytosis [175]. In addition, tyrosine phosphorylation of RabGDI2 (RabGDI β) has been shown to result in increased affinity for specific Rab GTPases [176]. Thus, regulation of RabGDIα downstream of MERTK activation likely serves to increase Rab GTPase cycling from one membrane compartment to the next during peaks of phagocytic uptake. The co-localization of Rab5 and RabGDIα in the RPE is consistent with an important and early role of Rab5 in phagosome formation downstream of MERTK activation. The novel finding that MERTK directly regulates effectors of membrane remodeling / trafficking adds to the evidence indicating that phagocytosis and endocytosis share multiple mechanistic features. This insight raises the exciting possibility that complementary studies of these mechanisms will inform efforts to intervene in situations where RPE function is compromised in disease and aging.

Outside Contributions: Kecia Feathers performed the initial dissections of rat RPE/choroid for the phosphotyrosine 2-D westerns and generated RNA for microarray analysis. Kendricks labs performed the 2D-westerns. Mary Ann Gawinowics performed MALDI-MS for RabGDIα identification. Lin Jia prepared sections for immunohistochemical analysis. Christina McHenry generated expression constructs for MERTK wild-type and the MERTK R844C mutant. Matthew Brooks performed the microarray analysis of the Rdh12-/- mice. Ritu Khanna analyzed microarray data from wild-type and Rdh12-/- mice.

Gene	Forward primers 5' to 3'	Reverse primers 5' to 3'
Rab 1	AGCTCATTCCTCCCCTTCCATTACC	CCTGCTGTGTCCCATATCTGAAGC
Rab 2A	TGGGATACAGCAGGGCAGGAGT	TGGAATGCTGACGGGCGTCT
Rab 4A	GAAGCCTCCAGGTTCGCACAA	GGTGACCGTAGCTGTCTCAAGG
Rab 4B	GGTGAAAACGTGGAAGAAGC	GCTGGTCCAGAAGAACAGGT
Rab 5A	CTTCAAAGGCAAGCAAGTCC	CTTCCTCTGGCTGAGTTTGC
Rab 5B	ACAAAGCTGACCTTGCCAAC	TTCTGGGGTTCACTCTTTGG
Rab 5C	CAAGCCTACGCAGATGACAA	AGGTAAGGGGCTCAGTTGCT
Rab 7A	GCATGGTAACAAGTCTGTCATC	TGCTGAAGGTCATCATCCTG
Rab 8A	GCCAGGGATATCAAAGCAAA	CAAATGGGCAGAGACCTTGT
Rab 8B	TGGAGACAAGTGCAAAATCG	GCAGAGAACACCGGAAGAAA
Rab 10	TGGGACACAGCAGGCCAGGAAC	ATGCTCCCTTGCAATCTGCTCTCCT
Rab 11A	ACGTCTGCATACTATCGTGGAGCA	AGGAACTGCCCTGAGATGACGT
Rab 11B	TTACCTCTGCGTACTACCGTGGTGC	CAAAGGCACGGGCCTCGTCA
Rab 14	AAGCAAGTGCAAAAACGGGAGAGA	CTGCGGGGCTGAGGGTTTGT
Rab 18	GGTGGGCAAGTCCAGCCTGC	ACCTTTCTTGACCAGCTGTATCCCA
Rab 22A	ATGGAGAGAGATGCCAAGGA	GGCTGTCTTCGGAGTTTGAA
Rab 23	AGGACGTCTGTGAAGGAGGA	CCACCGTTAAGGGAACTTGA
Rab 27	TCACCTGCAGTTATGGGACA	TCACAGCCCTCTGGTCTTCT
Rab 28	GCAGAAATCCTGGGAATCAA	GGGAAGAGCAGCCAGAACTA
Rab 32	GAAGGACAGCAGCCAGAGTC	AGACACATCAGCAGCACTGG
Rab 35	CTGAGCGGAAGGTGGTAGAG	ACATCGTTCTGTTGCTGCTG
Rab 38	ACCAGTTCTGCAAGGAGCAT	CCACGGGTTCTTTCTGTCAT
GDIα	CATTGGAGCTGTTGGAACCT	TGTTTGCGCTTCATGTTCTC
GDIβ	AGCATCAGCGACCTCTTTGT	TCTTGCGCTTCATTTCTTCA
GDIα	GGATCCCGAGGCCTGACCACGGACGAGGAAT	CTTAAGGCGGCCACAATCACTGCTCAGCT
Rab 5B	TGGATCCAATCTGGCCACGACTAGCAGAAG	TGAATTCAGCCACCCCCTCAGTTGCTACAA

Table III-1. Primer sequences used to generate RabGDIα and Rab GTPase expression constructs, and primers used for RT-PCR amplification of transcripts encoding Rab GTPases.

Measured mass, amu (average)	Calculated mass, amu (average)	error, amu	Sequence Position Start	End	Sequence
2900.29	2899.19	0.09	30	54	K.VLHMDRNPYYGGESSSITPLEELYK.R
1461.57	1460.65	-0.09	56	68	R.FQLLEGPPESMGR.G
1313.33	1312.47	-0.15	69	79	R.GRDWNVDLIPK.F
1126.12	1125.34	-0.23	90	98	K.MLLYTEVTR.Y
1793.07	1792.10	-0.04	90	103	K.MLLYTEVTRYLDFK.V
1656.30	1654.82	0.48	143	156	K.FLVFVANFDENDPK.T
1469.51	1468.59	-0.09	157	169	K.TFEGVDPQTTSMR.D
1867.72	1867.00	-0.29	194	208	R.TDDYLDQPCLETINR.I
939.08	938.04	0.04	211	218	K.LYSESLAR.Y
2142.25	2141.42	-0.18	222	240	K.SPYLYPLYGLGELPQGFAR.L
1491.77	1490.68	0.08	279	290	K.QLICDPSYIPDR.V
1209.02	1207.53	0.48	300	309	R.IICILSHPIK.N
2214.46	2213.39	0.06	310	328	K.NTNDANSCQIIIPQNQVNR.K
3428.71	3427.80	-0.10	349	379	K.YIAIASTTVETAEPEKEVEPALELLEPIDQK.F
4566.66	4565.89	-0.23	380	418	K.FVAISDLYEPIDDGSESQVFCSCSYDATTHFETTCNDIK.D
1504.68	1503.70	-0.03	424	436	R.MAGSAFDFENMKR.K

Table III-2. Identification of RabGDIα by MALDI-MS analysis. Tryptic peptides from Spot 4DA evaluated by MALDI-TOF. The protein was identified as Rab GDP dissociation inhibitor, Uniprot P50398. Measured masses from the MALDI-TOF spectrum are compared to calculated values. Masses listed represent 57% sequence coverage. MS-Fit MOWSE score: 1.38e+06; Mascot score 142, expect value 1.6e-10.

Rab	Probeset	Intensity	Function	Rab	Probeset	Intensity	Function
RPE Expression Reported in Literature				**ER and Golgi Transport**			
4B	1451643_a_at	8.243	Recycling endosomes	1	1416082_at	11.961	Transport; ER to Golgi
8A	1418692_at	8.832	Ciliary trafficking	1B	1424064_at	9.180	Transport; ER to Golgi
27A	1425285_a_at	6.877	Myosin recruitment to melano	2A	1419945_s_at	10.770	Transport; ER to Golgi
32	1416527_at	7.586	Post-Golgi trafficking	2B	1452667_at	7.826	Transport; ER to Golgi
38	1417700_at	10.170	Post-Golgi melano biogenesis	6	1448305_at	9.803	Retro transport; Golgi to ER
Endocytosis and Ciliary Trafficking				6B	1434914_at	8.673	Retro transport; Golgi to ER
5A	1416426_at	9.933	Early endo fusion	9	1448391_at	9.070	Transport; late endo to Golgi
5B	1422119_at	5.810	Early endo fusion	9B	1433791_at	3.812	Transport; late endo to Golgi
5C	1424684_at	8.844	Early endo fusion	10	1453095_at	10.567	Transport; Golgi to membrane
7	1415734_at	10.949	Transport to lysosomes	13	1424894_at	8.110	Tight junction biosysthesis
8B	1426799_at	8.889	Ciliary trafficking	18	1420900_a_at	10.077	Form lipid droplets from ER
12	1427992_a_at	8.433	Ciliary trafficking	19	1430148_at	5.787	Golgi
14	1419246_s_at	11.064	Early endo fusion	30	1426452_a_at	5.778	Golgi
17	1422178_a_at	6.437	Endosome recycling	33A	1417529_at	5.220	Retro transport; Golgi to ER
21	1437741_at	8.632	Endocytosis; Integrins	33B	1423083_at	9.064	Retro transport; Golgi to ER
22A	1424503_at	7.971	Endo to Golgi transport	39B	1435014_at	5.894	Golgi
23	1452113_a_at	7.029	Ciliary trafficking	42	1444450_at	4.232	Golgi
28	1423990_at	9.890	Endosomes	43	1425333_at	7.641	Golgi
35	1433922_at	7.946	Endosome recycling	**Exocytosis**			
Lysosome Distribution				3	1455922_at	8.672	Regulated exocytosis
34	1416591_at	9.475	Lysosomes	3A	1422589_at	8.289	Exocytosis; dock to membrane
36	1455064_at	6.781	Late endos and lyso	3B	1422583_at	6.948	Exocytosis; dock to membrane
Polarized Cell Recycling and transport				3C	1435047_at	6.336	Exocytosis; dock to membrane
4A	1449048_s_at	8.066	Endosome recycling	3D	1418891_a_at	8.497	Exocytosis; dock to membrane
11A	1449256_a_at	9.995	Transport; Golgi to apical endo	26	1435500_at	4.887	Regulated secretion of granules
11B	1423448_at	9.731	Transport; Golgi to apical endo	37	1433947_at	6.773	Mast Cell degranulation
15	1417829_a_at	7.696	Endosome recycling	**Rab Effector Proteins**			
25	1417738_at	8.912	Transport; Golgi to apical endo	GDI1	1451070_at	9.746	GDP dissociation inhibitor 1
40B	1436566_at	5.257	Transport; ER to Golgi endo	GDI2	1421742_at	3.918	GDP dissociation inhibitor 2
40C	1424331_at	8.738	Transport; ER to Golgi endo	CHM	1439824_at	8.308	Rab geranyl-geranyl transferase

Table III-3. Microarray analysis of Rab GTPase transcripts in RPE/choroid total RNA from 5 wk old wild-type (C57BL/6) mice. Average intensities from hybridizations using Affymetrix mouse 430_2.0 gene chips were calculated from normalized data from four replicates. When multiple probesets for a single gene were present, the one giving the highest intensity is shown.

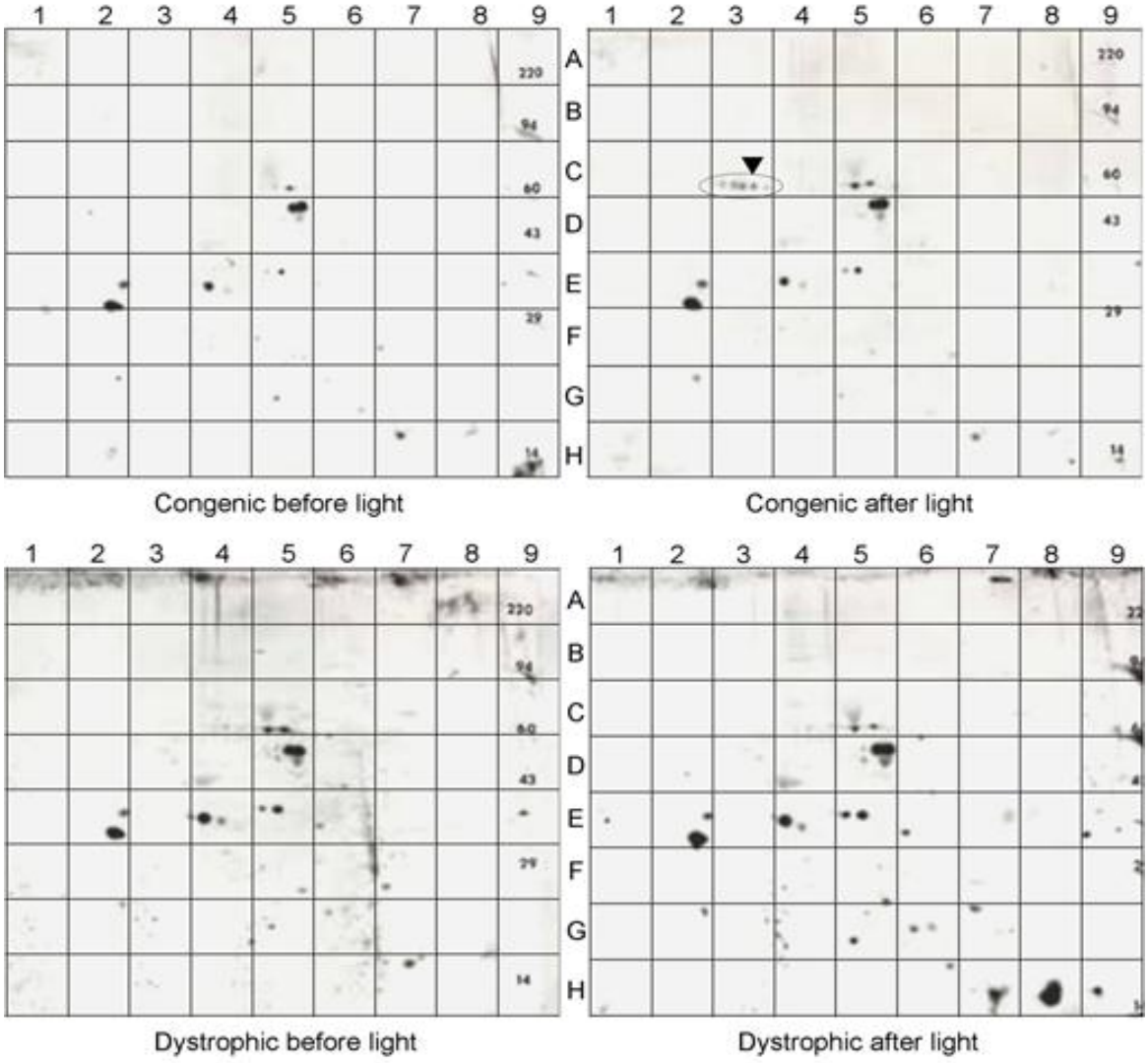

Figure III-1. Tyrosine-phosphorylated proteins in native RPE/choroid from RCS congenic and dystrophic rats. RPE/choroid protein homogenates from 4 wk old dystrophic and congenic RCS rats euthanized at 1.5 h before or 2 h after light onset were subjected to two-dimensional polyacrylamide gel electrophoresis, transferred to PVDF membranes, and probed with a monoclonal antibody specific for phosphotyrosine. Spot denoted with an arrowhead indicates the spot picked for MALDI-MS analysis.

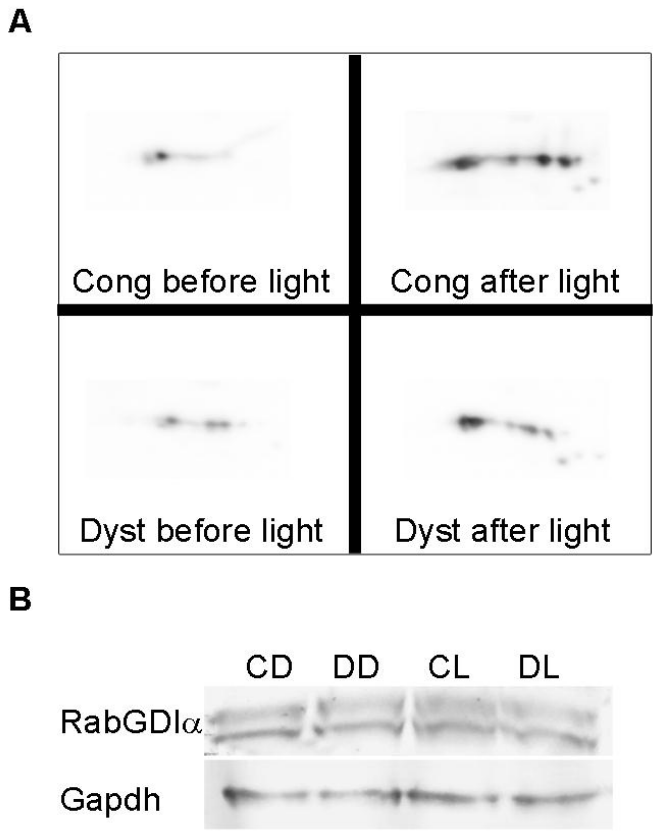

Figure III-2. Western analysis of RabGDIα expression in native RPE/choroid. RPE/choroid protein homogenates from RCS congenic and dystrophic animals were treated as described in Figure 1 and probed for RabGDIα immunoreactivity. (A) 2D western. (B) 1D western. CD, congenic rat RPE/choroid before light; DD, dystrophic rat RPE/choroid before light; CL, congenic rat RPE/choroid after light onset; DL, dystrophic rat RPE/choroid after light onset.

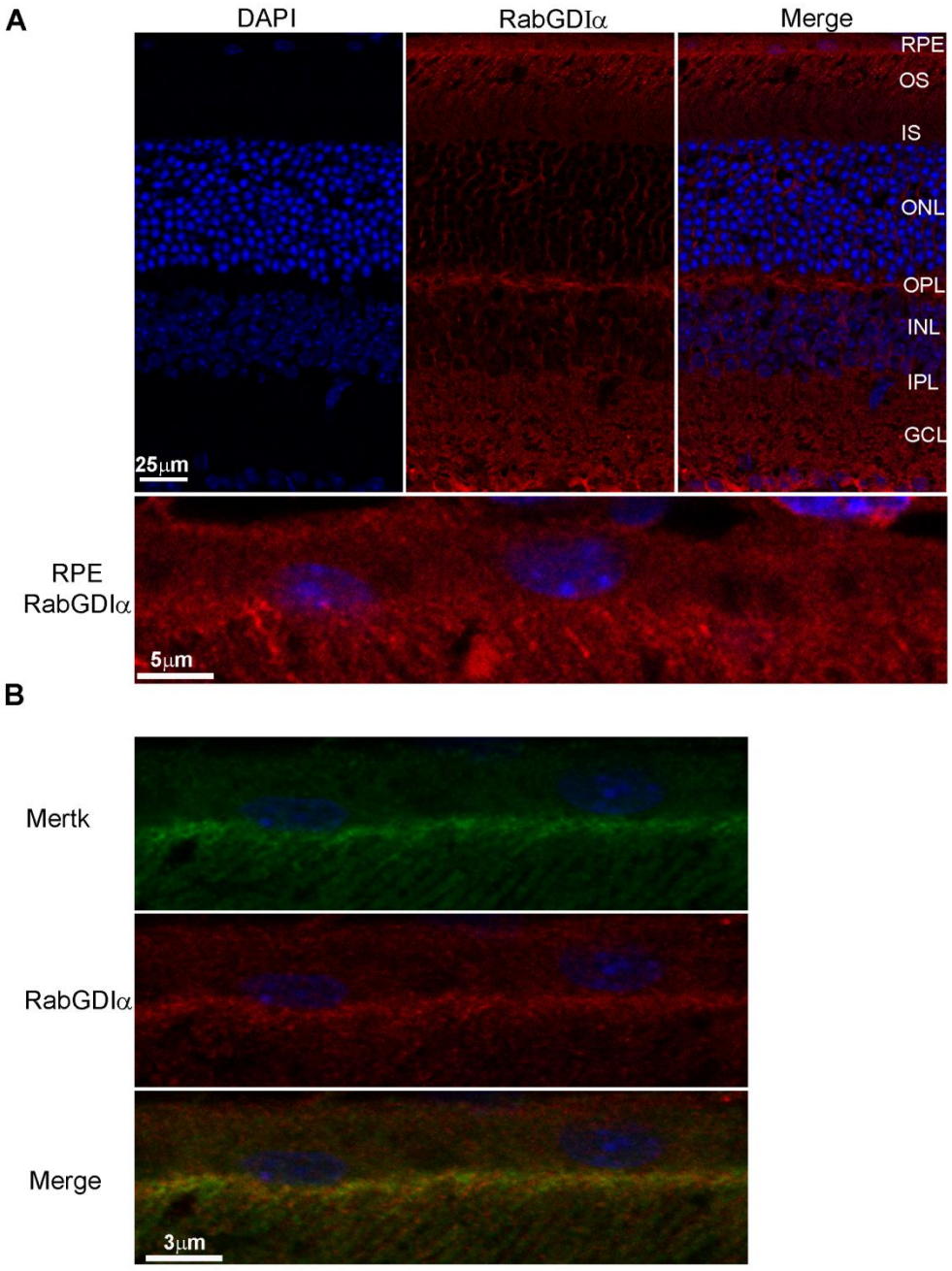

Figure III-3. Immunohistochemical analysis of RabGDIα localization expression in the RPE. (A) Retina/RPE/choroid cryosections from 4 wk old albino Balb/C mice were probed with anti-RabGDIα primary and AlexaFluor 555 secondary antibodies, and imaged using indirect fluorescence confocal microscopy. A selected area of RPE was enlarged to show localization in that cell layer. (B) Co-localization of anti-RabGDIα and anti-MERTK immunolabeling detected with AlexFluor 488 and 555 secondary antibodies, respectively. RPE, retinal pigment epithelium; OS, outer segments; IS, inner segments; ONL, outer nuclear layer; OPL, outer plexiform layer; INL, inner nuclear layer; IPL, inner plexiform layer. Nuclei were stained with DAPI (4′,6-diamidino-2-phenylindole).

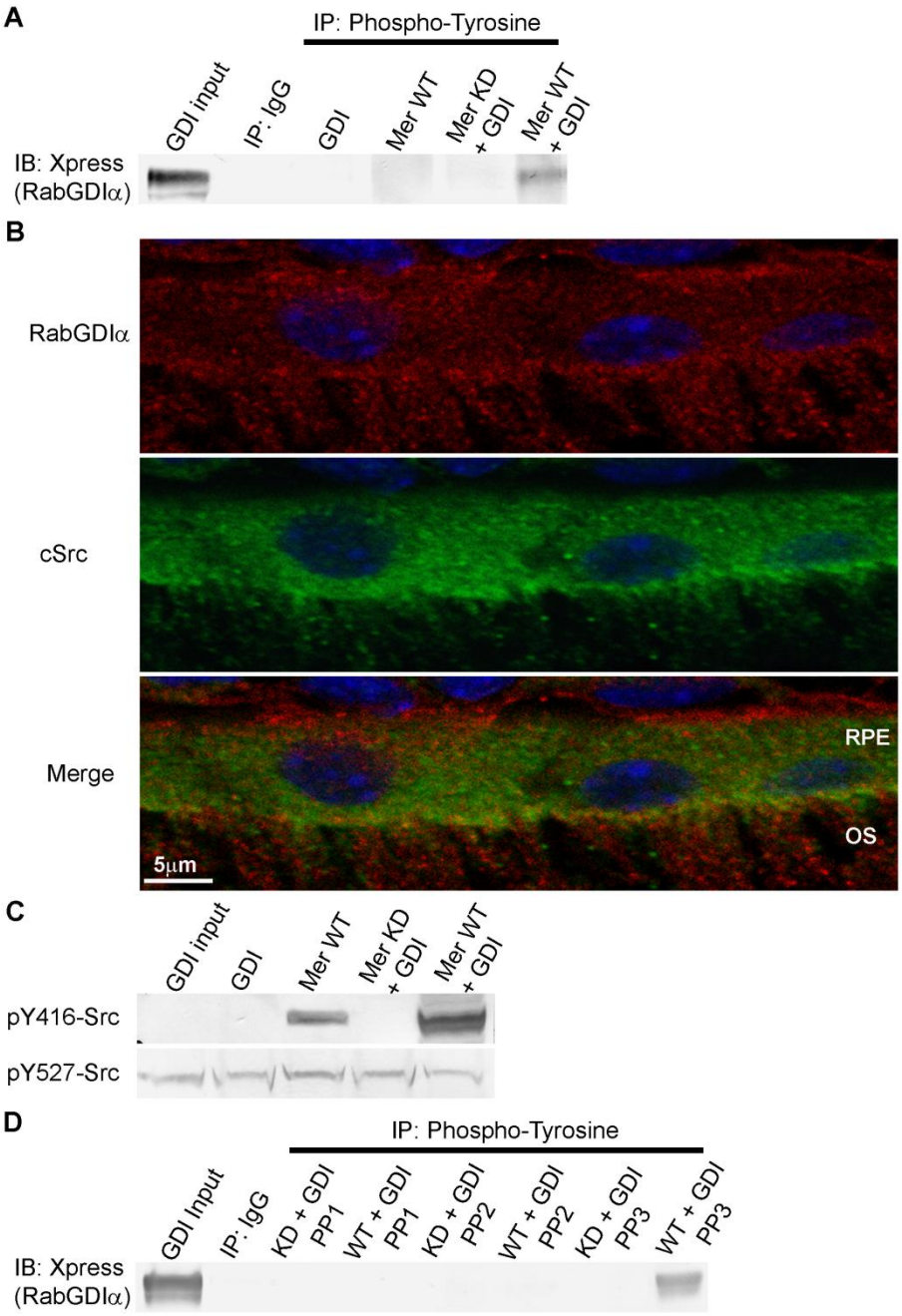

Figure III-4. RabGDIα phosphorylation and localization with cSrc. (A-B) Anti-phosphotyrosine immunopreciptations of transfected HEK-293T cells probed with anti-Xpress (RabGDIα) antibody. IgG, IgG control; GDI, rRabGDIα; Mer WT, full length wild-type MERTK; MerKD, kinase-dead R844C-MERTK mutant. (B) Immunostaining of the RPE layer of cryosections from albino Balb/C mice probed with anti-RabGDIα and anti-Src primary antibodies, and AlexFluor 488 and 555 secondary antibodies, respectively. (C) pY416Src and pY527-Src immunoreactivity on western blots of HEK-293T cells transfected with RabGDIα and wild-type MERTK or R844C-MERTK. (D) Immunoprecipitations as in (A) with PP1, PP2, and PP3 inhibitors of Src kinase activity included.

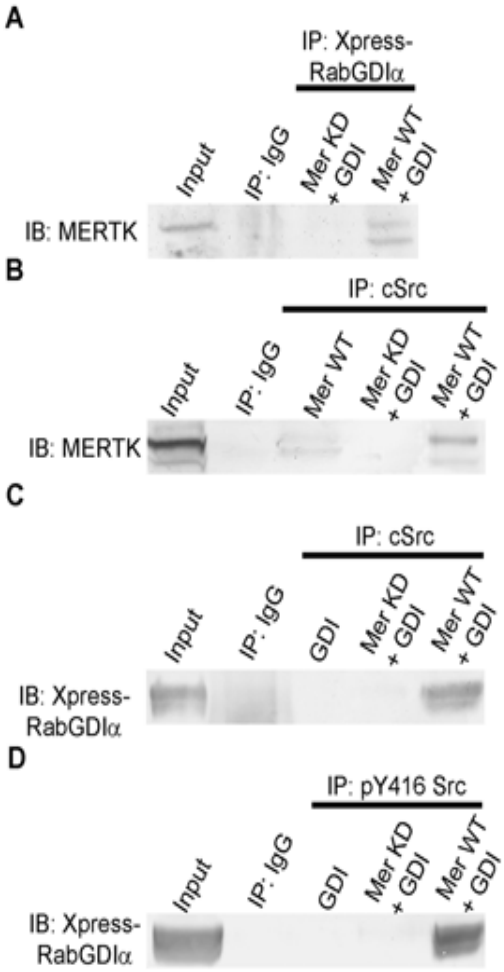

Figure III-5. RabGDIα interaction with MERTK and Src. HEK-293T cells transfected with RabGDIα and wild-type MERTK or R844C-MERTK were lysed and immunoprecipitations performed using antibodies against Src, pY416-Src, or Xpress (RabGDIα). (A) rRabGDIα (Xpress antibody) immunoprecipitations with western analysis of MERTK. (B) Src immunoprecipitations with western analysis of MERTK. (C) Src immunoprecipitations with western analysis with Xpress (rRabGDIα) (D) pY416-Src immunoprecipitations with western analysis of rRabGDIα (Xpress antibody).

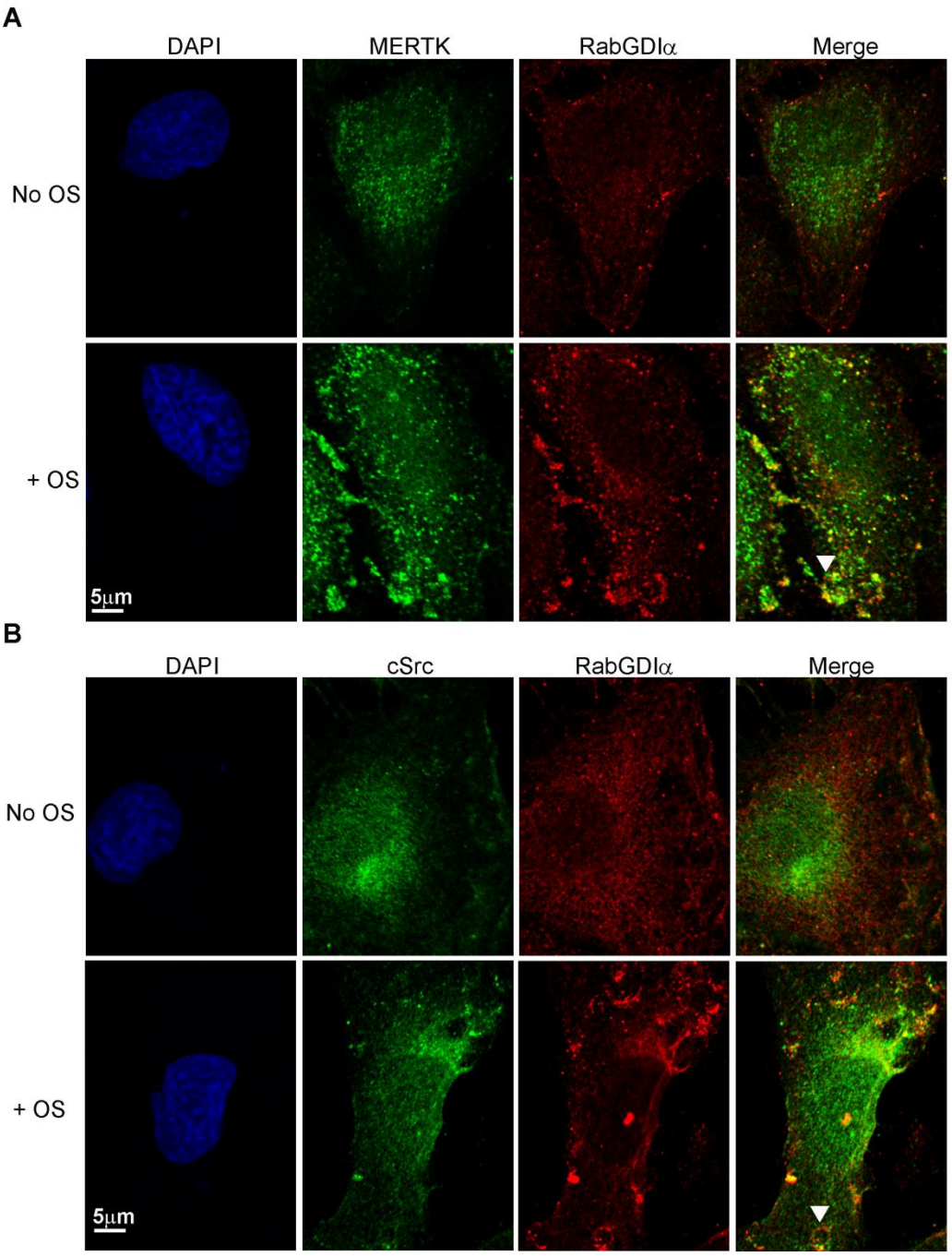

Figure III-6. RabGDIα co-localization with MERTK and cSrc in cultured cells during OS challenge. Immunofluorescence imaging of ingested phagosomes in confluent cultures of RPE-J cells incubated with bovine OS for 4 h, fixed, and labeled with primary antibodies to RabGDIα, MERTK, cSrc, and Alexa Fluor 488 (RabGDIα) or 555 (MERTK, Src) secondary antibodies, and imaged using indirect fluorescence confocal. (A) Co-localization of MERTK with RabGDIα in the presence or absence of added OS. (B) Co-localization of RabGDIα with Src as in (A). White arrowhead indicates phagosome.

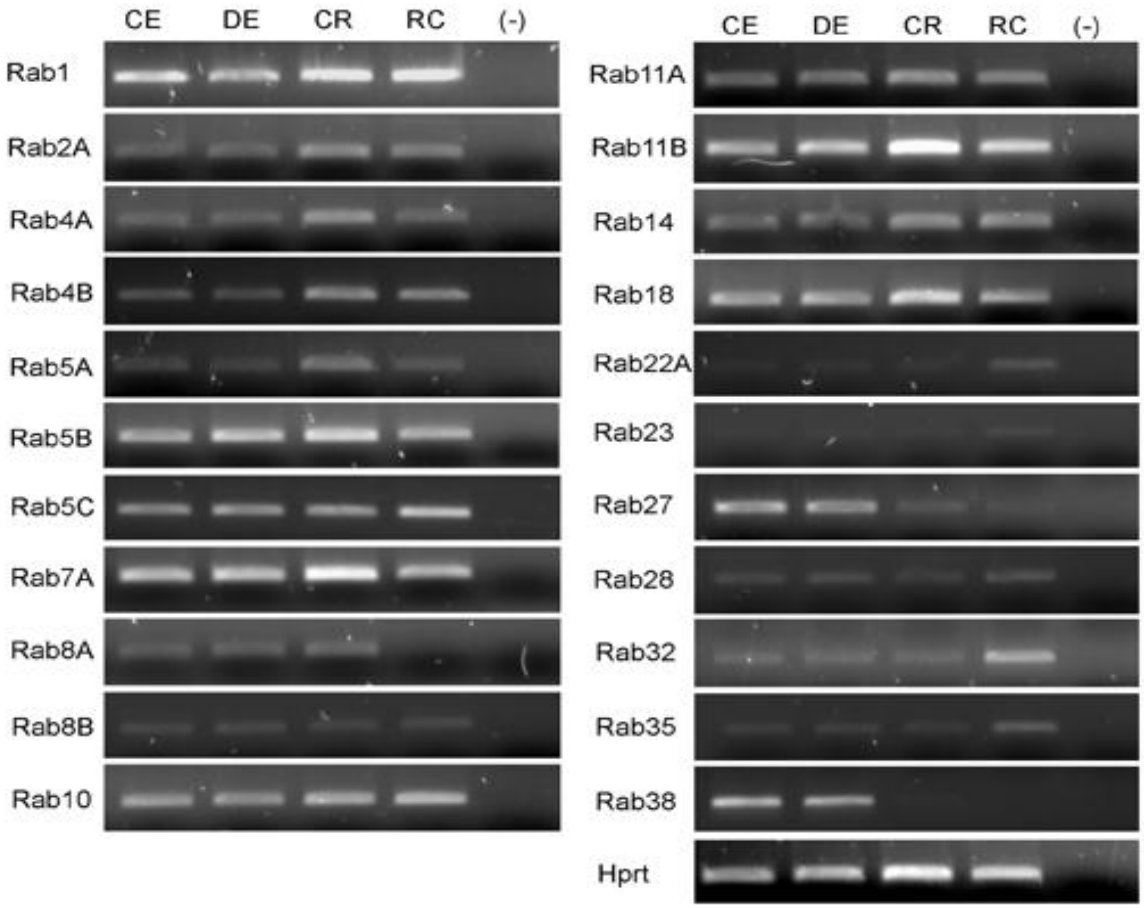

Figure III-7. RT-PCR analysis of Rab GTPase transcripts in rat RPE/choroid, retina, and RPE-J cells. RCS dystrophic and congenic rats reared in 12h/12h cyclic lighting were sacrificed 2 hr after light onset. Total RNA was isolated from dissected RPE/choroid, retina, and RPE-J cells, then reverse-transcribed and amplified with gene-specific primers flanking at least one intron in the genomic sequence. HPRT primers were used to confirm equal amounts of cDNA per reaction. CE, congenic rat RPE/choroid; DE, dystrophic rat RPE/choroid, CR, congenic rat retina; RC, RPE-J cells; (-), no cDNA.

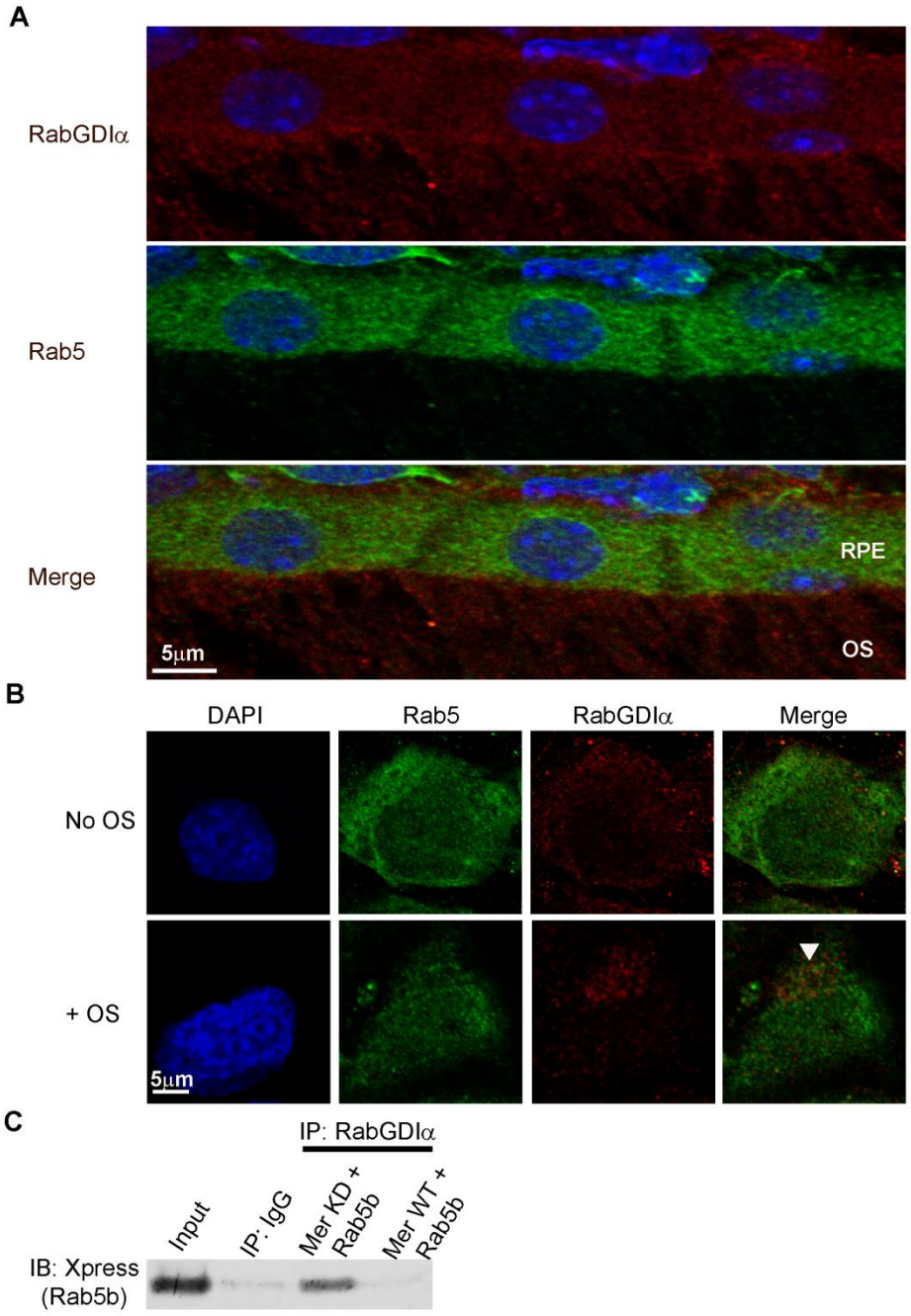

Figure III-8. Effect of RabGDI tyrosine phosphorylation on its interaction with Rab5 in the RPE. (A) RabGDIα and Rab5 co-localization in the RPE layer from albino mice imaged using indirect immunofluorescence with confocal microscopy. (B) Imaging of ingested phagosomes labeled with primary antibodies to RabGDIα and Rab5, with Alexa Fluor 488 or 555 secondary antibodies, as in Figure 6. (C) HEK-293T cells were transfected with constructs encoding rRab5B and wild-type MERTK or kinase-dead R844C-MERTK, and were immunoprecipitated with antibody against RabGDIα and probed for Rab5B using anti-Xpress antibody.

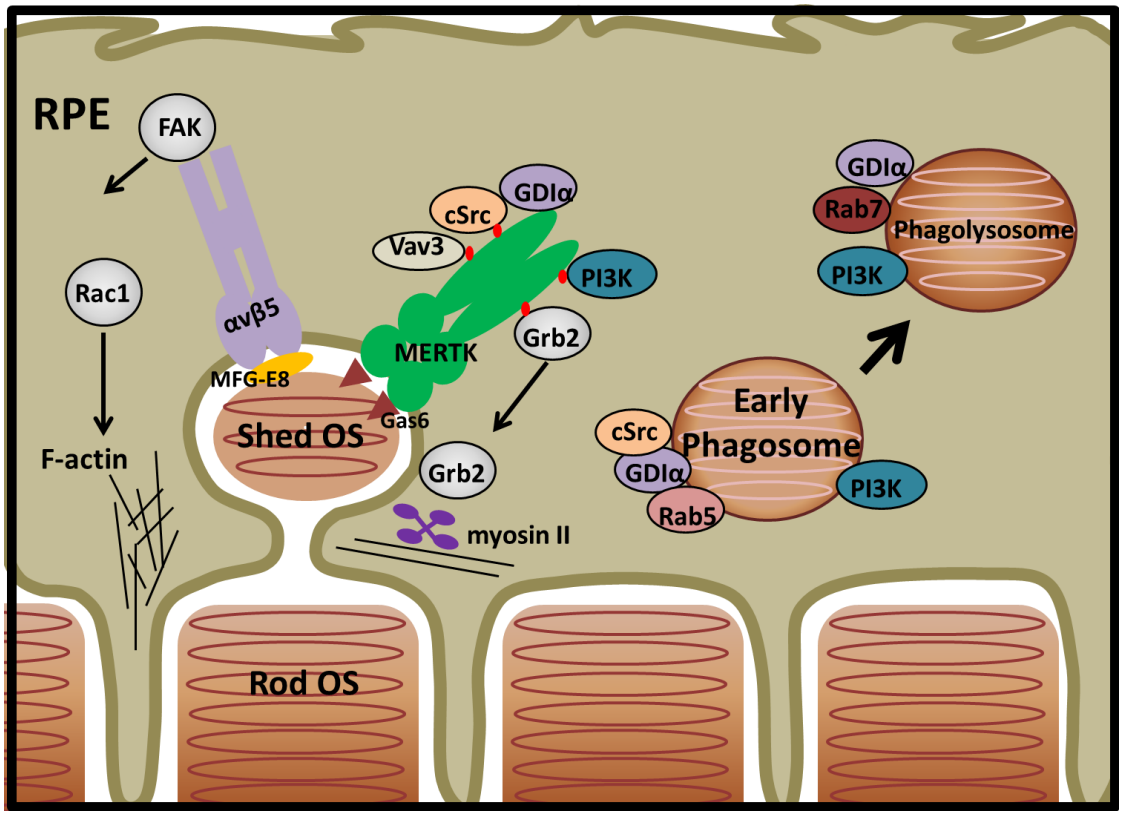

Figure III-9. Schematic of MERTK signaling to RabGDI in the RPE. The model shown depicts the signaling of MERTK to RabGDIα and Src in the RPE, in addition to a cohort of proteins including Grb2, p85α, and myosin II found to directly interact with the cytoplasmic domain of MERTK in the RPE. The model also depicts $\alpha_v\beta_5$ integrin signaling to FAK and Rac1.

CHAPTER IV

Discussion and Future Directions

The work described in this dissertation has contributed to further elucidating the mechanism of RPE phagocytosis. MERTK-mediated signaling is an essential aspect of RPE phagocytosis, and plays a variety of roles in the process including OS uptake and anti-inflammation. This body of work has implicated MERTK signaling in the regulation of cytoskeletal remodeling, and for the first time, in membrane trafficking. MERTK was found to interact with SH2-domain proteins important in a gambit of cellular functions, including those that regulate cytoskeletal rearrangement and membrane trafficking. MERTK was also shown to regulate the downstream tyrosine phosphorylation of an effector for the Rab family of GTPases important in membrane trafficking. These findings present a novel role of MERTK and serve to increase our understanding of MERTK-mediated signaling in RPE phagocytosis.

Direct interactions with MERTK

Previous studies identified signaling partners of MERTK in macrophages and dendritic cells following the uptake of apoptotic cells. These included GRB2, VAV1, PLCγ2, and SRC, as well as an indirect interaction with PI3K [59, 61, 62, 242]. In contrast, little was known about MERTK interacting

proteins in the RPE and their role in RPE phagocytosis. Myosin II was the sole known MERTK interacting protein shown to be necessary for phagocytic uptake of OS [89]. The current studies sought to identify SH2-domain proteins that interact with MERTK and to elucidate their functions in the RPE. The results showed that MERTK signaling partners overlap with those involved in apoptotic cell clearance in professional phagocytes, with some marked differences as detailed in Chapter II.

First, MERTK interaction with GRB2 was confirmed, and knockdown in cultured RPE cells showed a requirement for GRB2 in uptake but not binding of OS. Previous studies had shown that GRB2 is necessary in phagocytic uptake of apoptotic cells and control of the inflammatory response [59, 60]. The present data suggest that GRB2 may serve a similar dual function in the RPE. This possibility is of interest due to previously demonstrated interactions of GRB2 with an effector of the Ras signaling pathway and its association with dynamin and myosin [199, 212]. The findings from the current studies could indicate that GRB2 and myosin II may form an association in the RPE. Both myosin II and GRB2 have been shown to be required for phagocytic uptake [89]. Studies beyond the scope of this thesis would assess their interaction with one another and with other proteins in a complex with MERTK, to determine whether GRB2 signaling may directly regulate phagocytic uptake in the RPE.

Second, in contrast to previous findings, a direct interaction between PI3K and MERTK in the RPE was demonstrated in the present studies. PIK3R1 was found to localize to early phagosomes in a position to aid in membrane trafficking

by attracting Rab5 GTPase to the membrane. These findings suggest that MERTK-mediated activation of PI3K may lead to increased activity of PI3K in membrane trafficking in the RPE. Previous studies have shown multiple isoforms of PI3K are involved in membrane maturation and trafficking, specifically to synthesize the appropriate lipids needed to recruit additional proteins to the membrane [243]. The activation of PI3K is likely to recruit a cohort of proteins to the forming phagosome and phagolysosome in RPE phagocytosis in the same manner as in endocytosis and additional types of receptor mediated phagocytosis. It would be of interest to identify proteins that are recruited in response to activation of PI3K, as they may well be different isoforms of proteins or attracted in a different order than in other systems which could be attributed to the direct interaction of PI3K with MERTK.

Third, Vav1 was shown to interact with MERTK in vitro, but Vav3 was found to be the predominant isoform in the RPE. Neither Vav1 nor Vav3 were expressed in cultured RPE-J cells that maintain the ability to phagocytose OS. In addition, the Vav 2/3 -/- mouse exhibits a glaucoma-like phenotype, but no phagocytic defect or retinal dystrophy similar to the RCS rat, suggesting that the VAV family proteins are not required for phagocytic uptake in the RPE [208]. However, a recent study of Rac1 GTPase, for which the VAV family are known effectors, demonstrated that Rac1 functions downstream of integrins in RPE phagocytosis [63]. Taken together, these findings could point to a role of VAV proteins in the RPE involving their activation by MERTK, with additional crosstalk between VAV3 and integrin-mediated signaling being necessary for regulating

Rac1 activation. An alternative hypothesis that appears to be more likely is that VAV family proteins are not involved in phagocytic uptake due to the ability of ELMO and Dock180 proteins to form a bipartite GEF for Rac1 downstream of integrins [244].

Finally, the interaction of SRC and MERTK was confirmed and activation of SRC was shown to occur downstream of MERTK activation. The MERTK-mediated activation of SRC allows for a mechanism involving tyrosine phosphorylation and regulation of many subsequent proteins in the RPE. The reach of a receptor tyrosine kinase is highly dependent on activating a non-receptor tyrosine kinase to continue to conduct and direct the initiating signal in order to achieve the necessary cellular response. SRC is an appropriate candidate for this task and has been shown in multiple systems to function in the regulation of cytoskeletal rearrangement. Characterization of SRC protein interactions in the RPE would be of keen interest as it could identify multiple proteins that are directly involved in RPE phagocytosis.

MERTK-mediated tyrosine phosphorylation

As a receptor tyrosine kinase, an important aspect of MERTK regulation of cellular mechanisms is likely to involve secondary tyrosine phosphorylation of effector proteins. The disruption of the phagocytic mechanism in the RCS rat points to the importance of MERTK in maintenance of RPE cellular homeostasis. The present studies evaluated the differences in tyrosine phosphorylation between the congenic rat and the dystrophic RCS rat to identify RPE proteins modified downstream of MERTK activation. The tyrosine

phosphorylation profiles of congenic and dystrophic rats were compared during times of low phagocytic activity and times of peak phagocytic activity. The results showed significant overlap of tyrosine phosphorylation profiles in all samples, with one marked difference. Mass spectral analysis identified the differentially phosphorylated protein as RabGDIα, an effector of the Rab GTPases [174].

The work detailed in Chapter 3 describes the identification of RabGDIα and its regulation by MERTK, and the possible effects of tyrosine phosphorylation on RabGDIα function. RabGDIα expression was confirmed in the RPE using immunohistochemical analysis to demonstrate expression within the RPE and the apical microvilli, as well as co-localization with MERTK. Experiments were also conducted to confirm that MERTK activation was required for tyrosine phosphorylation of RabGDIα. As no phospho-specific antibodies for RabGDIα were available, phosphotyrosine immunoprecipitations were used to provide further evidence of the modification of RabGDIα in cultured cells. The intracellular protein kinase, Src, was also localized to the MERTK/RabGDIα complex, and the activated form of Src was required for tyrosine phosphorylation of RabGDIα. Studies in RPE-J cells also showed co-localization of RabGDIα with MERTK and Src upon ingestion of OS, suggesting that all three proteins form a complex to regulate membrane trafficking in the RPE. These findings are of significant interest in that they further confirm the direct interaction of MERTK with Src, and suggest that Src is specifically performing MERTK-mediated functions involved in regulation of proteins downstream of the receptor. In

addition, as the interaction of Src and RabGDIα demonstrates, identifying Src protein interactions could identify additional functions of MERTK in the RPE.

Further experiments examined the effect of RabGDIα tyrosine phosphorylation on its binding to Rab5 GTPase that functions in early endosome/phagosome formation. The results showed that RabGDIα has a lower affinity for Rab5 when tyrosine phosphorylated downstream of MERTK activation. This suggests that the tyrosine phosphorylation may serve to decrease the period of the Rab5 GTPase and RabGDIα interaction during peak phagocytosis to facilitate a more rapid formation and maturation process of phagosomes. These findings represent the first evidence that MERTK signaling regulates membrane trafficking in the RPE.

Altogether, the research presented in this thesis identifies a novel system of MERTK-mediated regulation of RPE phagocytosis. Direct interaction of MERTK with SH2-domain protein GRB2 likely aids in the facilitation of myosin II in phagocytic cup closure, while interaction with PI3K serves in the eventual recruitment of proteins required for membrane trafficking. The direct interaction of MERTK and Src and its subsequent activation has proven to be instrumental in the regulation of membrane trafficking through tyrosine phosphorylation of RabGDIα. The characterization of these interactions has revealed another facet of the MERTK signaling pathway, in addition to its roles in cytoskeletal rearrangement and anti-inflammatory control, which is now shown to include regulation of membrane trafficking.

Future Directions

The present studies implicate MERTK in the regulation of membrane trafficking in the RPE. This finding may represent a specialized function of MERTK occurring in a limited number of cell types. MERTK is primarily expressed in myeloid, epithelial, and reproductive cells [245, 246]. Although RabGDI is expressed in many tissues, the alpha isoform is present mainly in neural and cancerous cells [224]. In addition, RabGDIα is tyrosine phosphorylated in both cancerous cells and in brain tissue [226, 227]. MERTK has been shown to have high levels of expression and hyper-phosphorylation in cancerous cells including glioblastomas and lymphomas [247, 248]. This suggests that the phenomenon occurring in the RPE with MERTK-mediated tyrosine phosphorylation of RabGDIα may also occur in brain tissue and various cancerous cells. Thus, it would be of great interest to more completely understand the ramifications of this tyrosine phosphorylation on RabGDIα function. It is plausible that phosphorylation does not occur under normal conditions and it is a response to cellular stress and the Rab GTPase cycling system. In RPE phagocytosis, RabGDIα is tyrosine phosphorylated under conditions of peak phagocytic uptake which induces more turnover action of Rab GTPases. Comparatively, tyrosine phosphorylation of residue Y333 in cancer cells is likely downstream of MERTK hyper-phosphorylation, directly pointing to a stressful environment for many cellular processes and proteins including Rab GTPases. Studying the parallels of MERTK and RabGDIα tyrosine

phosphorylation in the RPE and cancer cells could yield interesting insights into this regulatory process.

Another interesting facet of the RabGDIα tyrosine phosphorylation story is the relationship between RabGDIα and Rab GTPases previously reported to be involved in RPE and OS specific functions. The current studies have shown specific high level expression of Rab27A and Rab38 in the RPE but not in the retina. Rab27A, Rab32, and Rab38 have been shown to be involved in melanosome transport in the RPE [180-182, 184]. The current studies have also shown high levels of Rab1, Rab11B, and Rab18 in the retina, which are involved in vesicle trafficking and fusion in OS [249]. As the current studies have shown that RabGDIα and Rab5 binding are affected by tyrosine phosphorylation of RabGDIα, it is reasonable to propose that this modification similarly influences RabGDIα interaction with other Rab GTPases in the RPE and neural retina. Studies using Rab GTPase clones generated during the present studies could easily be performed in cultured cells co-transfected with MERTK. If tyrosine phosphorylation of RabGDIα is found to occur in the OS, it would be interesting to determine which receptor(s) are involved and how the modification affects binding with various Rab GTPases.

The studies presented in Chapter II examined the expression of SRC-family kinases in the RPE using reverse-transcriptase PCR, finding Yes and Fyn to be two of the most abundant transcripts. In a previous model of MERTK-mediated phagocytic clearance of apoptotic cells, SRC-family kinases were implicated in the process, but no specific family member had been identified to

perform crosstalk between MERTK and αvβ5 integrin signaling to Rac1 and cytoskeletal reorganization [55]. To study SRC-family kinases in this crosstalk, the authors used a SRC/Yes/Fyn deficient mouse fibroblast cell line and observed down-regulation of FAK phosphorylation downstream of MERTK. The results of the present studies are consistent with the possibility that the SRC-family kinase that crosstalks between MERTK and αvβ5 integrin is SRC. The finding that SRC directly binds to Mertk provides an important clarification of this model, however the possibility remains that Yes or Fyn may be the actual family member involved. In addition, the pY416 SRC antibody used in the present studies cross-reacts with a number of SRC-family kinases including Yes and Fyn. In addition, SRC co-localization with RabGDIα in retinal cross sections and RPE-J cells challenged with OS was relatively weak compared to MERTK and RabGDIα co-localization. These results leave open the possibility that Yes or Fyn could be phosphorylating RabGDIα instead of SRC. Future studies of Fyn and Yes involvement in tyrosine phosphorylation of RabGDIα will be critical for obtaining a complete story of this MERTK-mediated regulation of Rab GTPases.

The field of vision research has experienced rapid progress in developing clinical treatments based on the identification of disease genes involved in critical cellular processes. This is due to the ability of the eye to provide an isolated environment for targeted therapies. For example, studies following the identification of MERTK as the defective gene in the dystrophic RCS rat showed that the phenotype could be corrected by subretinal injection of an adenoviral MERTK construct [87]. There are many other gene therapy studies that have

successfully restored vision in animals after the injection of viral constructs [250-252]. These studies could not have been completed without prior research that identified the genes, analyzed their functions, and identified the effect of their mutations on critical functions of the retina and the RPE. Phagocytosis is one of those critical functions and it is reasonable to propose that the genes encoding some of the proteins involved in MERTK signaling may also be identified as retinal dystrophy genes. Since most of the MERTK interacting partners are embryonic lethal in knockout animals, it is possible to exclude many of them as disease genes. Rab Escort Protein (REP1) is a disease gene found to be defective in Chorodermia [185]. Due to its importance in many different cell types, it is not likely that RabGDIs would be retinal dystrophy genes. In addition, mutations in RabGDIα residues L92 and R423 result in X-linked mental retardation [238, 239].

Finally, the findings reported in this dissertation may have relevance to studies of age-related macular degeneration (AMD). AMD is characterized by progressive retinal degeneration and loss of central vision that are accompanied with the formation of drusen, deposits of extracellular protein and lipid matter [253, 254]. Very little is known about the cellular processes that are compromised in AMD, as well as if the drusen is the cause of AMD or a symptom of another underlying disease process. Certainly issues affecting innate immunity and inflammation play important roles. The drusen are located between the RPE and Bruch's membrane and are thought to limit the nutrient uptake from the choroid by the RPE, thereby starving the retina [255]. One possibility is that the drusen

deposits are the result of a defective autophagy pathway [254]. Autophagy occurs within cells to remove spent cellular components from the cell, effectively inhibiting apoptotic cell death. As a post-mitotic cell layer, the RPE is a prime candidate for autophagy and has been shown to express autophagy markers [256, 257]. Autophagy and phagocytosis converge onto a common point at the lysosome, and share other common protein interactions and complexes at points before the formation of the lysosome. Both autophagosomes and phagosomes involve maturation processes that are facilitated by PI3K and its products [243]. In previous studies of murine macrophages that perform both autophagy and phagocytosis, it was shown that the autophagy marker LC3 was recruited to phagosomes to aid in maturation [258]. These studies provided the first link between autophagy and phagocytosis in professional phagocytes, which begging the question whether the same process may be occurring in RPE cells. Additionally, the present finding that MERTK mediates membrane trafficking may be relevant to AMD, since membrane trafficking will likely be defective in autophagy as well.

As a whole, the studies presented in this dissertation have provided new insight into the process of RPE phagocytosis, specifically the mechanism of MERTK signaling. The studies demonstrated a direct role of MERTK in membrane trafficking, and advanced the concept that the highly specialized mechanism of RPE phagocytosis represents a unique adaptation of that occurring in other phagocytic cell types.

Bibliography

1. Masland, R.H., *The fundamental plan of the retina.* Nat Neurosci, 2001. **4**(9): p. 877-86.
2. Wallace, V.A., *Making a Retina-From the Building Blocks to Clinical Applications.* Stem Cells, 2011.
3. Nickla, D.L. and J. Wallman, *The multifunctional choroid.* Prog Retin Eye Res, 2010. **29**(2): p. 144-68.
4. Strauss, O., *The retinal pigment epithelium in visual function.* Physiol Rev, 2005. **85**(3): p. 845-81.
5. Sung, C.H. and J.Z. Chuang, *The cell biology of vision.* J Cell Biol, 2010. **190**(6): p. 953-63.
6. Bok, D., *The retinal pigment epithelium: a versatile partner in vision.* J Cell Sci Suppl, 1993. **17**: p. 189-95.
7. Wasmeier, C., et al., *Melanosomes at a glance.* J Cell Sci, 2008. **121**(Pt 24): p. 3995-9.
8. Rizzolo, L.J., *Development and role of tight junctions in the retinal pigment epithelium.* Int Rev Cytol, 2007. **258**: p. 195-234.
9. Wislocki, G.B. and A.J. Ladman, *The demonstration of a blood-ocular barrier in the albino rat by means of the intravitam deposition of silver.* J Biophys Biochem Cytol, 1955. **1**(6): p. 501-10.
10. Rizzolo, L.J., *The distribution of Na+,K(+)-ATPase in the retinal pigmented epithelium from chicken embryo is polarized in vivo but not in primary cell culture.* Exp Eye Res, 1990. **51**(4): p. 435-46.
11. Rizzolo, L.J. and Z.Q. Li, *Diffusible, retinal factors stimulate the barrier properties of junctional complexes in the retinal pigment epithelium.* J Cell Sci, 1993. **106 (Pt 3)**: p. 859-67.
12. Saari, J.C., *Biochemistry of visual pigment regeneration: the Friedenwald lecture.* Invest Ophthalmol Vis Sci, 2000. **41**(2): p. 337-48.
13. Kennedy, B. and J. Malicki, *What drives cell morphogenesis: a look inside the vertebrate photoreceptor.* Dev Dyn, 2009. **238**(9): p. 2115-38.
14. Young, R.W., *The renewal of photoreceptor cell outer segments.* J Cell Biol, 1967. **33**(1): p. 61-72.
15. Young, R.W. and B. Droz, *The renewal of protein in retinal rods and cones.* J Cell Biol, 1968. **39**(1): p. 169-84.
16. Humphries, M.M., et al., *Retinopathy induced in mice by targeted disruption of the rhodopsin gene.* Nat Genet, 1997. **15**(2): p. 216-9.
17. Sung, C.H., et al., *A rhodopsin gene mutation responsible for autosomal dominant retinitis pigmentosa results in a protein that is defective in localization to the photoreceptor outer segment.* J Neurosci, 1994. **14**(10): p. 5818-33.
18. Chuang, J.Z., Y. Zhao, and C.H. Sung, *SARA-regulated vesicular targeting underlies formation of the light-sensing organelle in mammalian rods.* Cell, 2007. **130**(3): p. 535-47.

19. Young, R.W. and D. Bok, *Participation of the retinal pigment epithelium in the rod outer segment renewal process.* J Cell Biol, 1969. **42**(2): p. 392-403.
20. Anderson, D.H., S.K. Fisher, and R.H. Steinberg, *Mammalian cones: disc shedding, phagocytosis, and renewal.* Invest Ophthalmol Vis Sci, 1978. **17**(2): p. 117-33.
21. Strauss, O., et al., *The Royal College of Surgeons rat: an animal model for inherited retinal degeneration with a still unknown genetic defect.* Acta Anat, 1998. **162**(2-3): p. 101-11.
22. LaVail, M.M., *Legacy of the RCS rat: impact of a seminal study on retinal cell biology and retinal degenerative diseases.* Prog Brain Res, 2001. **131**: p. 617-27.
23. Sarangarajan, R. and S.P. Apte, *Melanization and phagocytosis: implications for age related macular degeneration.* Mol Vis, 2005. **11**: p. 482-90.
24. Young, R.W., *The daily rhythm of shedding and degradation of cone outer segment membranes in the lizard retina.* J Ultrastruct Res, 1977. **61**(2): p. 172-85.
25. Young, R.W., *The daily rhythm of shedding and degradation of rod and cone outer segment membranes in the chick retina.* Invest Ophthalmol Vis Sci, 1978. **17**(2): p. 105-16.
26. O'Day, W.T. and R.W. Young, *Rhythmic daily shedding of outer-segment membranes by visual cells in the goldfish.* J Cell Biol, 1978. **76**(3): p. 593-604.
27. LaVail, M.M., *Circadian nature of rod outer segment disc shedding in the rat.* Invest Ophthalmol Vis Sci, 1980. **19**(4): p. 407-11.
28. LaVail, M.M., *Rod outer segment disk shedding in rat retina: relationship to cyclic lighting.* Science, 1976. **194**(4269): p. 1071-4.
29. May, R.C. and L.M. Machesky, *Phagocytosis and the actin cytoskeleton.* J Cell Sci, 2001. **114**(Pt 6): p. 1061-77.
30. Kevany, B.M. and K. Palczewski, *Phagocytosis of retinal rod and cone photoreceptors.* Physiology (Bethesda), 2010. **25**(1): p. 8-15.
31. Swanson, J.A. and A.D. Hoppe, *The coordination of signaling during Fc receptor-mediated phagocytosis.* J Leukoc Biol, 2004. **76**(6): p. 1093-103.
32. Hafizi, S. and B. Dahlback, *Signalling and functional diversity within the Axl subfamily of receptor tyrosine kinases.* Cytokine Growth Factor Rev, 2006. **17**(4): p. 295-304.
33. Seitz, H.M., et al., *Macrophages and dendritic cells use different Axl/Mertk/Tyro3 receptors in clearance of apoptotic cells.* J Immunol, 2007. **178**(9): p. 5635-42.
34. Cox, D. and S. Greenberg, *Phagocytic signaling strategies: Fc(gamma)receptor-mediated phagocytosis as a model system.* Semin Immunol, 2001. **13**(6): p. 339-45.

35. Cougoule, C., et al., *Dissociation of recruitment and activation of the small G-protein Rac during Fcgamma receptor-mediated phagocytosis.* J Biol Chem, 2006. **281**(13): p. 8756-64.
36. Groves, E., et al., *Molecular mechanisms of phagocytic uptake in mammalian cells.* Cell Mol Life Sci, 2008. **65**(13): p. 1957-76.
37. Kiefer, F., et al., *The Syk protein tyrosine kinase is essential for Fcgamma receptor signaling in macrophages and neutrophils.* Mol Cell Biol, 1998. **18**(7): p. 4209-20.
38. Ridley, A.J., *Rho GTPases and actin dynamics in membrane protrusions and vesicle trafficking.* Trends Cell Biol, 2006. **16**(10): p. 522-9.
39. Massol, P., et al., *Fc receptor-mediated phagocytosis requires CDC42 and Rac1.* EMBO J, 1998. **17**(21): p. 6219-29.
40. Bustelo, X.R., *Regulatory and signaling properties of the Vav family.* Mol Cell Biol, 2000. **20**(5): p. 1461-77.
41. O'Bryan, J.P., et al., *axl, a transforming gene isolated from primary human myeloid leukemia cells, encodes a novel receptor tyrosine kinase.* Mol Cell Biol, 1991. **11**(10): p. 5016-31.
42. Janssen, J.W., et al., *A novel putative tyrosine kinase receptor with oncogenic potential.* Oncogene, 1991. **6**(11): p. 2113-20.
43. Mark, M.R., et al., *rse, a novel receptor-type tyrosine kinase with homology to Axl/Ufo, is expressed at high levels in the brain.* J Biol Chem, 1994. **269**(14): p. 10720-8.
44. Stitt, T.N., et al., *The anticoagulation factor protein S and its relative, Gas6, are ligands for the Tyro 3/Axl family of receptor tyrosine kinases.* Cell, 1995. **80**(4): p. 661-70.
45. Nagata, K., et al., *Identification of the product of growth arrest-specific gene 6 as a common ligand for Axl, Sky, and Mer receptor tyrosine kinases.* J Biol Chem, 1996. **271**(47): p. 30022-7.
46. Uehara, H. and E. Shacter, *Auto-oxidation and oligomerization of protein S on the apoptotic cell surface is required for Mer tyrosine kinase-mediated phagocytosis of apoptotic cells.* J Immunol, 2008. **180**(4): p. 2522-30.
47. Sasaki, T., et al., *Structural basis for Gas6-Axl signalling.* EMBO J, 2006. **25**(1): p. 80-7.
48. Nakano, T., et al., *Cell adhesion to phosphatidylserine mediated by a product of growth arrest-specific gene 6.* J Biol Chem, 1997. **272**(47): p. 29411-4.
49. Anderson, H.A., et al., *Serum-derived protein S binds to phosphatidylserine and stimulates the phagocytosis of apoptotic cells.* Nat Immunol, 2003. **4**(1): p. 87-91.
50. Wu, Y., N. Tibrewal, and R.B. Birge, *Phosphatidylserine recognition by phagocytes: a view to a kill.* Trends Cell Biol, 2006. **16**(4): p. 189-97.
51. Lemke, G. and C.V. Rothlin, *Immunobiology of the TAM receptors.* Nat Rev Immunol, 2008. **8**(5): p. 327-36.

52. Pawson, T., *Specificity in signal transduction: from phosphotyrosine-SH2 domain interactions to complex cellular systems.* Cell, 2004. **116**(2): p. 191-203.
53. Hubbard, S.R. and J.H. Till, *Protein tyrosine kinase structure and function.* Annu Rev Biochem, 2000. **69**: p. 373-98.
54. Scott, R.S., et al., *Phagocytosis and clearance of apoptotic cells is mediated by MER.* Nature, 2001. **411**(6834): p. 207-11.
55. Wu, Y., et al., *A role for Mer tyrosine kinase in alphavbeta5 integrin-mediated phagocytosis of apoptotic cells.* J Cell Sci, 2005. **118**(Pt 3): p. 539-53.
56. Araki, N., M.T. Johnson, and J.A. Swanson, *A role for phosphoinositide 3-kinase in the completion of macropinocytosis and phagocytosis by macrophages.* J Cell Biol, 1996. **135**(5): p. 1249-60.
57. Shankar, S.L., et al., *The growth arrest-specific gene product Gas6 promotes the survival of human oligodendrocytes via a phosphatidylinositol 3-kinase-dependent pathway.* J Neurosci, 2003. **23**(10): p. 4208-18.
58. Shankar, S.L., et al., *Gas6/Axl signaling activates the phosphatidylinositol 3-kinase/Akt1 survival pathway to protect oligodendrocytes from tumor necrosis factor alpha-induced apoptosis.* J Neurosci, 2006. **26**(21): p. 5638-48.
59. Georgescu, M.M., et al., *Biological effects of c-Mer receptor tyrosine kinase in hematopoietic cells depend on the Grb2 binding site in the receptor and activation of NF-kappaB.* Mol Cell Biol, 1999. **19**(2): p. 1171-81.
60. Tibrewal, N., et al., *Autophosphorylation docking site Tyr-867 in Mer receptor tyrosine kinase allows for dissociation of multiple signaling pathways for phagocytosis of apoptotic cells and down-modulation of lipopolysaccharide-inducible NF-kappaB transcriptional activation.* J Biol Chem, 2008. **283**(6): p. 3618-27.
61. Yi, Z., et al., *A novel role for c-Src and STAT3 in apoptotic cell-mediated MerTK-dependent immunoregulation of dendritic cells.* Blood, 2009. **114**(15): p. 3191-8.
62. Mahajan, N.P. and H.S. Earp, *An SH2 domain-dependent, phosphotyrosine-independent interaction between Vav1 and the Mer receptor tyrosine kinase: a mechanism for localizing guanine nucleotide-exchange factor action.* J Biol Chem, 2003. **278**(43): p. 42596-603.
63. Mao, Y. and S.C. Finnemann, *Essential diurnal Rac1 activation during retinal phagocytosis requires alphavbeta5 integrin but not tyrosine kinases focal adhesion kinase or Mer tyrosine kinase.* Mol Biol Cell, 2012. **23**(6): p. 1104-14.
64. Boesze-Battaglia, K. and A.D. Albert, *Phospholipid distribution among bovine rod outer segment plasma membrane and disk membranes.* Exp Eye Res, 1992. **54**(5): p. 821-3.

65. Ryeom, S.W., et al., *Binding of anionic phospholipids to retinal pigment epithelium may be mediated by the scavenger receptor CD36.* J Biol Chem, 1996. **271**(34): p. 20536-9.
66. Prasad, D., et al., *TAM receptor function in the retinal pigment epithelium.* Mol Cell Neurosci, 2006. **33**(1): p. 96-108.
67. Hall, M.O., et al., *Both protein S and Gas6 stimulate outer segment phagocytosis by cultured rat retinal pigment epithelial cells.* Exp Eye Res, 2005. **81**(5): p. 581-91.
68. Finnemann, S.C., et al., *Phagocytosis of rod outer segments by retinal pigment epithelial cells requires alpha(v)beta5 integrin for binding but not for internalization.* Proc Natl Acad Sci U S A, 1997. **94**(24): p. 12932-7.
69. Nandrot, E.F. and S.C. Finnemann, *Altered rhythm of photoreceptor outer segment phagocytosis in beta5 integrin knockout mice.* Adv Exp Med Biol, 2006. **572**: p. 119-23.
70. Nandrot, E.F., et al., *Essential role for MFG-E8 as ligand for alphavbeta5 integrin in diurnal retinal phagocytosis.* Proc Natl Acad Sci U S A, 2007. **104**(29): p. 12005-10.
71. Nandrot, E.F., et al., *Novel role for alphavbeta5-integrin in retinal adhesion and its diurnal peak.* Am J Physiol Cell Physiol, 2006. **290**(4): p. C1256-62.
72. Finnemann, S.C., *Focal adhesion kinase signaling promotes phagocytosis of integrin-bound photoreceptors.* Embo J, 2003. **22**(16): p. 4143-54.
73. Nandrot, E.F., et al., *Loss of synchronized retinal phagocytosis and age-related blindness in mice lacking alphavbeta5 integrin.* J Exp Med, 2004. **200**(12): p. 1539-45.
74. Chang, Y. and S.C. Finnemann, *Tetraspanin CD81 is required for the {alpha}vbeta5-integrin-dependent particle-binding step of RPE phagocytosis.* J Cell Sci, 2007. **120**(Pt 17): p. 3053-63.
75. LaVail, M.M., R.L. Sidman, and C.O. Gerhardt, *Congenic strains of RCS rats with inherited retinal dystrophy.* J Hered, 1975. **66**(4): p. 242-4.
76. Mullen, R.J. and M.M. LaVail, *Inherited retinal dystrophy: primary defect in pigment epithelium determined with experimental rat chimeras.* Science, 1976. **192**(4241): p. 799-801.
77. Tamai, M. and P.J. O'Brien, *Retinal dystrophy in the RCS rat: in vivo and in vitro studies of phagocytic action of the pigment epithelium on the shed rod outer segments.* Exp Eye Res, 1979. **28**(4): p. 399-411.
78. D'Cruz, P.M., et al., *Mutation of the receptor tyrosine kinase gene Mertk in the retinal dystrophic RCS rat.* Hum Mol Genet, 2000. **9**(4): p. 645-51.
79. Cohen, P.L., et al., *Delayed apoptotic cell clearance and lupus-like autoimmunity in mice lacking the c-mer membrane tyrosine kinase.* J Exp Med, 2002. **196**(1): p. 135-40.
80. Duncan, J.L., et al., *An RCS-like retinal dystrophy phenotype in mer knockout mice.* Invest Ophthalmol Vis Sci, 2003. **44**(2): p. 826-38.
81. Duncan, J.L., et al., *Inherited retinal dystrophy in Mer knockout mice.* Adv Exp Med Biol, 2003. **533**: p. 165-72.

82. Gal, A., et al., *Mutations in MERTK, the human orthologue of the RCS rat retinal dystrophy gene, cause retinitis pigmentosa.* Nat Genet, 2000. **26**(3): p. 270-1.
83. Thompson, D.A., et al., *Retinal dystrophy due to paternal isodisomy for chromosome 1 or chromosome 2, with homoallelism for mutations in RPE65 or MERTK, respectively.* Am J Hum Genet, 2002. **70**(1): p. 224-9.
84. McHenry, C.L., et al., *MERTK arginine-844-cysteine in a patient with severe rod-cone dystrophy: loss of mutant protein function in transfected cells.* Invest Ophthalmol Vis Sci, 2004. **45**(5): p. 1456-63.
85. Tada, A., et al., *Screening of the MERTK gene for mutations in Japanese patients with autosomal recessive retinitis pigmentosa.* Mol Vis, 2006. **12**: p. 441-4.
86. Cheong, H.S., et al., *MERTK polymorphisms associated with risk of haematological disorders among Korean SLE patients.* Rheumatology (Oxford), 2007. **46**(2): p. 209-14.
87. Vollrath, D., et al., *Correction of the retinal dystrophy phenotype of the RCS rat by viral gene transfer of Mertk.* Proc Natl Acad Sci U S A, 2001. **98**(22): p. 12584-9.
88. Feng, W., et al., *Mertk triggers uptake of photoreceptor outer segments during phagocytosis by cultured retinal pigment epithelial cells.* J Biol Chem, 2002. **277**(19): p. 17016-22.
89. Strick, D.J., W. Feng, and D. Vollrath, *Mertk Drives Myosin Ii Redistribution during Retinal Pigment Epithelium Phagocytosis.* Invest Ophthalmol Vis Sci, 2008.
90. Hall, M.O., et al., *The phagocytosis of os is mediated by the PI3-kinase linked tyrosine kinase receptor, mer, and is stimulated by GAS6.* Adv Exp Med Biol, 2003. **533**: p. 331-6.
91. Hall, M.O., T.A. Abrams, and T.W. Mittag, *ROS ingestion by RPE cells is turned off by increased protein kinase C activity and by increased calcium.* Exp Eye Res, 1991. **52**(5): p. 591-8.
92. Ryeom, S.W., J.R. Sparrow, and R.L. Silverstein, *CD36 participates in the phagocytosis of rod outer segments by retinal pigment epithelium.* J Cell Sci, 1996. **109**(Pt 2): p. 387-95.
93. Sparrow, J.R., et al., *CD36 expression is altered in retinal pigment epithelial cells of the RCS rat.* Exp Eye Res, 1997. **64**(1): p. 45-56.
94. Law, A.L., et al., *Annexin A2 regulates phagocytosis of photoreceptor outer segments in the mouse retina.* Mol Biol Cell, 2009. **20**(17): p. 3896-904.
95. Finnemann, S.C. and R.L. Silverstein, *Differential roles of CD36 and alphavbeta5 integrin in photoreceptor phagocytosis by the retinal pigment epithelium.* J Exp Med, 2001. **194**(9): p. 1289-98.
96. Kaplan, G., *Differences in the mode of phagocytosis with Fc and C3 receptors in macrophages.* Scand J Immunol, 1977. **6**(8): p. 797-807.
97. Castellano, F., P. Chavrier, and E. Caron, *Actin dynamics during phagocytosis.* Semin Immunol, 2001. **13**(6): p. 347-55.

98. Greenberg, S. and S. Grinstein, *Phagocytosis and innate immunity.* Curr Opin Immunol, 2002. **14**(1): p. 136-45.
99. Hall, A. and C.D. Nobes, *Rho GTPases: molecular switches that control the organization and dynamics of the actin cytoskeleton.* Philos Trans R Soc Lond B Biol Sci, 2000. **355**(1399): p. 965-70.
100. Caron, E. and A. Hall, *Identification of two distinct mechanisms of phagocytosis controlled by different Rho GTPases.* Science, 1998. **282**(5394): p. 1717-21.
101. Cox, D., et al., *Requirements for both Rac1 and Cdc42 in membrane ruffling and phagocytosis in leukocytes.* J Exp Med, 1997. **186**(9): p. 1487-94.
102. Takenawa, T. and S. Suetsugu, *The WASP-WAVE protein network: connecting the membrane to the cytoskeleton.* Nat Rev Mol Cell Biol, 2007. **8**(1): p. 37-48.
103. Miki, H., S. Suetsugu, and T. Takenawa, *WAVE, a novel WASP-family protein involved in actin reorganization induced by Rac.* EMBO J, 1998. **17**(23): p. 6932-41.
104. Tolias, K. and C.L. Carpenter, *In vitro interaction of phosphoinositide-4-phosphate 5-kinases with Rac.* Methods Enzymol, 2000. **325**: p. 190-200.
105. Edwards, D.C., et al., *Activation of LIM-kinase by Pak1 couples Rac/Cdc42 GTPase signalling to actin cytoskeletal dynamics.* Nat Cell Biol, 1999. **1**(5): p. 253-9.
106. Miki, H. and T. Takenawa, *Regulation of actin dynamics by WASP family proteins.* J Biochem, 2003. **134**(3): p. 309-13.
107. May, R.C., et al., *Involvement of the Arp2/3 complex in phagocytosis mediated by FcgammaR or CR3.* Nat Cell Biol, 2000. **2**(4): p. 246-8.
108. Firat-Karalar, E.N. and M.D. Welch, *New mechanisms and functions of actin nucleation.* Curr Opin Cell Biol, 2011. **23**(1): p. 4-13.
109. Machesky, L.M. and K.L. Gould, *The Arp2/3 complex: a multifunctional actin organizer.* Curr Opin Cell Biol, 1999. **11**(1): p. 117-21.
110. Welch, M.D., *The world according to Arp: regulation of actin nucleation by the Arp2/3 complex.* Trends Cell Biol, 1999. **9**(11): p. 423-7.
111. Aguda, A.H., et al., *The structural basis of actin interaction with multiple WH2/beta-thymosin motif-containing proteins.* Structure, 2006. **14**(3): p. 469-76.
112. Padrick, S.B., et al., *Hierarchical regulation of WASP/WAVE proteins.* Mol Cell, 2008. **32**(3): p. 426-38.
113. Rouiller, I., et al., *The structural basis of actin filament branching by the Arp2/3 complex.* J Cell Biol, 2008. **180**(5): p. 887-95.
114. Carlier, M.F. and D. Pantaloni, *Control of actin dynamics in cell motility.* J Mol Biol, 1997. **269**(4): p. 459-67.
115. Akin, O. and R.D. Mullins, *Capping protein increases the rate of actin-based motility by promoting filament nucleation by the Arp2/3 complex.* Cell, 2008. **133**(5): p. 841-51.

116. Iwasa, J.H. and R.D. Mullins, *Spatial and temporal relationships between actin-filament nucleation, capping, and disassembly.* Curr Biol, 2007. **17**(5): p. 395-406.
117. Cooper, J.A. and D. Sept, *New insights into mechanism and regulation of actin capping protein.* Int Rev Cell Mol Biol, 2008. **267**: p. 183-206.
118. Zigmond, S.H., et al., *Formin leaky cap allows elongation in the presence of tight capping proteins.* Curr Biol, 2003. **13**(20): p. 1820-3.
119. Bear, J.E., et al., *Antagonism between Ena/VASP proteins and actin filament capping regulates fibroblast motility.* Cell, 2002. **109**(4): p. 509-21.
120. Takeda, S., et al., *Two distinct mechanisms for actin capping protein regulation--steric and allosteric inhibition.* PLoS Biol, 2010. **8**(7): p. e1000416.
121. De La Cruz, E.M., *How cofilin severs an actin filament.* Biophys Rev, 2009. **1**(2): p. 51-59.
122. Bobkov, A.A., et al., *Cooperative effects of cofilin (ADF) on actin structure suggest allosteric mechanism of cofilin function.* J Mol Biol, 2006. **356**(2): p. 325-34.
123. Andrianantoandro, E. and T.D. Pollard, *Mechanism of actin filament turnover by severing and nucleation at different concentrations of ADF/cofilin.* Mol Cell, 2006. **24**(1): p. 13-23.
124. Matsui, S., et al., *LIM kinase 1 modulates opsonized zymosan-triggered activation of macrophage-like U937 cells. Possible involvement of phosphorylation of cofilin and reorganization of actin cytoskeleton.* J Biol Chem, 2002. **277**(1): p. 544-9.
125. Sumi, T., et al., *Cofilin phosphorylation and actin cytoskeletal dynamics regulated by rho- and Cdc42-activated LIM-kinase 2.* J Cell Biol, 1999. **147**(7): p. 1519-32.
126. Yin, H.L., J.H. Albrecht, and A. Fattoum, *Identification of gelsolin, a Ca2+-dependent regulatory protein of actin gel-sol transformation, and its intracellular distribution in a variety of cells and tissues.* J Cell Biol, 1981. **91**(3 Pt 1): p. 901-6.
127. Yin, H.L. and T.P. Stossel, *Control of cytoplasmic actin gel-sol transformation by gelsolin, a calcium-dependent regulatory protein.* Nature, 1979. **281**(5732): p. 583-6.
128. Yu, F.X., et al., *Identification of a polyphosphoinositide-binding sequence in an actin monomer-binding domain of gelsolin.* J Biol Chem, 1992. **267**(21): p. 14616-21.
129. Kwiatkowski, D.J., P.A. Janmey, and H.L. Yin, *Identification of critical functional and regulatory domains in gelsolin.* J Cell Biol, 1989. **108**(5): p. 1717-26.
130. Robinson, R.C., et al., *Domain movement in gelsolin: a calcium-activated switch.* Science, 1999. **286**(5446): p. 1939-42.
131. Kinosian, H.J., et al., *Ca2+ regulation of gelsolin activity: binding and severing of F-actin.* Biophys J, 1998. **75**(6): p. 3101-9.

132. Janmey, P.A. and T.P. Stossel, *Modulation of gelsolin function by phosphatidylinositol 4,5-bisphosphate.* Nature, 1987. **325**(6102): p. 362-4.
133. Serrander, L., et al., *Selective inhibition of IgG-mediated phagocytosis in gelsolin-deficient murine neutrophils.* J Immunol, 2000. **165**(5): p. 2451-7.
134. Berg, J.S., B.C. Powell, and R.E. Cheney, *A millennial myosin census.* Mol Biol Cell, 2001. **12**(4): p. 780-94.
135. Mermall, V., P.L. Post, and M.S. Mooseker, *Unconventional myosins in cell movement, membrane traffic, and signal transduction.* Science, 1998. **279**(5350): p. 527-33.
136. Araki, N., *Role of microtubules and myosins in Fc gamma receptor-mediated phagocytosis.* Front Biosci, 2006. **11**: p. 1479-90.
137. Swanson, J.A., et al., *A contractile activity that closes phagosomes in macrophages.* J Cell Sci, 1999. **112 (Pt 3)**: p. 307-16.
138. Cox, D., et al., *Myosin X is a downstream effector of PI(3)K during phagocytosis.* Nat Cell Biol, 2002. **4**(7): p. 469-77.
139. Diakonova, M., G. Bokoch, and J.A. Swanson, *Dynamics of cytoskeletal proteins during Fcgamma receptor-mediated phagocytosis in macrophages.* Mol Biol Cell, 2002. **13**(2): p. 402-11.
140. Araki, N., et al., *Phosphoinositide-3-kinase-independent contractile activities associated with Fcgamma-receptor-mediated phagocytosis and macropinocytosis in macrophages.* J Cell Sci, 2003. **116**(Pt 2): p. 247-57.
141. Olazabal, I.M., et al., *Rho-kinase and myosin-II control phagocytic cup formation during CR, but not FcgammaR, phagocytosis.* Curr Biol, 2002. **12**(16): p. 1413-18.
142. Chieregatti, E., et al., *Myr 7 is a novel myosin IX-RhoGAP expressed in rat brain.* J Cell Sci, 1998. **111 (Pt 24)**: p. 3597-608.
143. Al-Haddad, A., et al., *Myosin Va bound to phagosomes binds to F-actin and delays microtubule-dependent motility.* Mol Biol Cell, 2001. **12**(9): p. 2742-55.
144. Diakonova, M., et al., *Localization of five annexins in J774 macrophages and on isolated phagosomes.* J Cell Sci, 1997. **110 (Pt 10)**: p. 1199-213.
145. Turowski, P., et al., *Basement membrane-dependent modification of phenotype and gene expression in human retinal pigment epithelial ARPE-19 cells.* Invest Ophthalmol Vis Sci, 2004. **45**(8): p. 2786-94.
146. Smith, R.J., et al., *Clinical diagnosis of the Usher syndromes. Usher Syndrome Consortium.* Am J Med Genet, 1994. **50**(1): p. 32-8.
147. Petit, C., *Usher syndrome: from genetics to pathogenesis.* Annu Rev Genomics Hum Genet, 2001. **2**: p. 271-97.
148. Gibson, F., et al., *A type VII myosin encoded by the mouse deafness gene shaker-1.* Nature, 1995. **374**(6517): p. 62-4.
149. Liu, X., B. Ondek, and D.S. Williams, *Mutant myosin VIIa causes defective melanosome distribution in the RPE of shaker-1 mice.* Nat Genet, 1998. **19**(2): p. 117-8.
150. Liu, X., et al., *Myosin VIIa participates in opsin transport through the photoreceptor cilium.* J Neurosci, 1999. **19**(15): p. 6267-74.

151. Gibbs, D., J. Kitamoto, and D.S. Williams, *Abnormal phagocytosis by retinal pigmented epithelium that lacks myosin VIIa, the Usher syndrome 1B protein.* Proc Natl Acad Sci U S A, 2003. **100**(11): p. 6481-6.
152. Lopes, V.S., et al., *The Usher 1B protein, MYO7A, is required for normal localization and function of the visual retinoid cycle enzyme, RPE65.* Hum Mol Genet, 2011. **20**(13): p. 2560-70.
153. Schmitt, H.D., et al., *The ras-related YPT1 gene product in yeast: a GTP-binding protein that might be involved in microtubule organization.* Cell, 1986. **47**(3): p. 401-12.
154. Zerial, M. and H. McBride, *Rab proteins as membrane organizers.* Nat Rev Mol Cell Biol, 2001. **2**(2): p. 107-17.
155. Hutagalung, A.H. and P.J. Novick, *Role of Rab GTPases in membrane traffic and cell physiology.* Physiol Rev, 2011. **91**(1): p. 119-49.
156. Schwartz, S.L., et al., *Rab GTPases at a glance.* J Cell Sci, 2007. **120**(Pt 22): p. 3905-10.
157. Bucci, C. and M. Chiariello, *Signal transduction gRABs attention.* Cell Signal, 2006. **18**(1): p. 1-8.
158. Kinchen, J.M. and K.S. Ravichandran, *Phagocytic signaling: you can touch, but you can't eat.* Curr Biol, 2008. **18**(12): p. R521-4.
159. Colicelli, J., *Human RAS superfamily proteins and related GTPases.* Sci STKE, 2004. **2004**(250): p. RE13.
160. Kinchen, J.M., et al., *A pathway for phagosome maturation during engulfment of apoptotic cells.* Nat Cell Biol, 2008. **10**(5): p. 556-66.
161. Kinchen, J.M. and K.S. Ravichandran, *Phagosome maturation: going through the acid test.* Nat Rev Mol Cell Biol, 2008. **9**(10): p. 781-95.
162. Desnoyers, L., J.S. Anant, and M.C. Seabra, *Geranylgeranylation of Rab proteins.* Biochem Soc Trans, 1996. **24**(3): p. 699-703.
163. Farnsworth, C.C., et al., *Rab geranylgeranyl transferase catalyzes the geranylgeranylation of adjacent cysteines in the small GTPases Rab1A, Rab3A, and Rab5A.* Proc Natl Acad Sci U S A, 1994. **91**(25): p. 11963-7.
164. DerMardirossian, C. and G.M. Bokoch, *GDIs: central regulatory molecules in Rho GTPase activation.* Trends Cell Biol, 2005. **15**(7): p. 356-63.
165. Burton, J. and P. De Camilli, *A novel mammalian guanine nucleotide exchange factor (GEF) specific for rab proteins.* Adv Second Messenger Phosphoprotein Res, 1994. **29**: p. 109-19.
166. Strom, M., et al., *A yeast GTPase-activating protein that interacts specifically with a member of the Ypt/Rab family.* Nature, 1993. **361**(6414): p. 736-9.
167. Du, L.L. and P. Novick, *Yeast rab GTPase-activating protein Gyp1p localizes to the Golgi apparatus and is a negative regulator of Ypt1p.* Mol Biol Cell, 2001. **12**(5): p. 1215-26.
168. Will, E. and D. Gallwitz, *Biochemical characterization of Gyp6p, a Ypt/Rab-specific GTPase-activating protein from yeast.* J Biol Chem, 2001. **276**(15): p. 12135-9.

169. Seabra, M.C., et al., *Purification of component A of Rab geranylgeranyl transferase: possible identity with the choroideremia gene product.* Cell, 1992. **70**(6): p. 1049-57.
170. Seabra, M.C., et al., *Rab geranylgeranyl transferase. A multisubunit enzyme that prenylates GTP-binding proteins terminating in Cys-X-Cys or Cys-Cys.* J Biol Chem, 1992. **267**(20): p. 14497-503.
171. Cremers, F.P., et al., *REP-2, a Rab escort protein encoded by the choroideremia-like gene.* J Biol Chem, 1994. **269**(3): p. 2111-7.
172. Garrett, M.D., et al., *GDI1 encodes a GDP dissociation inhibitor that plays an essential role in the yeast secretory pathway.* EMBO J, 1994. **13**(7): p. 1718-28.
173. Wu, S.K., et al., *Structural insights into the function of the Rab GDI superfamily.* Trends Biochem Sci, 1996. **21**(12): p. 472-6.
174. Gilbert, P.M. and C.G. Burd, *GDP dissociation inhibitor domain II required for Rab GTPase recycling.* J Biol Chem, 2001. **276**(11): p. 8014-20.
175. Cavalli, V., et al., *The stress-induced MAP kinase p38 regulates endocytic trafficking via the GDI:Rab5 complex.* Mol Cell, 2001. **7**(2): p. 421-32.
176. Shisheva, A., S.R. Chinni, and C. DeMarco, *General role of GDP dissociation inhibitor 2 in membrane release of Rab proteins: modulations of its functional interactions by in vitro and in vivo structural modifications.* Biochemistry, 1999. **38**(36): p. 11711-21.
177. Yoshimura, S., et al., *Functional dissection of Rab GTPases involved in primary cilium formation.* J Cell Biol, 2007. **178**(3): p. 363-9.
178. Westlake, C.J., et al., *Primary cilia membrane assembly is initiated by Rab11 and transport protein particle II (TRAPPII) complex-dependent trafficking of Rabin8 to the centrosome.* Proc Natl Acad Sci U S A, 2011. **108**(7): p. 2759-64.
179. Futter, C.E., et al., *The role of Rab27a in the regulation of melanosome distribution within retinal pigment epithelial cells.* Mol Biol Cell, 2004. **15**(5): p. 2264-75.
180. Klomp, A.E., et al., *Analysis of the linkage of MYRIP and MYO7A to melanosomes by RAB27A in retinal pigment epithelial cells.* Cell Motil Cytoskeleton, 2007. **64**(6): p. 474-87.
181. Gibbs, D., et al., *Role of myosin VIIa and Rab27a in the motility and localization of RPE melanosomes.* J Cell Sci, 2004. **117**(Pt 26): p. 6473-83.
182. Lopes, V.S., et al., *The ternary Rab27a-Myrip-Myosin VIIa complex regulates melanosome motility in the retinal pigment epithelium.* Traffic, 2007. **8**(5): p. 486-99.
183. Ramalho, J.S., et al., *Myrip uses distinct domains in the cellular activation of myosin VA and myosin VIIA in melanosome transport.* Pigment Cell Melanoma Res, 2009. **22**(4): p. 461-73.
184. Lopes, V.S., et al., *Melanosome maturation defect in Rab38-deficient retinal pigment epithelium results in instability of immature melanosomes during transient melanogenesis.* Mol Biol Cell, 2007. **18**(10): p. 3914-27.

185. Alory, C. and W.E. Balch, *Organization of the Rab-GDI/CHM superfamily: the functional basis for choroideremia disease.* Traffic, 2001. **2**(8): p. 532-43.
186. Merry, D.E., et al., *Isolation of a candidate gene for choroideremia.* Proc Natl Acad Sci U S A, 1992. **89**(6): p. 2135-9.
187. Gordiyenko, N.V., et al., *Silencing of the CHM gene alters phagocytic and secretory pathways in the retinal pigment epithelium.* Invest Ophthalmol Vis Sci, 2010. **51**(2): p. 1143-50.
188. Mecklenburg, L. and U. Schraermeyer, *An overview on the toxic morphological changes in the retinal pigment epithelium after systemic compound administration.* Toxicol Pathol, 2007. **35**(2): p. 252-67.
189. Sauve, Y., et al., *Preservation of visual responsiveness in the superior colliculus of RCS rats after retinal pigment epithelium cell transplantation.* Neuroscience, 2002. **114**(2): p. 389-401.
190. Vicente-Manzanares, M. and F. Sanchez-Madrid, *Role of the cytoskeleton during leukocyte responses.* Nat Rev Immunol, 2004. **4**(2): p. 110-22.
191. Goody, R.S., A. Rak, and K. Alexandrov, *The structural and mechanistic basis for recycling of Rab proteins between membrane compartments.* Cell Mol Life Sci, 2005. **62**(15): p. 1657-70.
192. Tschernutter, M., et al., *Clinical characterisation of a family with retinal dystrophy caused by mutation in the Mertk gene.* Br J Ophthalmol, 2006. **90**(6): p. 718-23.
193. Brea-Fernandez, A.J., et al., *Novel splice donor site mutation in MERTK gene associated with retinitis pigmentosa.* Br J Ophthalmol, 2008. **92**(10): p. 1419-23.
194. Mackay, D.S., et al., *Novel mutations in MERTK associated with childhood onset rod-cone dystrophy.* Mol Vis, 2010. **16**: p. 369-77.
195. Caberoy, N.B., Y. Zhou, and W. Li, *Tubby and tubby-like protein 1 are new MerTK ligands for phagocytosis.* EMBO J, 2010. **29**(23): p. 3898-910.
196. Graham, D.K., et al., *Cloning and mRNA expression analysis of a novel human protooncogene, c- mer.* Cell Growth Differ, 1994. **5**(6): p. 647-57.
197. Ling, L., D. Templeton, and H.J. Kung, *Identification of the major autophosphorylation sites of Nyk/Mer, an NCAM-related receptor tyrosine kinase.* J Biol Chem, 1996. **271**(31): p. 18355-62.
198. Huang, X., et al., *Structural insights into the inhibited states of the Mer receptor tyrosine kinase.* J Struct Biol, 2009. **165**(2): p. 88-96.
199. Giubellino, A., T.R. Burke, Jr., and D.P. Bottaro, *Grb2 signaling in cell motility and cancer.* Expert Opin Ther Targets, 2008. **12**(8): p. 1021-33.
200. LaVail, M.M., *Photoreceptor characteristics in congenic strains of RCS rats.* Invest Ophthalmol Vis Sci, 1981. **20**(5): p. 671-5.
201. Zoncu, R., A. Efeyan, and D.M. Sabatini, *mTOR: from growth signal integration to cancer, diabetes and ageing.* Nat Rev Mol Cell Biol, 2011. **12**(1): p. 21-35.
202. Simonsen, A., et al., *EEA1 links PI(3)K function to Rab5 regulation of endosome fusion.* Nature, 1998. **394**(6692): p. 494-8.

203. Vieira, O.V., et al., *Distinct roles of class I and class III phosphatidylinositol 3-kinases in phagosome formation and maturation.* J Cell Biol, 2001. **155**(1): p. 19-25.
204. Christoforidis, S., et al., *Phosphatidylinositol-3-OH kinases are Rab5 effectors.* Nat Cell Biol, 1999. **1**(4): p. 249-52.
205. Majeed, M., et al., *Role of Src kinases and Syk in Fcgamma receptor-mediated phagocytosis and phagosome-lysosome fusion.* J Leukoc Biol, 2001. **70**(5): p. 801-11.
206. Sather, S., et al., *A soluble form of the Mer receptor tyrosine kinase inhibits macrophage clearance of apoptotic cells and platelet aggregation.* Blood, 2007. **109**(3): p. 1026-33.
207. Law, A.-L., et al., *The Extracellular Part Of MerTK Is Shed By RPE Cells Both In Vitro And In Vivo.* ARVO Abstract, 2011: p. #904.
208. Fujikawa, K., et al., *VAV2 and VAV3 as candidate disease genes for spontaneous glaucoma in mice and humans.* PLoS One, 2010. **5**(2): p. e9050.
209. Qin, S. and G.A. Rodrigues, *Roles of alphavbeta5, FAK and MerTK in oxidative stress inhibition of RPE cell phagocytosis.* Exp Eye Res, 2012. **94**(1): p. 63-70.
210. Zhang, Y. and H. Wang, *Integrin signalling and function in immune cells.* Immunology, 2012. **135**(4): p. 268-75.
211. Huveneers, S. and E.H. Danen, *Adhesion signaling - crosstalk between integrins, Src and Rho.* J Cell Sci, 2009. **122**(Pt 8): p. 1059-69.
212. Jeong, S.J., et al., *Increased association of dynamin II with myosin II in ras transformed NIH3T3 cells.* Acta Biochim Biophys Sin (Shanghai), 2006. **38**(8): p. 556-62.
213. Liu, B.A., et al., *SH2 domains recognize contextual peptide sequence information to determine selectivity.* Mol Cell Proteomics, 2010. **9**(11): p. 2391-404.
214. Sen, P., et al., *Apoptotic cells induce Mer tyrosine kinase-dependent blockade of NF-kappaB activation in dendritic cells.* Blood, 2007. **109**(2): p. 653-60.
215. Peterson, G.L., *A simplification of the protein assay method of Lowry et al. which is more generally applicable.* Anal Biochem, 1977. **83**(2): p. 346-56.
216. Papermaster, D.S., *Preparation of retinal rod outer segments.* Methods Enzymol, 1982. **81**: p. 48-52.
217. Colwill, K. and S. Graslund, *A roadmap to generate renewable protein binders to the human proteome.* Nat Methods, 2011. **8**(7): p. 551-8.
218. Hed, J., *Methods for distinguishing ingested from adhering particles.* Methods Enzymol, 1986. **132**: p. 198-204.
219. Clark, V.M., *The cell biology of the retinal pigment epithelium.* The Retina, Part II, 1986: p. 129-168.
220. Alory, C. and W.E. Balch, *Molecular evolution of the Rab-escort-protein/guanine-nucleotide-dissociation-inhibitor superfamily.* Mol Biol Cell, 2003. **14**(9): p. 3857-67.

221. Hanke, J.H., et al., *Discovery of a novel, potent, and Src family-selective tyrosine kinase inhibitor. Study of Lck- and FynT-dependent T cell activation.* J Biol Chem, 1996. **271**(2): p. 695-701.
222. Traxler, P., et al., *Use of a pharmacophore model for the design of EGF-R tyrosine kinase inhibitors: 4-(phenylamino)pyrazolo[3,4-d]pyrimidines.* J Med Chem, 1997. **40**(22): p. 3601-16.
223. Pfeffer, S.R., A.B. Dirac-Svejstrup, and T. Soldati, *Rab GDP dissociation inhibitor: putting rab GTPases in the right place.* J Biol Chem, 1995. **270**(29): p. 17057-9.
224. Nishimura, N., et al., *Molecular cloning and characterization of two rab GDI species from rat brain: brain-specific and ubiquitous types.* J Biol Chem, 1994. **269**(19): p. 14191-8.
225. Bachner, D., et al., *Expression patterns of two human genes coding for different rab GDP-dissociation inhibitors (GDIs), extremely conserved proteins involved in cellular transport.* Hum Mol Genet, 1995. **4**(4): p. 701-8.
226. Rush, J., et al., *Immunoaffinity profiling of tyrosine phosphorylation in cancer cells.* Nat Biotechnol, 2005. **23**(1): p. 94-101.
227. Ballif, B.A., et al., *Large-scale identification and evolution indexing of tyrosine phosphorylation sites from murine brain.* J Proteome Res, 2008. **7**(1): p. 311-8.
228. DerMardirossian, C., et al., *Phosphorylation of RhoGDI by Src regulates Rho GTPase binding and cytosol-membrane cycling.* Mol Biol Cell, 2006. **17**(11): p. 4760-8.
229. Smart, J.E., et al., *Characterization of sites for tyrosine phosphorylation in the transforming protein of Rous sarcoma virus (pp60v-src) and its normal cellular homologue (pp60c-src).* Proc Natl Acad Sci U S A, 1981. **78**(10): p. 6013-7.
230. Proikas-Cezanne, T., et al., *Rab14 is part of the early endosomal clathrin-coated TGN microdomain.* FEBS Lett, 2006. **580**(22): p. 5241-6.
231. Feng, Y., et al., *Expression and properties of Rab7 in endosome function.* Methods Enzymol, 2001. **329**: p. 175-87.
232. Bucci, C., et al., *The small GTPase rab5 functions as a regulatory factor in the early endocytic pathway.* Cell, 1992. **70**(5): p. 715-28.
233. Niedergang, F. and P. Chavrier, *Regulation of phagocytosis by Rho GTPases.* Curr Top Microbiol Immunol, 2005. **291**: p. 43-60.
234. Vieira, O.V., R.J. Botelho, and S. Grinstein, *Phagosome maturation: aging gracefully.* Biochem J, 2002. **366**(Pt 3): p. 689-704.
235. Vieira, O.V., et al., *Modulation of Rab5 and Rab7 recruitment to phagosomes by phosphatidylinositol 3-kinase.* Mol Cell Biol, 2003. **23**(7): p. 2501-14.
236. Hoppe, G., et al., *Oxidized low density lipoprotein-induced inhibition of processing of photoreceptor outer segments by RPE.* Invest Ophthalmol Vis Sci, 2001. **42**(11): p. 2714-20.

237. Cremers, F.P., et al., *Deletions in patients with classical choroideremia vary in size from 45 kb to several megabases.* Am J Hum Genet, 1990. **47**(4): p. 622-8.
238. Bienvenu, T., et al., *Non-specific X-linked semidominant mental retardation by mutations in a Rab GDP-dissociation inhibitor.* Hum Mol Genet, 1998. **7**(8): p. 1311-5.
239. D'Adamo, P., et al., *Mutations in GDI1 are responsible for X-linked non-specific mental retardation.* Nat Genet, 1998. **19**(2): p. 134-9.
240. Steele-Mortimer, O., J. Gruenberg, and M.J. Clague, *Phosphorylation of GDI and membrane cycling of rab proteins.* FEBS Lett, 1993. **329**(3): p. 313-8.
241. Zahner, J.E. and C.M. Cheney, *A Drosophila homolog of bovine smg p25a GDP dissociation inhibitor undergoes a shift in isoelectric point in the developmental mutant quartet.* Mol Cell Biol, 1993. **13**(1): p. 217-27.
242. Todt, J.C., B. Hu, and J.L. Curtis, *The receptor tyrosine kinase MerTK activates phospholipase C gamma2 during recognition of apoptotic thymocytes by murine macrophages.* J Leukoc Biol, 2004. **75**(4): p. 705-13.
243. Vanhaesebroeck, B., et al., *The emerging mechanisms of isoform-specific PI3K signalling.* Nat Rev Mol Cell Biol, 2010. **11**(5): p. 329-41.
244. Brugnera, E., et al., *Unconventional Rac-GEF activity is mediated through the Dock180-ELMO complex.* Nat Cell Biol, 2002. **4**(8): p. 574-82.
245. Graham, D.K., et al., *Cloning and developmental expression analysis of the murine c-mer tyrosine kinase.* Oncogene, 1995. **10**(12): p. 2349-59.
246. Graham, D.K., et al., *Cloning and mRNA expression analysis of a novel human protooncogene, c-mer.* Cell Growth Differ, 1994. **5**(6): p. 647-57.
247. Linger, R.M., et al., *TAM receptor tyrosine kinases: biologic functions, signaling, and potential therapeutic targeting in human cancer.* Adv Cancer Res, 2008. **100**: p. 35-83.
248. Wang, Y., et al., *Mer receptor tyrosine kinase promotes invasion and survival in glioblastoma multiforme.* Oncogene, 2012.
249. Kwok, M.C., et al., *Proteomics of photoreceptor outer segments identifies a subset of SNARE and Rab proteins implicated in membrane vesicle trafficking and fusion.* Mol Cell Proteomics, 2008. **7**(6): p. 1053-66.
250. Le Meur, G., et al., *Restoration of vision in RPE65-deficient Briard dogs using an AAV serotype 4 vector that specifically targets the retinal pigmented epithelium.* Gene Ther, 2007. **14**(4): p. 292-303.
251. Beltran, W.A., et al., *Gene therapy rescues photoreceptor blindness in dogs and paves the way for treating human X-linked retinitis pigmentosa.* Proc Natl Acad Sci U S A, 2012. **109**(6): p. 2132-7.
252. Deng, W.T., et al., *Tyrosine-mutant AAV8 delivery of human MERTK provides long-term retinal preservation in RCS rats.* Invest Ophthalmol Vis Sci, 2012. **53**(4): p. 1895-904.
253. Buschini, E., et al., *Age related macular degeneration and drusen: neuroinflammation in the retina.* Prog Neurobiol, 2011. **95**(1): p. 14-25.

254. Mitter, S.K., et al., *Autophagy in the retina: a potential role in age-related macular degeneration.* Adv Exp Med Biol, 2012. **723**: p. 83-90.
255. Wang, A.L., et al., *Autophagy and exosomes in the aged retinal pigment epithelium: possible relevance to drusen formation and age-related macular degeneration.* PLoS One, 2009. **4**(1): p. e4160.
256. Wang, A.L., et al., *Using LC3 to monitor autophagy flux in the retinal pigment epithelium.* Autophagy, 2009. **5**(8): p. 1190-3.
257. Krohne, T.U., et al., *Effects of lipid peroxidation products on lipofuscinogenesis and autophagy in human retinal pigment epithelial cells.* Exp Eye Res, 2010. **90**(3): p. 465-71.
258. Sanjuan, M.A., et al., *Toll-like receptor signalling in macrophages links the autophagy pathway to phagocytosis.* Nature, 2007. **450**(7173): p. 1253-7.